UNIVERSITY OF CALIFORNIA

SANTA CRUZ

Highly Conserved 3' Region of 16S Ribosomal RNA Supports

Translational Reading Frame Fidelity

A dissertation submitted in partial satisfaction
of the requirements for the degree of

DOCTOR OF PHILOSOPHY

in

CHEMISTRY

by

Alexandria Smart

December 2022

The dissertation of Alexandria Smart is approved:

_____
Professor Michael Stone, chair

_____
Professor Alan Zahler

_____
Professor Harry Noller

_____
Peter Biehl, Vice Provost and Dean of Graduate Studies

TABLE OF CONTENTS

ABSTRACT

Alexandria Smart

Highly Conserved 3' Region of 16S Ribosomal RNA Supports Translational Reading Frame Fidelity

Translocation of mRNA unidirectionally through the ribosome is coupled to subunit rotation. Based on our observation that A1503 of 16S rRNA intercalates between mRNA bases during specific rotational states, we tested the possibility that it could play a role in maintenance of the reading frame. We eliminated the possibility of intercalation by creating ribosomes containing an abasic site at position 1503 of 16S rRNA. This was done by site-specifically cleaving and sequentially ligating a synthetic RNA oligonucleotide containing abasic 1503. While directing ligation of the synthetic RNA to cleaved 16S rRNA, we were able to preserve higher-order structure by using a tailed DNA splint which could be removed quantitatively under mild conditions. Reconstituted ribosomes containing the abasic site were fully active in protein synthesis but showed an increased level of spontaneous frameshifting. In testing our control ligation constructs that did not contain abasic 1503, we established that semi-synthetic 16S rRNA has slightly elevated rates of frameshifting. We confirm that this finding is attribute to the demethylated 16S rRNA bases A1518 and A1519, which are universally methylated in natural ribosomes.

Dedicated to my sisters, Amanda and Katie

Acknowledgements

This thesis is a beautiful culmination of work between myself and members of the Noller group. Specifically, this work could not be completed without Laura Lancaster, John Paul Donohue, Dustin Niblett, and Harry F. Noller, as well as without helpful discussions from Gillian Rexroad. I have also had the benefit of learning and working within a community of RNA researchers in the Center for Molecular Biology of RNA, which have allowed for great conversation about my thesis and related topics. The support from this community have helped me more than I can accurately describe. Speaking of community, this work would not have been possible without the family and friends that have helped me along the way. I am lucky enough to have too large of a community to list them all, but I can especially thank my parents, Steven and Jenny Smart. My grandpa (who, along with my grandma also deserve acknowledgement) used to always brag that I was “Smart” before I was born, and that’s thanks to them.

INTRODUCTION

Translation follows a universally conserved pathway

Ribosomes can have variability from species to species, but the overall structure and function are conserved (Sauert et al., 2015). In all species two subunits composed primarily of ribosomal RNA (rRNA) and decorated with ribosomal proteins form a larger complex that is responsible for the production of all proteins in an organism. In bacteria the larger 50S subunit is composed of two rRNAs, the 23S and the 5S, while the smaller 30S subunit consists of a single large rRNA, the 16S. The universally conserved pathway for protein synthesis consists of ribosomal initiation at a messenger RNA (mRNA) start site, elongation of the peptide chain through rounds of translocation, followed by termination at a stop site. Cycles of elongation consist of aminoacyl-tRNA binding to the ribosomal A site, peptide bond formation, then translocation of mRNA and transfer RNA (tRNA) to the peptidyl (P) site. Synchronized and unidirectional translocation of both the mRNA and tRNA(s) is crucial for proper translation. The ribosome goes through large scale structural rearrangements when undergoing sequential rounds of translocation. Over the past several decades, improvements in structure studies have generated a wealth of information about the molecular

mechanism of these rearrangements during elongation, allowing researchers to build a model for ribosomal processivity.

During elongation, cycles of translocation are accomplished by the rotational movements of the two ribosomal subunits—first with respect to each other (intersubunit rotation) and then within the context of the 30S subunit only. In a single cycle of elongation the ribosome begins and ends in the unrotated classical state, moving spontaneously into a hybrid state characterized by 6-10^{o} of intersubunit rotation, followed by reversal of intersubunit rotation coupled with 30S subunit head domain rotation of 18-21^{o} forming the chimeric hybrid state before return to classical (Fig. 1) (Mohan et al., 2014). Throughout this dynamic series of higher order rearrangements, the tRNAs and mRNA must maintain perfect codon-anticodon pairing or there's risk of losing the correct reading frame.

Frameshifting

While the reading frame is initially determined by binding to a start codon, errors can occur to shift the ribosome out of frame. Ribosomal frameshifting occurs when mRNA positioning shifts with respect to the tRNAs in either the 5' or 3' direction thus translating a new reading frame of -1 or +1 respectively. Spontaneous frameshifting without designated sequence specificity is deleterious to the cell, producing missense proteins or, since 3 of 64 codons is a stop, it is likely that a frameshift event leads to an early stop codon and truncated proteins. Translation of these aberrant mRNAs could

lead to deleterious gain-of-function activity of the resulting mis-translated proteins (Chang et al., 2007). These errors in coding can cause toxicity in all organisms and are the most dangerous mistakes that can be made during translation of the genetic code (Wills and Atkins, 2006; Drummond and Wilke, 2008; Stochmanski et al., 2012). For this reason, eukaryotes have evolved elaborate nonsense-mediated decay systems for avoiding truncated products by eliminating mRNA transcripts that contain premature stop codons (Baker and Parker, 2004). On the other hand, programmed ribosomal frameshifting dictated by structured mRNA and mRNA containing 'slippery' sequences allows for sufficient translation of an out of frame alternate gene product and thus expands the genetic information within a single mRNA (Larsen et al., 1997; Li et al., 2001; Chen et al., 2009; Ritchie et al., 2012). Since frameshifting is a regulatory mechanism used as a universal gene expression system (Craigen and Caskey, 1986; Flower and Mchenry, 1990; Matsufuji et al., 1996; Namy et al., 2004; Belew et al., 2008) it seems then, that evolution would have built a ribosome that never frameshifts unless directly beneficial, as encoded by the mRNA, tRNA, and stimulatory factors.

When programmed frameshifting occurs the ribosome has been shown to adjust conformational states, pausing in a non-canonical highly rotated state making the ribosome susceptible to frameshifting (Tinoco Jr. et al., 2013; Chen et al., 2014; Kim et al., 2014; Qin et al., 2014). However, an aberrant frameshift is also most likely to occur in the highly rotated chimeric

hybrid state (Hong et al., 2018; Zhou et al., 2019; Demo et al., 2020). In this susceptible state, the interactions keeping the mRNA in place within the ribosomal reading frame are the tRNA codon-anticodon interactions and Elongation Factor-G (EF-G) (Savelsbergh et al., 2003; Dunkle et al., 2011; Niblett et al., 2021). While the tRNAs are actively translocated through the ribosome, the mRNA movement is passive and relies on the strength of codon-anticodon interactions. However, these are too weak to account for the high fidelity of mRNA reading frame maintenance alone (Labuda et al., 1982; Turner, 1996). EF-G makes stabilizing interactions with the codon-anticodon pair as the A-site tRNA translocates to the P-site and structural evidence of spontaneous translocation in the absence of EF-G shows how frameshifting could occur without those stabilizing interactions (Zhou et al., 2019). While this allows for reading frame fidelity of the A and P sites, there lacks monitoring of the exit (E) site during translocation.

A1503: ribosome structure finding implicates function

While researchers can use the wealth of published ribosome structures to gain clues about aspects of function, a hypothesis must be tested with either *in vivo* or *in vitro* study. With that being said, this entire project was born out of a surprising finding from a ribosome structure of a translocation intermediate. A crystal structure of the ribosome trapped in the chimeric hybrid state at 3.5 Å resolution allowed authors to visualize density for intercalation of 16S rRNA base A1503 into mRNA nucleotides between

positions -1 and -2 (relative to AUG start codon; Fig. 2) (Zhou et al., 2013). Since then, many more high-resolution structures have been reported of complexes trapped in different rotational states. Using deposited ribosome structures in the protein data bank (PDB), we assembled a comprehensive list of those that showed A1503 intercalation. We found that A1503 stacks between mRNA bases invariably in the chimeric hybrid state and in the classical state with vacant or non-cognate E-site tRNA. However, we have not found evidence of A1503 interacting with mRNA in the hybrid state. Considering that RNA base stacking interactions are energetically favorable as well as easily reversible (Norberg and Nilsson, 1995; Šponer et al., 2008; Condon et al., 2015), is there a possible functional role for A1503 stacking between specific mRNA bases? There is a structural implication for reading frame maintenance of the E-site codon since intercalation of A1503 would sterically block the mRNA from moving in the forward or reverse direction. This would be a barrier for translocation unless intercalation was then followed by retraction in a correctly timed manner to allow mRNA movement with the tRNA.

Given the prevalence of A1503 intercalation in deposited structures, we sought to directly test its potential role in reading frame maintenance using *in vitro* translation. Although single-base substitution of A1503 alters the free energy of base stacking to some degree, all four nucleotides should make stable stacking interactions (Walter and Turner, 1994; Šponer et al., 2008;

Jafilan et al., 2012). For this reason, we built ribosomes with 16S rRNA base A1503 completely removed from the RNA backbone using ligation of truncated 16S to a chemically synthesized RNA oligonucleotide containing an abasic site. This was done under gentle conditions to maintain functional 16S rRNA for reconstitution into 70S ribosomes. Using *in vitro* translation of mRNA containing a 'slippery sequence' (Niblett et al., 2021), we measured the rate of ribosomal frameshifting. Ribosomes containing an abasic site at position 1503 showed an increased frequency of frameshifting compared to wild-type and single-base substitutions. With our *in vitro* findings and the comprehensive structural evidence, we propose that A1503 intercalation is involved in reading frame fidelity.

An unexpected result leads to study of 16S rRNA dimethyl adenosines

When testing our abasic 1503 ribosomes, we compared the rate of frameshifting with a control set of ribosomes that had been reconstituted with 16S rRNA built with a completely wild-type chemically synthesized RNA oligonucleotide. We found that a semi-synthetic wild-type 16S rRNA lead to slightly increased levels of frameshifting, which allowed us to uncover further functional roles of the 16S rRNA 3'-end. While this control carried the wild type 16S rRNA sequence, it was missing two universally conserved modifications left out in the synthesis, dimethylation at A1518 and A1519. Previous work has shown demethylated 3' adenosines on 16S rRNA resulted in leaky translation and conferred resistance to kasugamycin (Helser et al.,

1971, 1972; Buul et al., 1984). This led us to study the function of these dimethylated adenosines in our *in vitro* translation system with frameshift mRNAs.

We obtained strains lacking the conserved methyltransferase, KsgA, responsible for specific methylation of A1518 and A1519 in 30S biogenesis (-KsgA strain) (Poldermans et al., 1980; Connolly et al., 2008) to purify demethylated ribosomes. These ribosomes showed the same rate of frameshifting seen in the ligation control construct, indicating that the lack of methylation on the synthetic 3' end was likely responsible for increased frameshifting. Furthermore, we purified active KsgA enzyme and methylated our 30S subunits from the -KsgA strain *in vitro,* finding the activity could be rescued. Upon *in vitro* methylation and reassociation into 70S, the ribosomes showed lowered rates of frameshifting equivalent to that of naturals. These findings agree with early studies in kasugamycin resistant strains and allow us to build upon previous models for functional the importance of dimethylation at A1518 and A1519.

A non-denaturing method for ligation of large functional RNAs

Maintaining inherent functionality of the 16S rRNA was vital when building the abasic 1503 semi-synthetic construct. We started with cleavage of 16S rRNA by colicin E3 RNase generating a small 49 nucleotide fragment from 1494-1542, which conveniently contains 1503 (Boon, 1971a; Bowman et al., 1971; Baan et al., 1976; Heus and van Knippenberg, 1988). We then

ligated the native 1493 nucleotide truncated 16S with a synthetic RNA bearing an abasic site at position 1503 but otherwise consisting of wild-type sequence. However, techniques in the literature rendered the 16S rRNA inactive.

RNA researchers have long used introduction of site-specific nucleotide modifications to probe the structure and function of these important biological molecules. Improvements in RNA ligation techniques have allowed for synthesis of novel constructs containing site-specific internal modifications such as nucleotides with 2'-deoxy or 2'-O-methyl (Moore and Sharp, 1992), photo-cross-linkable groups (Golden et al., 1996), fluorescent dyes (Akiyama and Stone, 2009) or radioactive phosphates (Huang and Yu, 2013). Bridging two RNAs with a DNA splint and then sealing the nicked RNA with T4 DNA Ligase (Kleppe et al., 1970; Fareed et al., 1971; Moore and Sharp, 1992; Kershaw and O'Keefe, 2012) or T4 RNA Ligase 2 (Ho and Shuman, 2002; Nandakumar et al., 2004) has become the most efficient way to build modified RNAs with minimal off-target side products (Moore and Query, 2000; Stark et al., 2006).

An important remaining hurdle to this powerful approach lies in purification of the desired RNA products from their hybridized DNA splint oligonucleotides while preserving the structure of the RNA. This purification has primarily been achieved using polyacrylamide gel electrophoresis under denaturing conditions. However, this method typically results in low yields,

especially with larger RNAs, contamination with fragments of polyacrylamide and disruption of the higher-order structure of the RNA. While it is possible to use non-denaturing methods such as sucrose gradient centrifugation or size-exclusion chromatography to separate large ligation products from small un-ligated fragments, there have not been successful methods for removal of the annealed DNA splint oligonucleotide while avoiding denaturation of the ligated RNA product. Removal of the DNA splint using DNase digestion is often inefficient, and typically requires denaturing gel purification to remove any remaining DNA fragments that may be able to re-hybridize to the RNA ligation product. For these reasons, we sought to develop a method by which DNA splints can be quantitatively removed from RNA ligation products on a preparative scale under non-denaturing conditions.

In our approach, we designed DNA splints complementary to the junction of the RNA ligation targets but flanked by non-complementary 5' and 3' tails (Fig. 3). The non-complementary tails then allow removal of the DNA splint by annealing to an antisplint DNA with complete complementarity to the tailed splint DNA (Fig. 3). The antisplint DNA efficiently outcompetes the RNA ligation product for hybridization with the tailed splint and remains stably annealed to the antisplint while the RNA product is purified under non-denaturing conditions. We find that this ligation strategy allows for site directed modification of large functional RNAs such as those found in the ribosome.

Figures and tables

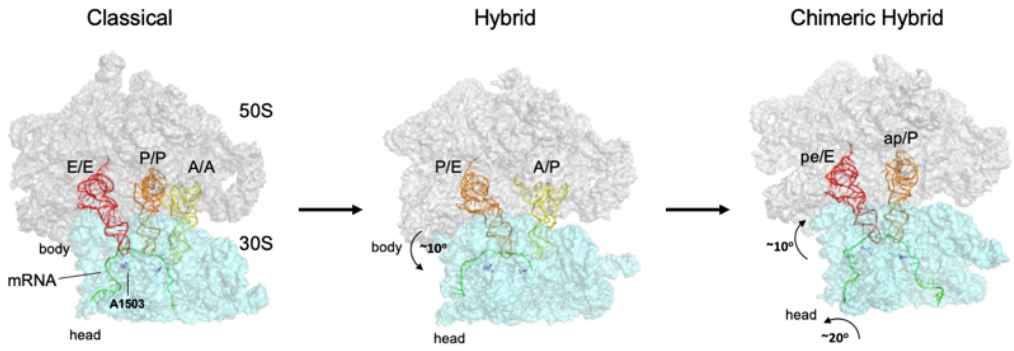

Figure 1. Large scale rotational rearrangements of ribosomal subunits undergoing translocation. Each translocation cycle begins and ends in the classical, unrotated state. While in the classical state, tRNAs are in the same binding site with respect to both subunits as denoted by A/A, P/P, and E/E (where 30S/50S). From there, the 30S subunit rotates 5-10^{o} with respect to the 50S forming the hybrid state. The hybrid state is further characterized by the tRNAs positioning with their acceptor stems in the next binding site (P and E sites) while the anticodon ends remain bound to the initial site (A and P sites), as denoted by A/P and P/E. Next, the chimeric hybrid state occurs once intersubunit rotation has reversed and the 30S head domain rotates ~20^{o} forward. In this state the tRNAs have fully translocated into the next binding site of the 50S subunit and are around 2/3 translocated within the 30S, denoted by ap/P and pe/E.

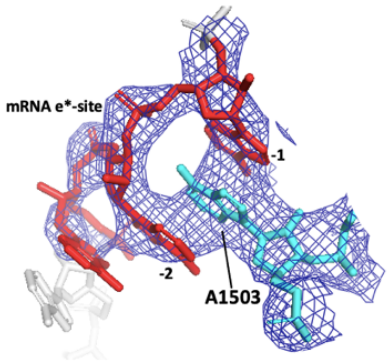

Figure 2. Example of A1503 intercalation. The first report of A1503 intercalation into mRNA bases -1 and -2 (relative to AUG start codon) was in the chimeric hybrid state (PDB 4V9K, Zhou 2013). The $2F_o - F_c$ electron density map is shown in blue, contoured at 1.5σ. A1503 is shown in cyan and mRNA e*-site codon in red.

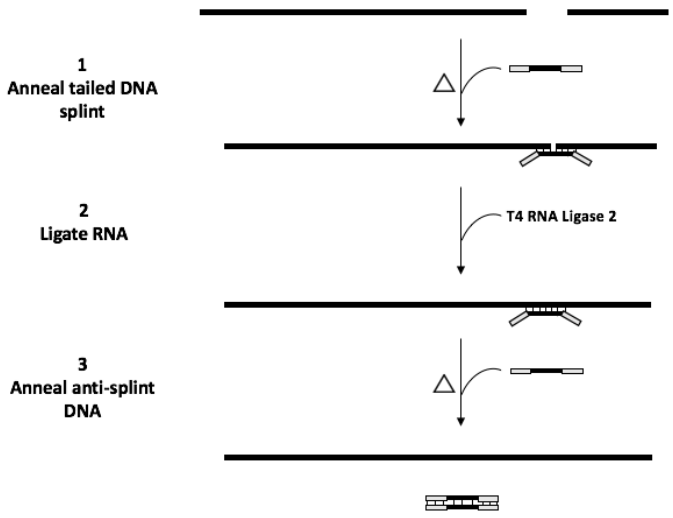

Figure 3. Scheme for tailed DNA splint displacement by annealing to a tailed anti-splint DNA. In step 1 a tailed DNA splint containing a middle region of high sequence specificity flanked by non-complementary tails is annealed to target RNAs. Following ligation (step 2), a DNA oligonucleotide bearing a complement sequence to the tailed splint is added. This antisplint DNA outcompetes the RNA ligation product such that contaminating DNA splint is easily isolated from the RNA and removed under gentle conditions.

References

ABDI, N.M., and FREDRICK, K. (2005). Contribution of 16S rRNA nucleotides forming the 30S subunit A and P sites to translation in Escherichia coli. RNA *11*, 1624–1632.

Akiyama, B.M., and Stone, M.D. (2009). Chapter 2 - Assembly of Complex RNAs by Splinted Ligation. In Methods in Enzymology, (Academic Press), pp. 27–46.

Baan, R.A., Charldorp, R.V., Leerdam, E.V., Knippenberg, P.H.V., and Bosch, L. (1976). The 3'-terminus of 16 S ribosomal RNA of Escherichia coli. Isolation and purification of the terminal 49-nucleotide fragment at a milligram scale. FEBS Lett. *71*, 351–355.

Baba, T., Ara, T., Hasegawa, M., Takai, Y., Okumura, Y., Baba, M., Datsenko, K.A., Tomita, M., Wanner, B.L., and Mori, H. (2006). Construction of Escherichia coli K-12 in-frame, single-gene knockout mutants: the Keio collection. Mol. Syst. Biol. *2*, 2006.0008.

Baker, K.E., and Parker, R. (2004). Nonsense-mediated mRNA decay: terminating erroneous gene expression. Curr. Opin. Cell Biol. *16*, 293–299.

Bank, R.P.D. RCSB PDB: Policies.

Baranov, P.V., Gesteland, R.F., and Atkins, J.F. (2002). Recoding: translational bifurcations in gene expression. Gene *286*, 187–201.

Belew, A.T., Hepler, N.L., Jacobs, J., and Dinman, J. (2008). PRFdb: A database of computationally predicted eukaryotic programmed -1 ribosomal frameshift signals. BMC Genomics.

Boon, T. (1971a). Inactivation of Ribosomes In Vitro by Colicin E3 and Its Mechanism of Action. 4.

Boon, T. (1971b). Inactivation of Ribosomes In Vitro by Colicin E3. Proc. Natl. Acad. Sci. *68*, 2421–2425.

Bowman, C.M., Dahlberg, J.E., Ikemura, T., Konisky, J., and Nomura, M. (1971). Specific Inactivation of 16S Ribosomal RNA Induced by Colicin E3 In Vivo. Proc. Natl. Acad. Sci. *68*, 964–968.

Brown, R.F., Andrews, C.T., and Elcock, A.H. (2015). Stacking free energies of all DNA and RNA nucleoside pairs and dinucleoside-monophosphates computed using recently revised AMBER parameters and compared with experiment. J. Chem. Theory Comput. *11*, 2315–2328.

Buul, C.P.J.J. van, Visser, W., and Knippenberg, P.H. van (1984). Increased translational fidelity caused by the antibiotic kasugamycin and ribosomal ambiguity in mutants harbouring the ksgA gene. FEBS Lett. *177*, 119–124.

Chang, Y.-F., Imam, J.S., and Wilkinson, M.F. (2007). The Nonsense-Mediated Decay RNA Surveillance Pathway. Annu. Rev. Biochem. *76*, 51–74.

Chen, C., Stevens, B., Kaur, J., Smilansky, Z., Cooperman, B.S., and Goldman, Y.E. (2011). Allosteric vs. spontaneous exit-site (E-site) tRNA dissociation early in protein synthesis. Proc. Natl. Acad. Sci. *108*, 16980–16985.

Chen, G., Chang, K.-Y., Chou, M.-Y., Bustamante, C., and Tinoco, I. (2009). Triplex structures in an RNA pseudoknot enhance mechanical stability and increase efficiency of –1 ribosomal frameshifting. Proc. Natl. Acad. Sci. *106*, 12706–12711.

Chen, J., Petrov, A., Johansson, M., Tsai, A., O'Leary, S.E., and Puglisi, J.D. (2014). Dynamic pathways of −1 translational frameshifting. Nature *512*, 328–332.

Choi, J., and Puglisi, J.D. (2017). Three tRNAs on the ribosome slow translation elongation. Proc. Natl. Acad. Sci. *114*, 13691–13696.

Condon, D.E., Kennedy, S.D., Mort, B.C., Kierzek, R., Yildirim, I., and Turner, D.H. (2015). Stacking in RNA: NMR of Four Tetramers Benchmark Molecular Dynamics. J. Chem. Theory Comput. *11*, 2729–2742.

Connolly, K., Rife, J.P., and Culver, G. (2008). Mechanistic insight into the ribosome biogenesis functions of the ancient protein KsgA. Mol. Microbiol. *70*, 1062–1075.

Craigen, W.J., and Caskey, C.T. (1986). Expression of peptide chain release factor 2 requires high-efficiency frameshift. Nature *322*, 273–275.

Davis, R.C., and Tinoco, I. (1968). Temperature-dependent properties of dinucleoside phosphates. Biopolymers *6*, 223–242.

Demirci, H., Murphy, F., Belardinelli, R., Kelley, A.C., Ramakrishnan, V., Gregory, S.T., Dahlberg, A.E., and Jogl, G. (2010). Modification of 16S ribosomal RNA by the KsgA methyltransferase restructures the 30S subunit to optimize ribosome function. RNA *16*, 2319–2324.

Demo, G., Loveland, A.B., Svidritskiy, E., Gamper, H.B., Hou, Y.-M., and Korostelev, A.A. (2020). Structural basis for +1 ribosomal frameshifting during EF-G-catalyzed translocation. BioRxiv 2020.12.29.424751.

Douthwaite, S., Powers, T., Lee, J.Y., and Noller, H.F. (1989). Defining the structural requirements for a helix in 23 S ribosomal RNA that confers erythromycin resistance. J. Mol. Biol. *209*, 655–665.

Drummond, D.A., and Wilke, C.O. (2008). Mistranslation-Induced Protein Misfolding as a Dominant Constraint on Coding-Sequence Evolution. Cell *134*, 341–352.

Dunkle, J.A., Wang, L., Feldman, M.B., Pulk, A., Chen, V.B., Kapral, G.J., Noeske, J., Richardson, J.S., Blanchard, S.C., and Cate, J.H.D. (2011). Structures of the Bacterial Ribosome in Classical and Hybrid States of tRNA Binding. Science *332*, 981–984.

Fareed, G.C., Wilt, E.M., and Richardson, C.C. (1971). Enzymatic Breakage and Joining of Deoxyribonucleic Acid: VIII. HYBRIDS OF RIBO- AND DEOXYRIBONUCLEOTIDE HOMOPOLYMERS AS SUBSTRATES FOR POLYNUCLEOTIDE LIGASE OF BACTERIOPHAGE T4. J. Biol. Chem. *246*, 925–932.

Flower, A.M., and Mchenry, C.S. (1990). The γ subunit of DNA polymerase III holoenzyme of Escherichia coli is produced by ribosomal frameshifting. 5.

Frilander, M.J., and Steitz, J.A. (2001). Dynamic Exchanges of RNA Interactions Leading to Catalytic Core Formation in the U12-Dependent Spliceosome. Mol. Cell *7*, 217–226.

Golden, B.L., Gooding, A.R., Podell, E.R., and Cech, T.R. (1996). X-ray crystallography of large RNAs: heavy-atom derivatives by RNA engineering. RNA *2*, 1295–1305.

Helser, T.L., Davies, J.E., and Dahlberg, J.E. (1971). Change in Methylation of 16S Ribosomal RNA Associated with Mutation to Kasugamycin Resistance in Escherichia coli. Nature. New Biol. *233*, 12–14.

Helser, T.L., Davies, J.E., and Dahlberg, J.E. (1972). Mechanism of Kasugamycin Resistance in Escherichia coli. Nature. New Biol. *235*, 6–9.

Heus, H.A., and van Knippenberg, P.H. (1988). The 3' terminal colicin fragment of Escherichia coli 16S ribosomal RNA. Conformational details revealed by enzymic and chemical probing. J. Biomol. Struct. Dyn. *5*, 951–963.

Ho, C.K., and Shuman, S. (2002). Bacteriophage T4 RNA ligase 2 (gp24.1) exemplifies a family of RNA ligases found in all phylogenetic domains. Proc. Natl. Acad. Sci. *99*, 12709–12714.

Hong, S., Sunita, S., Maehigashi, T., Hoffer, E.D., Dunkle, J.A., and Dunham, C.M. (2018). Mechanism of tRNA-mediated +1 ribosomal frameshifting. Proc. Natl. Acad. Sci. *115*, 11226–11231.

Huang, C., and Yu, Y.-T. (2013). Synthesis and Labeling of RNA In Vitro. Curr. Protoc. Mol. Biol. Ed. Frederick M Ausubel Al *0 4*, Unit4.15.

Jafilan, S., Klein, L., Hyun, C., and Florián, J. (2012). Intramolecular Base Stacking of Dinucleoside Monophosphate Anions in Aqueous Solution. J. Phys. Chem. B *116*, 3613–3618.

Jenner, L.B., Demeshkina, N., Yusupova, G., and Yusupov, M. (2010). Structural aspects of messenger RNA reading frame maintenance by the ribosome. Nat. Struct. Mol. Biol. *17*, 555–560.

Kershaw, C.J., and O'Keefe, R.T. (2012). Splint ligation of RNA with T4 DNA ligase. Methods Mol. Biol. Clifton NJ *941*, 257–269.

Kibbe, W.A. (2007). OligoCalc: an online oligonucleotide properties calculator. Nucleic Acids Res. *35*, W43–W46.

Kim, H.-K., Liu, F., Fei, J., Bustamante, C., Gonzalez, R.L., and Tinoco, I. (2014). A frameshifting stimulatory stem loop destabilizes the hybrid state and impedes ribosomal translocation. Proc. Natl. Acad. Sci. U. S. A. *111*, 5538–5543.

Kleppe, K., Sande, J.H. van de, and Khorana, H.G. (1970). Polynucleotide Ligase-Catalyzed Joining of Deoxyribo-oligonucleotides on Ribopolynucleotide Templates

and of Ribo-oligonucleotides on Deoxyribopolynucleotide Templates. Proc. Natl. Acad. Sci. *67*, 68–73.

Korostelev, A., Asahara, H., Lancaster, L., Laurberg, M., Hirschi, A., Zhu, J., Trakhanov, S., Scott, W.G., and Noller, H.F. (2008). Crystal structure of a translation termination complex formed with release factor RF2. Proc. Natl. Acad. Sci. *105*, 19684–19689.

Kunkel, T.A. (1985). Rapid and efficient site-specific mutagenesis without phenotypic selection. Proc. Natl. Acad. Sci. *82*, 488–492.

Kurland, C.G. (1992). Translational Accuracy and the Fitness of Bacteria. Annu. Rev. Genet. *26*, 29–50.

Labuda, D., Grosjean, H., Striker, G., and Pörschke, D. (1982). Codon:Anticodon and anticodon:Anticodon interaction. Evaluation of equilibrium and kinetic parameters of complexes involving a G:U wobble. Biochim. Biophys. Acta BBA - Gene Struct. Expr. *698*, 230–236.

Lancaster, L., and Noller, H.F. (2005). Involvement of 16S rRNA Nucleotides G1338 and A1339 in Discrimination of Initiator tRNA. Mol. Cell *20*, 623–632.

Larsen, B., Gesteland, R.F., and Atkins, J.F. (1997). Structural probing and mutagenic analysis of the stem-loop required for Escherichia coli dnaX ribosomal frameshifting: programmed efficiency of 50%11Edited By D. E. Draper. J. Mol. Biol. *271*, 47–60.

Li, Z., Stahl, G., and Farabaugh, P.J. (2001). Programmed +1 frameshifting stimulated by complementarity between a downstream mRNA sequence and an error-correcting region of rRNA. RNA *7*, 275–284.

Lingner, J., and Cech, T.R. (1996). Purification of telomerase from Euplotes aediculatus: requirement of a primer 3’ overhang. Proc. Natl. Acad. Sci. *93*, 10712–10717.

Matsufuji, S., Matsufuji, T., Wills, N.M., Gesteland, R.F., and Atkins, J.F. (1996). Reading two bases twice: mammalian antizyme frameshifting in yeast. EMBO J. *15*, 1360.

Moazed, D., and Noller, H. (1989a). Interaction of tRNA with 23S rRNA in the ribosomal A, P, and E sites. Cell.

Moazed, D., and Noller, H.F. (1989b). Intermediate states in the movement of transfer RNA in the ribosome. Nature *342*, 142–148.

Mohan, S., Donohue, J.P., and Noller, H.F. (2014). Molecular mechanics of 30S subunit head rotation. Proc. Natl. Acad. Sci. *111*, 13325–13330.

Moore, M.J., and Query, C.C. (2000). [7] Joining of RNAs by splinted ligation. In Methods in Enzymology, (Academic Press), pp. 109–123.

Moore, M.J., and Sharp, P.A. (1992). Site-specific modification of pre-mRNA: the 2'-hydroxyl groups at the splice sites. Science *256*, 992–997.

Namy, O., Rousset, J.-P., Napthine, S., and Brierley, I. (2004). Reprogrammed Genetic Decoding in Cellular Gene Expression. Mol. Cell *13*, 157–168.

Nandakumar, J., Ho, C.K., Lima, C.D., and Shuman, S. (2004). RNA Substrate Specificity and Structure-guided Mutational Analysis of Bacteriophage T4 RNA Ligase 2 *. J. Biol. Chem. *279*, 31337–31347.

Niblett, D., Nelson, C., Leung, C.S., Rexroad, G., Cozy, J., Zhou, J., Lancaster, L., and Noller, H.F. (2021). Mutations in domain IV of elongation factor EF-G confer −1 frameshifting. RNA *27*, 40–53.

Noller, H.F., Donohue, J.P., and Gutell, R.R. (2022). The universally conserved nucleotides of the small subunit ribosomal RNAs. RNA *28*, 623–644.

Norberg, J., and Nilsson, L. (1995). Stacking Free Energy Profiles for All 16 Natural Ribodinucleoside Monophosphates in Aqueous Solution. J. Am. Chem. Soc. *117*, 10832–10840.

O'Farrell, H.C., Pulicherla, N., Desai, P.M., and Rife, J.P. (2006). Recognition of a complex substrate by the KsgA/Dim1 family of enzymes has been conserved throughout evolution. RNA *12*, 725–733.

Peng, B.-Z., Bock, L.V., Belardinelli, R., Peske, F., Grubmüller, H., and Rodnina, M.V. (2019). Active role of elongation factor G in maintaining the mRNA reading frame during translation. Sci. Adv. *5*, eaax8030.

Poldermans, B., Bakker, H., and Van Knippenberg, P.H. (1980). Studies on the function of two adjacent N6,N6-dimethyladenosines near the 3' end of 16S ribosomal RNA of Escherichia coli. IV. The effect of the methylgroups on ribosomal subunit interaction. Nucleic Acids Res. *8*, 143–151.

Qin, P., Yu, D., Zuo, X., and Cornish, P.V. (2014). Structured mRNA induces the ribosome into a hyper-rotated state. EMBO Rep. *15*, 185–190.

Ritchie, D.B., Foster, D.A.N., and Woodside, M.T. (2012). Programmed −1 frameshifting efficiency correlates with RNA pseudoknot conformational plasticity, not resistance to mechanical unfolding. Proc. Natl. Acad. Sci. U. S. A. *109*, 16167–16172.

Sanders, C.L., and Curran, J.F. (2007). Genetic analysis of the E site during RF2 programmed frameshifting. RNA *13*, 1483–1491.

Sauert, M., Temmel, H., and Moll, I. (2015). Heterogeneity of the translational machinery: Variations on a common theme. Biochimie *114*, 39–47.

Savelsbergh, A., Katunin, V.I., Mohr, D., Peske, F., Rodnina, M.V., and Wintermeyer, W. (2003). An Elongation Factor G-Induced Ribosome Rearrangement Precedes tRNA-mRNA Translocation. Mol. Cell *11*, 1517–1523.

Schluenzen, F., Takemoto, C., Wilson, D.N., Kaminishi, T., Harms, J.M., Hanawa-Suetsugu, K., Szaflarski, W., Kawazoe, M., Shirouzu, M., Nierhaus, K.H., et al. (2006). The antibiotic kasugamycin mimics mRNA nucleotides to destabilize tRNA binding and inhibit canonical translation initiation. Nat. Struct. Mol. Biol. *13*, 871–878.

Schürer, H., Lang, K., Schuster, J., and Mörl, M. (2002). A universal method to produce in vitro transcripts with homogeneous 3′ ends. Nucleic Acids Res. *30*, e56.

Schuwirth, B.S., Day, J.M., Hau, C.W., Janssen, G.R., Dahlberg, A.E., Cate, J.H.D., and Vila-Sanjurjo, A. (2006). Structural analysis of kasugamycin inhibition of translation. Nat. Struct. Mol. Biol. *13*, 879–886.

Senior, B.W., and Holland, I.B. (1971). Effect of Colicin E3 upon the 30S Ribosomal Subunit of Escherichia coli. Proc. Natl. Acad. Sci. U. S. A. *68*, 959–963.

Šponer, J., E. Riley, K., and Hobza, P. (2008). Nature and magnitude of aromatic stacking of nucleic acid bases. Phys. Chem. Chem. Phys. *10*, 2595–2610.

Stark, M.R., Pleiss, J.A., Deras, M., Scaringe, S.A., and Rader, S.D. (2006). An RNA ligase-mediated method for the efficient creation of large, synthetic RNAs. RNA *12*, 2014–2019.

Stephan, N.C., Ries, A.B., Boehringer, D., and Ban, N. (2021). Structural basis of successive adenosine modifications by the conserved ribosomal methyltransferase KsgA. Nucleic Acids Res. *49*, 6389–6398.

Stochmanski, S.J., Therrien, M., Laganière, J., Rochefort, D., Laurent, S., Karemera, L., Gaudet, R., Vyboh, K., Van Meyel, D.J., Di Cristo, G., et al. (2012). Expanded ATXN3

frameshifting events are toxic in Drosophila and mammalian neuron models. Hum. Mol. Genet. *21*, 2211–2218.

Thammana, P., and Held, W.A. (1974). Methylation of 16S RNA during ribosome assembly in vitro. Nature *251*, 682–686.

Tinoco Jr., I., Kim, H.-K., and Yan, S. (2013). Frameshifting dynamics. Biopolymers *99*, 1147–1166.

Traub, P., and Nomura, M. (1968). Structure and function of E. coli ribosomes. V. Reconstitution of functionally active 30S ribosomal particles from RNA and proteins. Proc. Natl. Acad. Sci. U. S. A. *59*, 777–784.

Traub, P., and Nomura, M. (1969). Structure and function of Escherichia coli ribosomes: VI. Mechanism of assembly of 30 s ribosomes studied in vitro. J. Mol. Biol. *40*, 391–413.

Traub, P., Mizushima, S., Lowry, C.V., and Nomura, M. (1971a). [41] Reconstitution of ribosomes from subribosomal components. In Methods in Enzymology, (Academic Press), pp. 391–407.

Traub, P., Mizushima, S., Lowry, C.V., and Nomura, M. (1971b). [41] Reconstitution of ribosomes from subribosomal components. In Methods in Enzymology, (Academic Press), pp. 391–407.

Turner, D.H. (1996). Thermodynamics of base pairing. Curr. Opin. Struct. Biol. *6*, 299–304.

Uemura, S., Aitken, C.E., Korlach, J., Flusberg, B.A., Turner, S.W., and Puglisi, J.D. (2010). Real-time tRNA transit on single translating ribosomes at codon resolution. Nature *464*, 1012–1017.

Van Charldorp, R., Heus, H.A., and Van Knippenberg, P.H. (1981). Adenosine dimethylation of 16S ribosomal RNA: effect of the methylgroups on local conformational stability as deduced from electrophoretic mobility of RNA fragments in denaturing polyacrylamide gels. Nucleic Acids Res. *9*, 267–275.

Varshney, U., Lee, C.P., and RajBhandary, U.L. (1991). Direct analysis of aminoacylation levels of tRNAs in vivo. Application to studying recognition of Escherichia coli initiator tRNA mutants by glutaminyl-tRNA synthetase. J. Biol. Chem. *266*, 24712–24718.

Walter, A.E., and Turner, D.H. (1994). Sequence dependence of stability for coaxial stacking of RNA helixes with Watson-Crick base paired interfaces. Biochemistry *33*, 12715–12719.

Watson, Z.L., Ward, F.R., Méheust, R., Ad, O., Schepartz, A., Banfield, J.F., and Cate, J.H. (2020). Structure of the bacterial ribosome at 2 Å resolution. ELife *9*.

Wills, N.M., and Atkins, J.F. (2006). The potential role of ribosomal frameshifting in generating aberrant proteins implicated in neurodegenerative diseases. RNA *12*, 1149–1153.

Zhou, J., Lancaster, L., Donohue, J.P., and Noller, H.F. (2013). Crystal Structures of EF-G-Ribosome Complexes Trapped in Intermediate States of Translocation. Science *340*, 1236086–1236086.

Zhou, J., Lancaster, L., Donohue, J.P., and Noller, H.F. (2019). Spontaneous ribosomal translocation of mRNA and tRNAs into a chimeric hybrid state. Proc. Natl. Acad. Sci. *116*, 7813–7818.

CHAPTER II

Intercalation of 16S rRNA base A1503 into mRNA and Maintenance of the Translational Reading Frame

Abstract

During the translocation step of protein synthesis, tRNA is moved actively by rotation of the head domain of the small ribosomal subunit. However, translocation of mRNA is passive, relying on its base pairing to the tRNA anticodon, which risks shifting the translational reading frame. Based on the observation that A1503 of 16S rRNA intercalates between mRNA bases in specific intermediate states of translocation, we tested the possibility that it plays a role in maintenance of the reading frame. By constructing ribosomes with an abasic site at 16S position 1503, we eliminated the possibility of A1503 intercalation. This was done by cleaving 16S rRNA uniquely at position 1493 using the colicin E3 endonuclease and replacing the 3'-terminal 49mer fragment with a synthetic oligonucleotide containing the abasic site. Ligation of the synthetic 49mer to the large 1493mer was facilitated by a tailed DNA splint which could be removed quantitatively under mild conditions to preserve higher-order structure in the RNA. Reconstituted ribosomes

containing the abasic site were highly active in protein synthesis but showed an elevated level of spontaneous frameshifting into both the -1 and +1 reading frames.

Introduction

Advancements in ribosome structure studies have allowed researchers to trap complexes in translation intermediates such as the chimeric hybrid state. Previously, a crystal structure of the ribosome trapped in the chimeric hybrid state at 3.5 Å resolution led to a surprising discovery (Zhou et al., 2013). The authors noted distinct density for intercalation of 16S rRNA base A1503 into mRNA nucleotides at positions -1 and -2 (relative to AUG start codon; Fig. 1). Since then, many more high-resolution structures have been reported of complexes trapped in different states of translocation. Using deposited ribosome structures in the protein data bank (PDB), we assembled a comprehensive list of those that showed A1503 intercalation. We found that A1503 stacks between mRNA bases invariably in the chimeric hybrid state and in the classical state with vacant or non-cognate E-site tRNA. However, we have not found evidence of A1503 interacting with mRNA in the hybrid state. Considering that RNA base stacking interactions are energetically favorable as well as easily reversible (Norberg and Nilsson, 1995; Šponer et

al., 2008; Condon et al., 2015), is there a possible functional role for A1503 stacking between specific mRNA bases?

Synchronous movement of mRNA and tRNAs is required during sequential rounds of translocation to maintain the translational reading frame. While tRNAs are actively translocated through the ribosome, mRNA movement is passive and relies on codon-anticodon base pairing. These interactions are too weak to account for the high fidelity of mRNA reading frame maintenance alone (Labuda et al., 1982; Turner, 1996). The highly conserved GTPase, elongation factor EF-G (EF-2 in eukaryotes), has been shown to play an important role in reading frame maintenance by stabilizing the codon-anticodon duplex during translocation from the aminoacyl (A) to peptidyl (P) site (Savelsbergh et al., 2003; Dunkle et al., 2011; Peng et al., 2019; Niblett et al., 2021). While this allows for reading frame fidelity of the A and P sites, there lacks monitoring of the exit (E) site during translocation. Since ribosomal frameshifting leads to incorporation of incorrect amino acids until finally terminating at an out of frame stop codon, these types of errors are the most dangerous mistakes that can be made during translation (Kurland, 1992; Wills and Atkins, 2006; Drummond and Wilke, 2008; Stochmanski et al., 2012).

Given the prevalence of A1503 intercalation in deposited structures, we sought to directly test its potential role in reading frame maintenance using *in vitro* translation. Although single-base substitution of A1503 alters the free

energy of base stacking to some degree, all four nucleotides should make stable stacking interactions (Walter and Turner, 1994; Šponer et al., 2008; Jafilan et al., 2012). For this reason, we built ribosomes with 16S rRNA base A1503 completely removed from the RNA backbone. Cleavage with colicin E3 RNase generates a small 49 nucleotide fragment of 16S rRNA from 1494-1542, which conveniently contains 1503 (Boon, 1971a; Bowman et al., 1971; Baan et al., 1976; Heus and van Knippenberg, 1988). We then ligated the native 1493 nucleotide truncated 16S with a synthetic RNA bearing an abasic site at position 1503 but otherwise consisting of wild-type sequence. This was done under gentle conditions (see chapter 4) to maintain functional 16S rRNA for reconstitution into 70S ribosomes. Using *in vitro* translation of mRNA containing a 'slippery sequence' (Niblett et al., 2021), we found the rate of ribosomal frameshifting. Ribosomes containing an abasic site at position 1503 showed an increased frequency of frameshifting compared to wild-type and single-base substitutions. With our *in vitro* findings and the comprehensive structural evidence, we propose that A1503 intercalation is involved in reading frame fidelity.

Results

Intercalation of A1503 Between mRNA Bases

In order to understand the prevalence of structure reports with A1503 intercalation, we examined the density maps for 144 structures selected to encompass ribosomes in varying rotational states with different factors and tRNA occupancies (Table S1). We found that 47 of those had sufficient resolution and local order to accurately model the position of A1503 and nearby mRNA bases (Table S2). Ribosome complexes were classified according to their intersubunit and 30S head rotation values into classical (non-rotated), hybrid (6°-10° intersubunit rotation) or chimeric hybrid (18°-21° 30S head rotation) (Mohan et al., 2014). Of the 47 structures with convincing A1503 and mRNA density, we found 37 structures in the classical state, 2 in the hybrid state, and 9 in the chimeric-hybrid state (Table 1). Most striking, is that A1503 intercalates between positions -1 and -2 (defined by +1 as the A in the AUG start codon) of the mRNA in 8 of the 9 chimeric-hybrid state complexes and in the single complex where A1503 does not intercalate, it stacks on position -2 (Table 1). In classical state structures, A1503 intercalates between positions -3 and -4 of the mRNA (defined by +1 as the A in the AUG start codon; note this is the P-site in classical state and pe* in chimeric hybrid) in 15 of 37 complexes and stacks on either position -3 or -4 in another 11 complexes (Table 1; Fig. 1). Classical state ribosomes with A1503 intercalation have either a vacant E-site or a non-cognate E-tRNA such that mRNA base -3 is free from pairing with the anticodon. In the remaining 11 classical state structures that did not have evidence of A1503

intercalation, the E-site was occupied by either cognate or near-cognate tRNA with the anticodon bound to the -3 mRNA base. This suggests intercalation in the classical state depends on the availability of the mRNA -3 base to allow stacking with A1503. Interestingly, though the E-site is vacant in hybrid state structures, A1503 was not found to intercalate, and the mRNA was largely found to be disordered (Table 1; S1). Though we looked at the density of 9 hybrid state structures, we found that only 2 had mRNA density outside of the codon-anticodon interactions.

Additionally, it was previously observed that C1397 of 16S rRNA stacks on bases +9 or +10 in the chimeric hybrid state (Zhou et al., 2013) and bases +7 or +8 in the classical state (Korostelev et al., 2008; Jenner et al., 2010). This interaction is similar to A1503 intercalation in that it follows the pattern of interacting with mRNA primarily in the chimeric hybrid and classical state (Fig 1). The main difference between A1503 and C1397, is that instead of intercalating C1397 primarily makes stacking interactions with the upstream mRNA residue when the ribosome is in a classical state and stacks on the downstream mRNA base in the chimeric hybrid state (Table S3). Though in our data set the mRNA density downstream of the A-site codon is weak in the hybrid state, C1397 does not look to be making any stacking interactions. Intercalation can occur when the distance between A1503 and nearby mRNA bases accommodates stable stacking interactions. To understand the optimal distance for intercalation as well as define a distance that removes A1503

from mRNA, we measured the distance between the nearby mRNA bases and A1503 in our 47 structure data set (Table 2; see methods section). Furthermore, we noticed that when not intercalated into mRNA bases, A1503 adopted a slightly different conformation, which we defined as a retracted state. We found that in general, intercalation results when A1503 is 3.2 Å from mRNA bases and retraction results when A1503 is 5.1 Å or farther from mRNA bases (Table 2, Table S1). In fact, A1503 has a 5.2 Å range of motion when swiveling between the intercalated and retracted states (Fig. 2). Since we previously saw C1397 stacking in many of the structures that had A1503 intercalation, we also measured the distance between C6 of A1503 and C4 of C1397 in each state, suspecting coordinated movement of the two bases. In structures that showed A1503 and C1397 intercalation, we saw an average distance of 36.4Å between the two bases, in an extended orientation (Fig. 3A, 3B). In structures that did not show A1503 or C1397 intercalation, we measured an average distance of 33.4Å between A1503 and C1397, in a more compact state (Fig. 3C, 3D). The movement of A1503 and C1397 involves swiveling from a compacted and retracted state to an extended and intercalated state, thus increasing the distance between the two bases by around 3Å (Fig. 3E).

Next, using the distance between A1503 and mRNA bases we surveyed 819 ribosome structures for evidence of intercalation. We graphed complexes as points with 30S head rotation on the x-axis and intersubunit rotation on the y-

axis then highlighted hits of A1503 intercalation as indicated (Fig. 4). We found that A1503 intercalation hits clustered around specific rotational values corresponding to the classical and the chimeric hybrid state, whereas hybrid state rotational values did not return any evidence of A1503 intercalation. We also used this data set of 819 complexes to survey C1397 stacking with A1503 intercalation. In doing so, we tested the correlation between A1503 and C1397 using McNemar's test for significance. A two-tailed P-value less than 0.0001 was returned, indicating statistical significance.

Constructing Ribosomes with an Abasic Nucleotide at Position 1503 of 16S rRNA

With the frequency of observed A1503 intercalation, particularly in chimeric-hybrid state complexes, we sought to test its possible functional importance. This was achieved by eliminating intercalation of A1503 into mRNA by introducing an abasic site into 70S ribosomes. Abasic 30S subunits were reconstituted *in vitro* from 16S rRNA bearing an abasic nucleotide at position 1503. We built abasic 16S rRNA using splinted RNA ligation of a truncated 16S rRNA from *E. coli* and a short, synthetic RNA oligonucleotide carrying an abasic site. Site-specific cleavage by colicin E3 breaks the phosphodiester linkage of 16S rRNA between positions 1493 and 1494 in the context of 70S ribosomes (Boon, 1971a; Bowman et al., 1971; Baan et al., 1976; Heus and van Knippenberg, 1988). The resulting large 1493-nucleotide

product was then ligated to a synthetic 49-nucleotide RNA containing an abasic site at position 1503 (Fig. 5A). Splinted RNA ligation using a tailed DNA splint allowed it to be removed quantitatively under mild conditions, preserving the higher-order structure of the RNA (Fig. 5B; see methods). The ligation product was reconstituted *in vitro* with total 30S proteins (Traub et al., 1971a) and combined with natural 50S subunits, creating 70S ribosomes containing an abasic nucleotide at position 1503 of 16S rRNA (Fig. 5C). Reconstituted 70S ribosomes were tested for their activity *in vitro* by translating an mRNA encoding a 27 kDa protein (Niblett et al., 2021). Abasic 70S translational activity was 71% of that of tight-couple 70S ribosomes (Fig. 6), compared with 76% for control ribosomes reconstituted from 16S rRNA ligated with wild-type synthetic 49-mer, indicating that the abasic 16S rRNA ligation product maintained its ability to fold correctly and assemble into active 70S ribosomes *in vitro*.

Abasic 1503 Ribosomes Have Increased Levels of Frameshifting

The mRNA used in our -1-frameshift *in vitro* translation assay contains a 'slippery sequence' that promotes -1 frameshifting (-1-FS), generating a prematurely terminated 16 kDa product when in the -1-frame and a 27 kDa product when in the 0-frame. We measured the frameshifting frequency of the abasic 1503 ribosomes by quantification of the amount of 16 kDa truncated product relative to full-length, 27 kDa product (Fig. 7) (Niblett 2021). We

compared the frameshifting rate of abasic 1503 ribosomes with other reconstituted controls as well as with natural tight-coupled ribosomes (Fig. 7). Our reconstituted controls consisted of 16S rRNAs that had either been ligated with a wild-type synthetic 49mer, treated with a mock ligation, colicin E3 digested, or left untreated. Tight-coupled 70S ribosomes produce a ratio of 0.57 -1 frameshift product to 0-frame product, while abasic 1503 ribosomes accumulated almost twice as much frameshift product (Table 3; Fig. 7A). Though ribosomes reconstituted from the wild-type synthetic 49mer ligation product showed statistically significant elevated levels of -1-FS, abasic 1503 ribosomes had by far the highest rate of -1-FS. This indicates that absence of a base at position 1503, and not the ligation process itself, is responsible for increased frameshifting (Table 3; Fig. 7A). We also tested ribosomes containing 30S subunits with single-base substitutions at position 1503. These constructs were purified from endogenous subunits using an MS2-coat protein affinity purification strategy (Lancaster and Noller, 2005). When compared to wild-type MS2-tagged constructs, there was only a minimal increase in -1-FS with the A1503U mutant, no change in A1503C, and a decrease in -1-FS with A1503G (Fig. 7A)

Since -1 frameshifting is further stimulated by mRNA secondary structure downstream from a slippery sequence (Ritchie et al., 2012), we tested frameshifting using an mRNA annealed to a complementary DNA oligonucleotide (Fig. 7B). The added structure nearly doubled the rate of -1-

FS by each ribosomal construct, yet abasic 1503 ribosomes continued to show the highest rate of frameshifting (Fig. 7B). Any effects of abasic 1503 on reading frame maintenance are not disproportionally elevated by unwinding a structured mRNA. Though a -1 frameshift is more common naturally (Baranov et al., 2002), we also investigated the effects of removing base A1503 on frequency of +1 frameshifting. For this assay, we used an mRNA designed to produce a full-length 27 kDa protein translated in a +1-frame, but a truncated 16 kDa product when translating in the 0-frame (Sanders and Curran, 2007) (Fig. 7C). Again, we observed heightened levels of frameshifting for the abasic 1503 ribosomes relative to all other constructs (Fig. 7C). The single-base substitutions A1503U and A1503C behaved nearly identical to wild-type MS2-tagged ribosomes. On the other hand, A1503G showed a lower rate of shifting into the +1 frame but again was less active overall (Fig. 7C).

Discussion

Intercalation of A1503 in published structures

To build on the finding that A1503 intercalation occurs between mRNA positions -1 and -2 in the chimeric hybrid state (Zhou et al., 2013), we looked at a sample size of 144 published ribosome structures encompassing ribosomes in all rotational states and bound to different factors, tRNAs, and antibiotics (Table S1). Of these, 47 had sufficient local resolution and order to accurately model mRNA near A1503 (Table S2). Classical state ribosomes

with A1503 intercalation have either a vacant E-site or a non-cognate E-tRNA, in which case mRNA position -3 is unbound to the anticodon. This suggests intercalation in the classical state depends on the availability of mRNA position -3 base to stack. When the E-site codon is bound to the anticodon of the tRNA as in a cognate complex, mRNA position -3 is not free to interact with A1503. Though it is unclear how frequently classical state ribosomes remain bound to E-site tRNA during elongation (Uemura et al., 2010; Chen et al., 2011; Choi and Puglisi, 2017), A1503 intercalation between mRNA bases -3 and -4 would likely destabilize codon–anticodon pairing. Positioning of A1503 near the mRNA is structurally achieved by stabilizing interactions with a cluster of universally conserved nucleotides (Noller et al., 2022). Covalent linkage to G1504, which is ‘clamped’ between 16S rRNA bases 1505, 1502 and 1501, stabilizes A1503 positioning relative to G926. Base G926 is known to contact phosphate +3 of mRNA in the chimeric hybrid state and +1 in the classical state. Further stabilizing A1503 near mRNA and G926 is a hydrogen bond between the phosphate of A1503 and the two-amino group of G925 (Noller et al., 2022). Not only does G1504 stabilize A1503 near the mRNA, but this interaction also links A1503 to C1397 through Watson-Crick pair G1504—C1399. This invariable and strong interaction tethers the two intercalating bases and is likely responsible for the highly corelated movement of C1397 with A1503 (Fig. 3).

Effects of single-base-substitution

Given the high conservation of A1503 and the wealth of structural evidence of intercalation into mRNA bases, we sought to test how de-stabilizing intercalation with single-base substitution would affect protein synthesis and rates of frameshifting. Our *in vitro* translation assay allows us to test ribosomes in translating an mRNA containing a 'slippery' sequence to detect heightened frameshifting. Using translation of a -1-frameshift mRNA, we detected modest differences in frameshifting in the mutants as compared to wild-type. Interestingly, A1503G mutagenesis resulted in a decrease of -1 and +1 frameshifted product (Fig. 7A, 7C) but less activity overall (Fig. 6). Together, these findings indicate that substitution to a guanosine at 1503 shifts the dynamics of stacking with mRNA in a way that makes ribosomes less active but more accurate when translating a slippery sequence. Conversely, an A1503U mutation only modestly increased the rate of -1-FS with no measurable effect on +1-FS and showed comparable activity to wild-type (Fig. 7A, 7C). These results are not surprising since guanosine has the lowest free energy for stacking interactions and thus favors very stable base stacking (Davis and Tinoco, 1968; Norberg and Nilsson, 1995; Šponer et al., 2008; Jafilan et al., 2012; Brown et al., 2015). On the other hand, pyrimidine bases have a higher base stacking free energy and compared to guanosine, have less stable stacking interactions. Furthermore, A1503 is extremely conserved but the only mutations that are tolerated are A1503U or A1503C

(Noller et al., 2022). The highly stable base stacking interactions caused by A1503 mutagenesis to guanosine has not been tolerated evolutionarily. Adenosine ranks in the middle as far as free energy of stacking, so there could have been an evolutionary pressure for 1503 to be adenosine.

Effects of an Abasic Nucleotide at A1503

Since all four bases are capable of intercalation and mutagenesis resulted in very minimal frameshifting changes, we reasoned that the only way to eliminate intercalation would be to remove base A1503 altogether. This was achieved by reconstituting ribosomes composed of colicin E3 digested 16S rRNA ligated to synthetic 49mer RNA containing an abasic site. Ribosomes bearing an abasic 1503 16S rRNA frequently shifted out of frame in both the -1 and +1 direction (Fig. 7), though did not have significantly decreased activity (Fig. 6). As predicted, removal of base A1503 from the 16S rRNA backbone eliminated the possibility of intercalation between mRNA bases and resulted in higher frequencies of slipping out of the 0-frame. Elimination of A1503 intercalation near the E-site codon may be solely enough to explain this increase in frameshifting. It's also possible that without A1503 intercalation, the coordinated movement of C1397 is disrupted enough to affect mRNA stacking dynamics of C1397 as well. Though movement of C1397 and A1503 are correlated, we cannot determine if A1503 directly facilitates C1397 movement.

A1503 and the translational reading frame

Why does A1503 of the 16S rRNA intercalate into mRNA bases during specific intermediates of translocation? Our current model is that A1503 intercalation into mRNA bases is coordinated with mRNA movement to allow for translocation while still assisting in reading frame maintenance of elongating ribosomes. In the hybrid state, we did not see evidence of A1503 intercalation, and mRNA bases outside of codon-anticodon interactions appeared mostly disordered. In hybrid state intermediates, tRNAs spontaneously move into the P- and E-site of the 50S subunit, sampling this state until EF-G binds and commits the ribosome to translocation. Once committed to translocation in the chimeric hybrid state, 30S body domain residues A1503 and C1397, intercalate between -1, -2 and +9, +10 respectively to stabilize the mRNA reading frame. In trapped chimeric hybrid complexes, each codon has partially translocated in the 30S. From here, translocation of a full codon is established upon 30S head rotation back to the classical state. Accordingly, the mRNA -1, -2 positions in the ap*, pe* chimeric hybrid state become -3, -4 in the post-translocated P, E classical state. Once in the non-rotated classical state, A1503 remains intercalated for an unknown amount of time, but may stack with the -3 mRNA base such that codon-anticodon interactions are weakened in the E-site. In this way, A1503 intercalation may de-stabilize E-site tRNA anticodon binding and favor

dissociation upon return to classical state for a subsequent round of translocation. Studies of E-site tRNA dissociation dynamics with mutagenized 1503 ribosomes will need to be explored to further test this theory.

Experimental Procedures

Structural analysis of A1503 interactions

Structural alignment and imaging were done using PyMOL to fetch and align PDB files from the protein databank. All alignments were done on the 16S body residues 1-939, 1345-1542. Initial measurements between A1503 and mRNA as well as A1503 swivel distance were conducted using the measurement wizard in PyMOL with our 48-structure data set after comparing models and maps of 144 structures. Models were compared to maps for correlation quality using COOT. Ribosomes were obtained from the PDB using a blast search on E. coli 16S (7K00 chain A, default blast settings) resulting in 994 ribosomes. They were further filtered by completeness, resolution, number of tRNA, factors, mRNA, and experimental methods resulting in 819 ribosomes. We typically found X-ray structures to have better density for the residues of interest, which resulted in 481 structures. We defined A1503 intercalation evidence in structures where A1503 is within 3.8Å of two consecutive mRNA bases using PDB 7K00 as our reference. Residue

1503 was examined using pymol scripts to find mRNA residues in the appropriate neighborhood. The centroid distance between residue 1503 and nearby mRNA residues was calculated. If two adjacent residues were surrounding residue 1503 within 3.8Å, it was classified as intercalating. The rotation values were measured using the Euler-Rodriguez method as previously described (Mohan et al., 2014). The angles were measured relative to the 2Å resolution reference structure 7K00 (Watson et al., 2020). The intersubunit rotation was determined by aligning the 23S to the reference and calculating the angle of the small subunit body relative to the reference. The head rotation was measured similarly, aligning the small subunit bodies and calculating the resulting angle of the head.

Buffer, Ribosomes, Factors, tRNA, mRNA

Tight-couple 70S ribosomes were purified as described (Moazed and Noller, 1989a). IF1, IF2, and IF3 were prepared as described (Lancaster and Noller, 2005). In vitro-transcribed $tRNA^{Met}$ was prepared according to Niblett (Niblett et al., 2021). Following transcription and gel purification, 2′,3′-cyclic phosphate was removed from the 3′ end of $tRNA^{Met}$ by incubation with T4 polynucleotide kinase (NEB) (Schürer et al., 2002). Aminoacylation (Moazed and Noller, 1989a) of transcribed $tRNA^{Met}$ was shown to be >95% as monitored by acid gel electrophoresis (Varshney et al., 1991). S100 extract was prepared from 10 g of E. coli MRE600 cells purified over DEAE resin

according to previously published protocols (Traub et al., 1971a). Total tRNA from MRE600 was purified (insert). The frameshift mRNA was constructed as described previously (Niblett et al., 2021).

Sequences of mRNAs:

-1 frameshift mRNA:

5'-

AUGCACCACCACCACCACCACGCAACUGUUUCCAUGCGCGACAUGCUC
AAGGCUGGUGUUCACUUCGGUCACCAGACCCGUUACUGGAACCCGAA
AAUGAAGCCGUUCAUCUUCGGUGCGCGUAACAAAGUUCACAUCAUCAA
CCUUGAGAAAACUGUACCGAUGUUCAACGAAGCUCUGGCUGAACUGAA
CAAGAUUGCUUCUCGCAAAGGUAAAAUCCUUUUCGUUGGUACUAAACG
CGCUGCAAGCGAAGCGGUGAAAGACGCUGCUCUGAGCUGCGACCAGU
UCUUCGUGAACCAUCGCUGGCUGGGCGGUAUGCUGACUAACUGGAAA
ACCGUUCGUCAGUCCAUCAAACGUCUGAAAGACCUGGAAACUCAGUCU
CAGGGAGGUACUUUCGGAAAAAAGACCAAGAAAGAAGCGCUGAUGCG
CACUCGUGAGCUGGAGAAACUGGAAAACAGCCUGGGCGGUAUCAAAG
ACAUGGGCGGUCUGCCGGACGCUCUGUUUGUAAUCGAUGCUGACCAC
GAACACAUUGCUAUCAAAGAAGCAAACAACCUGGGUAUUCCGGUAUUU
GCUAUCGUUGAUACCAACUCUGAUCCGGACGGUGUUGACUUCGUUAU
CCCGGGUAACGACGACGCAAUCCGUGCUGUGACCCUGUACCUGGGCG
CUGUUGCUGCAACCGUACGUGAAGGCCGUUCUCAGGAUCUGGCUUCC

CAGGCGGAAGAAAGCUUCGUAGAAGCUGAGUAAGGAUCCGAAUUCGA

GCUCCGUCGACAAGCUUGCGGCCGCAGGACUCCGGAGGAGACUCCGG

AGUCCCUCGAG

+1 frameshift mRNA

5'-

AUGCACCACCACCACCACCACGCAACUGUUUCCAUGCGCGACAUGCUC

AAGGCUGGUGUUCACUUCGGUCACCAGACCCGUUACUGGAACCCGAA

AAUGAAGCCGUUCAUCUUCGGUGCGCGUAACAAAGUUCACAUCAUCAA

CCUUGAGAAAACUGUACCGAUGUUCAACGAAGCUCUGGCUGAACUGAA

CAAGAUUGCUUCUCGCAAAGGUAAAAUCCUUUUCGUUGGUACUAAACG

CGCUGCAAGCGAAGCGGUGAAAGACGCUGCUCUGAGCUGCGACCAGU

UCUUCGUGAACCAUCGCUGGCUGGGCGGUAUGCUGACUAACUGGAAA

ACCGUUCGUCAGUCCAUCAAACGUCUGAAAGACCUGGAAACUCAGUCC

AGGGGGUUUCUUUGACUACACCAAGAAAGAAGCGCUGAUGCGCACUC

GUGAGCUGGAGAAACUGGAAAACAGCCUGGGCGGUAUCAAAGACAUG

GGCGGUCUGCCGGACGCUCUGUUUGUAAUCGAUGCUGACCACGAACA

CAUUGCUAUCAAAGAAGCAAACAACCUGGGUAUUCCGGUAUUUGCUAU

CGUUGAUACCAACUCUGAUCCGGACGGUGUUGACUUCGUUAUCCCGG

GUAACGACGACGCAAUCCGUGCUGUGACCCUGUACCUGGGCGCUGUU

GCUGCAACCGUACGUGAAGGCCGUUCUCAGGAUCUGGCUUCCCAGGC

GGAAGAAAGCUUCGUAGAAGCUGAGUAAGGAUCCGAAUUCGAGCUCC

GUCGACAAGCUUGCGGCCGCAGGACUCCGGAGGAGACUCCGGAGUCC
CUCGAG

Construction of A1503 mutants and MS2 purification

Site directed mutagenesis (Kunkel, 1985) was used to construct A1503 mutants in plasmid pKF207 (Abdi and Fredrick, 2005). This plasmid contains an altered anti-SD sequence that allows for specific translation of β-galactosidase under control of an arabinose-inducible promotor. An Ms2-tagged construct was used for A1503 mutant 30S subunit purification as previously described (Lancaster and Noller, 2005). In order to purify the Ms2-tagged 30S subunits, each was put into the pLK35 plasmid which contains the rrnB operon under control of the lambda P_L promoter for temperature inducible expression (Douthwaite et al., 1989). To make the pLK35_Ms2 16S rRNA constructs, the mutants were cut from the pKF207 plasmid with KpnI and BamHI, upstream of the altered anti-SD sequence such that the altered anti-SD would not be retained in the pLK35 plasmid. Next, pLK35 plasmid was digested with BamHI and BstE restriction enzymes to retain a natural anti-SD sequence in the 16S rRNA. Restriction digested DNA segments of interest were purified by agarose gel electrophoresis and subsequently ligated to construct the pLK35_Ms2 A1503 mutagenesis products. Purification of the Ms2-affinity tagged wild type and mutant 30S subunits encoded from pLK35 were expressed in strain MOPOP and purified as previously described

(Lancaster and Noller, 2005). The MS2 tag affinity sequence on extracted 16S rRNA was detected by extending [^{32}P] primer 5'-CCCGTCCGCCACTCGTCAGC-3' in absence of dCTP, and the proportion of 16S rRNA containing the sequence was determined using a phosphor imager (Molecular Dynamics). Each affinity purified 30S subunit construct was associated with natural 50S subunits for *in vitro* assays described below.

Construction of abasic 1503 and wild type synthetic ligated 16SrRNA containing ribosomes

DNA splinted RNA ligation under non-denaturing conditions was used to construct an abasic 1503 16S rRNA *in vitro* (Smart 2022). As described previously, a colicin E3 cut 1493 nucleotide segment of 16S rRNA was ligated to a synthetic RNA oligonucleotide containing the 3' end 16S rRNA sequence as well as one with an abasic site modification at position 1503 (bold and underlined): 5'-GUCGUAACA**A**GGUAACCGUAGGGGAACCUGCGGUUGGAUCACCUCCUUA-3' (Dharmacon). Following splint-directed ligation, the tailed-DNA splint was removed from the RNA ligation products by annealing a complementary DNA oligonucleotide under gentle conditions (Smart 2022). The semi-synthetic 16S rRNA ligation products were then reconstituted with TP30 proteins and natural 50S subunits to construct functional 70S particles, which were purified by 10-35% sucrose gradient in 25 mM Tris-HCl (pH 7.5), 100

mM NH_4Cl, 15 mM $MgCl_2$, 5 mM β-mercaptoethanol as previously described (Moazed and Noller, 1989).

***In vitro* translational activity and quantification**

The activity of ribosomes containing A1503 mutations as well as containing 16S rRNA ligation, mock ligation, or colicin E3 cut 1493mer segment was tested by *in vitro* translation of a full-length protein as previously described (Niblett et al., 2021), with the modification that no excess EF-G or EF-Tu was added to reaction mixtures in this study. Results were analyzed by electrophoresis on a 4%-15% SDS polyacrylamide gel, dried under vacuum for 30 minutes at 80°C, and pump then visualized and quantified using ImageJ software.

Tables and Figures

Table 1. Intercalation and stacking of A1503 in mRNA [a]

State	Number of structures	Number Intercalated (mRNA position)	Percent Intercalated	Number stacked (mRNA position)	Percent Stacked
Classical (E-site occupied)	31	13 (-3/-4)	42%	5 (-3) 5 (-4)	32%
Classical (E-site vacant)	6	2 (-3/-4)	33%	1(-4)	17%
Hybrid	2	0	0%	0	0%
Chimeric Hybrid	9	8 (-1/-2)	89%	1 (-2)	11%

[a] Position of A1503 interaction with mRNA is determined by P or pe* site convention. Intercalation occurs directly between two mRNA bases, indicated

by (downstream base/upstream base). Stacking results from A1503 interacting preferentially with either the upstream or downstream mRNA base.

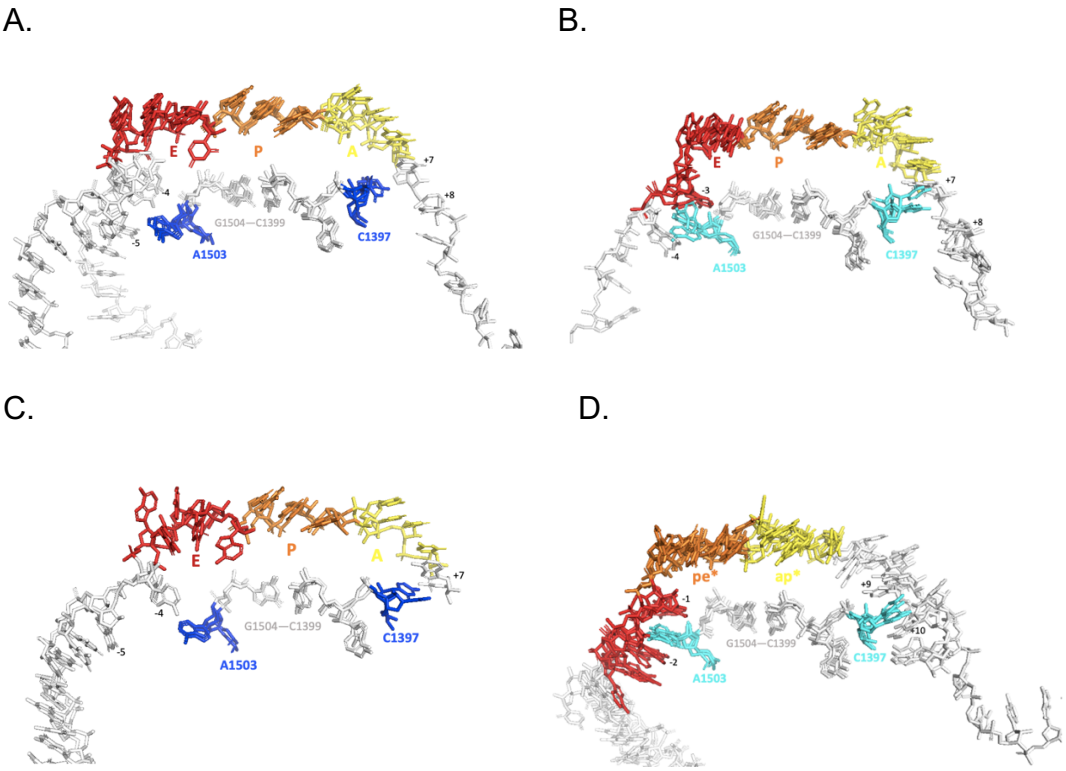

Figure 1. A1503 and C1397 intercalation occurs during specific stages of translocation. Intercalation and retraction movements of A1503 and C1397 with mRNAs in different states. Alignments of two or more structures from different studies but similar translocation intermediate states were aligned in PyMOL on the 16S body domain (residues 1-939, 1346-1542). The classical state where A1503 and C1397 are seen retracted from mRNA (A)

are modeled by PDB 4V6F, 4V9D, and 4V5F. The classical state ribosomes that have A1503 and C1397 intercalating between mRNA positions -3, -3 and +7, +8 respectively (B) are demonstrated by PDBs 4V51, 4WZD, 4WQ1, and 4WZO. In hybrid state ribosomes (PDB 6WDG, and 4V9D), the mRNA is more dynamic between structures, and we do not see A1503 or C1397 intercalation (C). Chimeric hybrid states with the highest degree of 30S head rotation (PDB 4W29, 4V9K, 4V9L, 6N1D), show intercalation of A1503 and C1397 into mRNA bases -1, -2 and +9, +10 respectively (D).

Table 2. Average distance between A1503 and nearby mRNA bases

State	A1503 Distance (Å)
Classical –without intercalation	5.4
Classical – with intercalation	3.2
Hybrid	5.1
Chimeric Hybrid	3.2

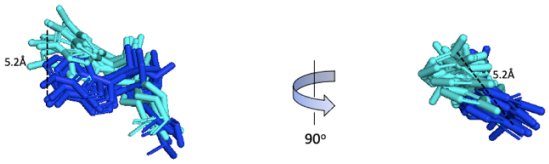

Figure 2. When moving from a retracted position to an intercalated position, A1503 adopts 2 major states. As A1503 moves from a retracted position (blue) to an intercalated position (cyan), the base swivels 5.2 Å as seen by aligning the 16S rRNA body from ribosomes in classical, hybrid, and

chimeric hybrid states (PDB 4WZD, 4W29, 4V9L, 6WDG, 4V6F, 6WD5, 4WQ1, 4WRA, 4WZO, 4V9D, 4V5F).

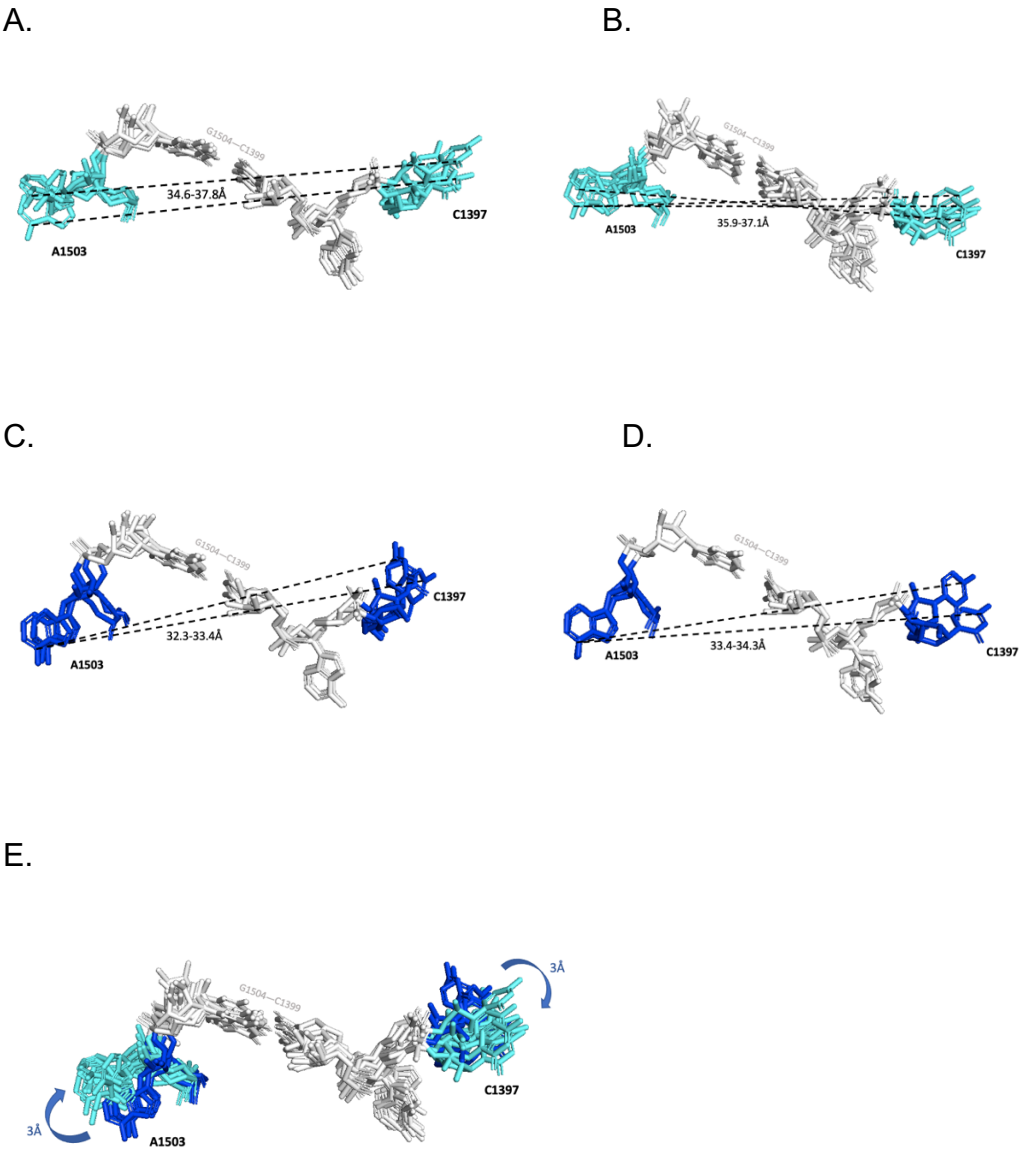

Figure 3. Intercalation and retraction of A1503 and C1397 movement is coordinated. Intercalating 16S rRNA bases A1503 and C1397 swivel between retracted position (blue) and intercalated position (cyan) in a

coordinated fashion, joined by Watson-crick pair G1504 and C1399. When A1503 and C1397 intercalate in a classical state (A; PDB 4V51, 4WZD, 4WQ1, 4WZO) or in the chimeric hybrid state (B; 4W29, 4V9K, 4V9L, 6N1D) A1503 and C1397 are extended. However, when A1503 and C1397 adopt a retracted position in either the classical state (C; PDB 4V6F, 4V9D, 4V5F) or the hybrid state (D; PDB 6WDG, 4V9D), the bases are retracted. This coordinated swivel results in a retraction or extension of bases A1503 and C1397 changing the distance between the two intercalating bases by around 3Å (E) on average.

A.

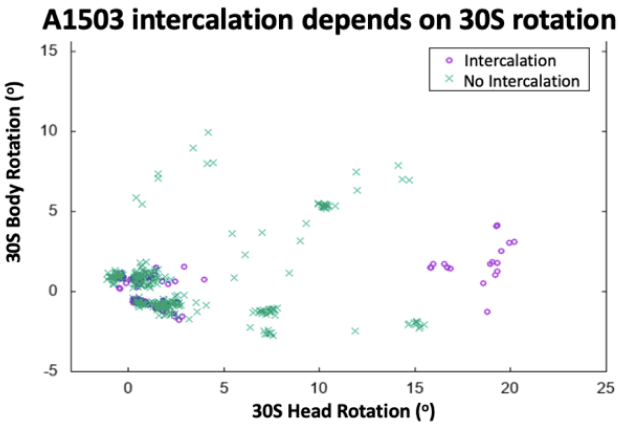

B.

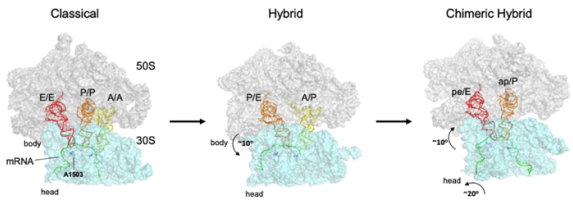

Figure 4. Intercalation of 16S rRNA base A1503 into mRNA occurs within specific 30S rotational states. (A) There are two populations of rotational states that result in A1503 intercalation (purple circles). Intercalation of A1503 into mRNA occurs only with low 30S body rotations of 5° or less. Higher 30S body rotations such as those found in the hybrid state, may move mRNA in a way that disrupts A1503 intercalation or coordinate retraction of A1503 and C1397 from mRNA. (B) The 30S rotational values correspond to the three major ribosomal states during translocation.

A.

Sequences:

Synthetic wild type 49mer (position 1503 underlined and bold):

5' –

GUCGUAACA**A**GGUAACCGUAGGGGAACCUGCGGUUGGAUCACCUCCU

UA – 3'

Synthetic abasic 1503 49mer:

5' –

GUCGUAACA**.rab.**GGUAACCGUAGGGGAACCUGCGGUUGGAUCACCUC

CUUA – 3'

Tailed DNA splint (non-complementary tails italicized):

5' – *GAGTAT*

CGGTTACCTTGTTACGACTTCACCCCAGTCATGAATCACAAAG

ACCATTCGCGG –'3

DNA anti-splint:

5’ –

CCGCGAATGGTCTTTGTGATTCATGACTGGGGTGAAGTCGTAACAAGGT

AACCGATACTC – ‘3

B.

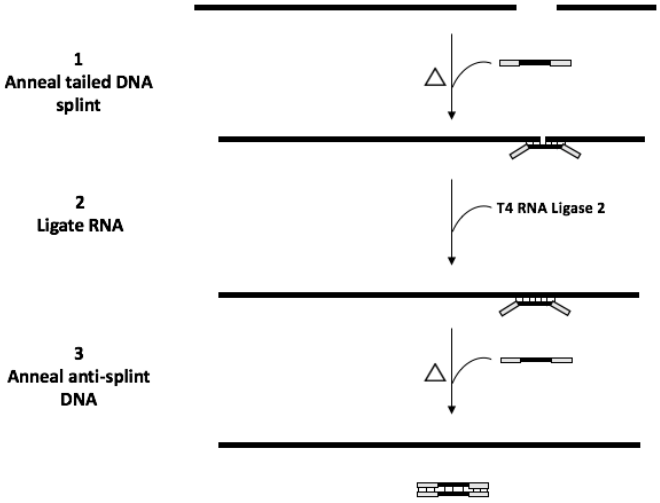

C.

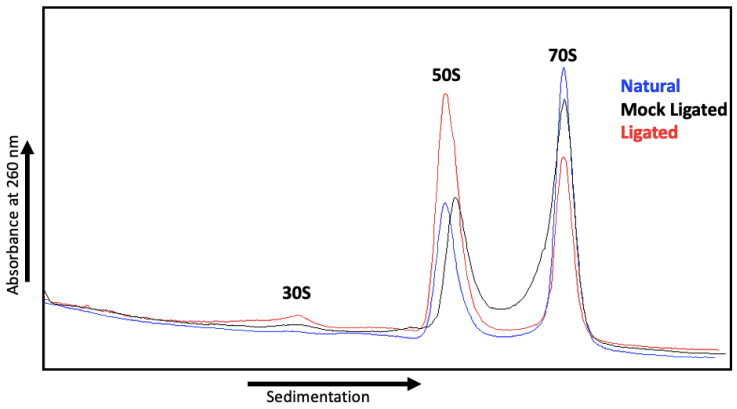

Figure 5. Creating abasic site with splinted ligation. We used a tailed DNA splint mediated RNA ligation strategy to build the abasic and synthetic wild-type 16S rRNA. (A) Sequences of synthetic RNA oligonucleotides as well as the tailed DNA splint and its corresponding anti-splint DNA. (B) Schematic of the splinted RNA ligation strategy using a tailed DNA splint for easy removal under gentle conditions. (C) Reconstitution of 16S rRNA with 30S subunit proteins and natural 50S. Schematic of 10% - 35% sucrose gradient scanned at 260nm absorbance to indicate reconstitution of ribosomes with natural 16S rRNA (blue), a mock ligated 16S rRNA (black) and ligated 16S product (red).

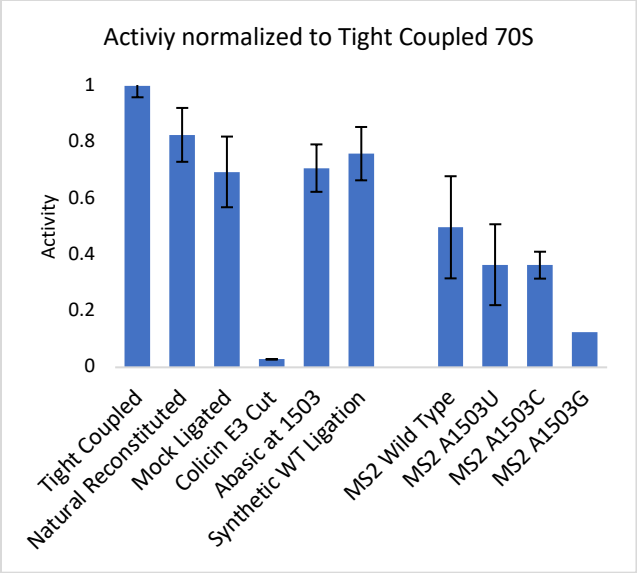

Figure 6. Activity of Ribosome Constructs. *In vitro* translation activity was determined by ^{35}S-Met incorporation into either full length or truncated S2 protein product by -1 frameshift mRNA (n=4 for MS2 A1503 mutants; n=8 for all others).

A.

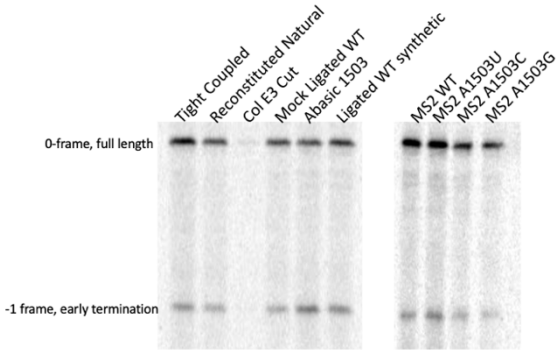
Tight Coupled
Reconstituted Natural
Col E3 Cut
Mock Ligated WT
Abasic 1503
Ligated WT synthetic
MS2 WT
MS2 A1503U
MS2 A1503C
MS2 A1503G
0-frame, full length
-1 frame, early termination

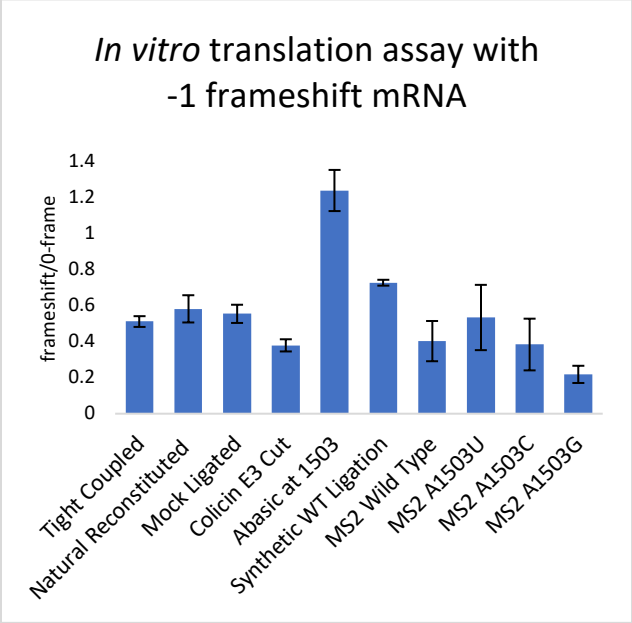
In vitro translation assay with
-1 frameshift mRNA
frameshift/0-frame
1.4
1.2
1
0.8
0.6
0.4
0.2
0
Tight Coupled
Natural Reconstituted
Mock Ligated
Colicin E3 Cut
Abasic at 1503
Synthetic WT Ligation
MS2 Wild Type
MS2 A1503U
MS2 A1503C
MS2 A1503G

B.

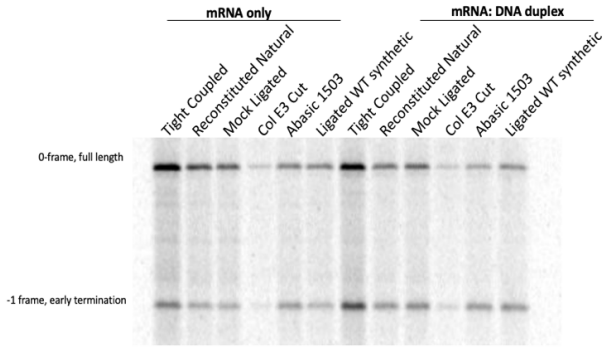
mRNA only
mRNA: DNA duplex
Tight Coupled
Reconstituted Natural
Mock Ligated
Col E3 Cut
Abasic 1503
Ligated WT synthetic
Tight Coupled
Reconstituted Natural
Mock Ligated
Col E3 Cut
Abasic 1503
Ligated WT synthetic
0-frame, full length
-1 frame, early termination

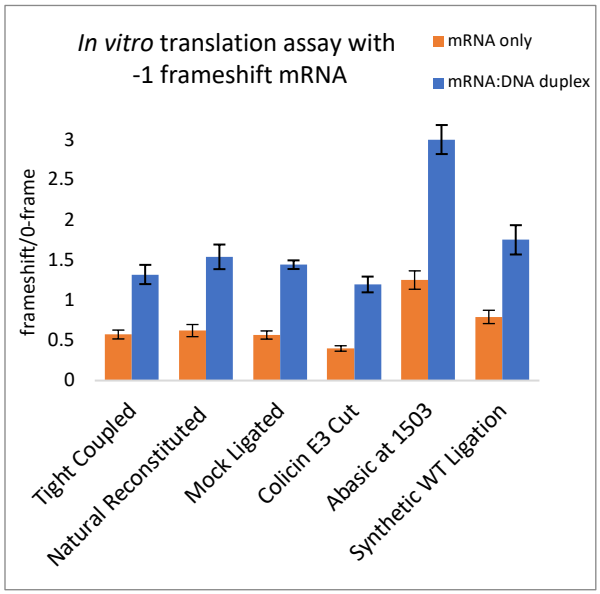
In vitro translation assay with
-1 frameshift mRNA
mRNA only
mRNA:DNA duplex
frameshift/0-frame
3
2.5
2
1.5
1
0.5
0
Tight Coupled
Natural Reconstituted
Mock Ligated
Colicin E3 Cut
Abasic at 1503
Synthetic WT Ligation

C.

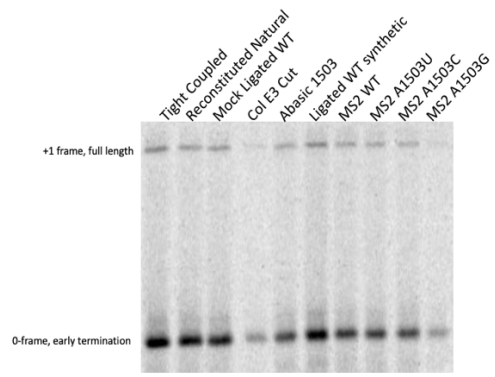

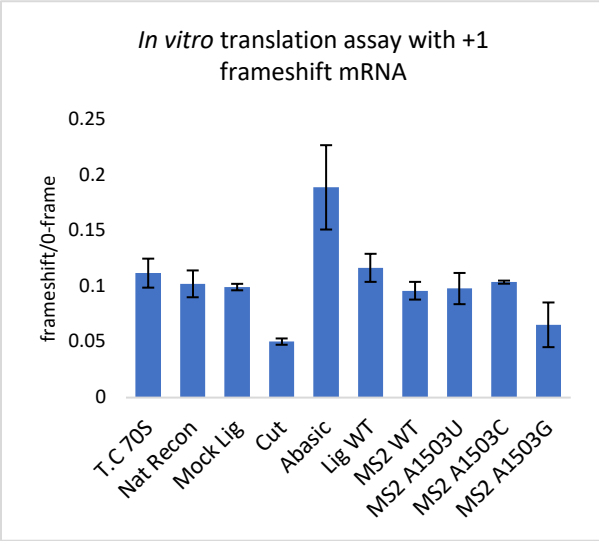

Figure 7. Ribosomes with abasic site at 16S rRNA position 1503 frameshift with high frequency by *in vitro* translation assay. *In vitro* translation assays were visualized by ^{35}S-Met incorporation into either full length or truncated S2 protein product by -1 frameshift mRNA (A), duplexed -1 frameshift mRNA (B) or +1 frameshift mRNA (C) (n=4 for MS2 A1503 mutants; n=8 for all others).

Table 3. Stimulation of -1 Frameshifting by Abasic 1503 Ribosomes [a]

70S Construct	% Frameshift	Frameshift/0-Frame
Tight Coupled	33.8±1.3	0.51±0.03
Natural Reconstituted	36.8±2.7	0.58±0.08
Mock Ligated	35.7±2.2	0.56±0.05
Colicin E3 Cut	27.5±1.8	0.38±0.03
Abasic 1503	55.4±2.4	1.24±0.11
Ligated WT	42.1±0.5	0.73±0.01
MS2 Wild Type	28.3±4.6	0.40±0.11
MS2 A1503U	33.9±6.3	0.53±0.18
MS2 A1503C	27.0±6.1	0.38±0.14
MS2 A1503G	17.8±2.6	0.22±0.07

[a] Efficiencies of -1 frameshifting by each ribosomal construct (Fig. 8A). (% Frameshift) percent of product from -1 frameshift out of total product translated; (Frameshift/0-Frame) ratio of frameshifted product to 0-frame product.

References

ABDI, N.M., and FREDRICK, K. (2005). Contribution of 16S rRNA nucleotides forming the 30S subunit A and P sites to translation in Escherichia coli. RNA *11*, 1624–1632.

Akiyama, B.M., and Stone, M.D. (2009). Chapter 2 - Assembly of Complex RNAs by Splinted Ligation. In Methods in Enzymology, (Academic Press), pp. 27–46.

Baan, R.A., Charldorp, R.V., Leerdam, E.V., Knippenberg, P.H.V., and Bosch, L. (1976). The 3'-terminus of 16 S ribosomal RNA of Escherichia coli. Isolation and purification of the terminal 49-nucleotide fragment at a milligram scale. FEBS Lett. *71*, 351–355.

Baba, T., Ara, T., Hasegawa, M., Takai, Y., Okumura, Y., Baba, M., Datsenko, K.A., Tomita, M., Wanner, B.L., and Mori, H. (2006). Construction of Escherichia coli K-12

in-frame, single-gene knockout mutants: the Keio collection. Mol. Syst. Biol. *2*, 2006.0008.

Baker, K.E., and Parker, R. (2004). Nonsense-mediated mRNA decay: terminating erroneous gene expression. Curr. Opin. Cell Biol. *16*, 293–299.

Bank, R.P.D. RCSB PDB: Policies.

Baranov, P.V., Gesteland, R.F., and Atkins, J.F. (2002). Recoding: translational bifurcations in gene expression. Gene *286*, 187–201.

Belew, A.T., Hepler, N.L., Jacobs, J., and Dinman, J. (2008). PRFdb: A database of computationally predicted eukaryotic programmed -1 ribosomal frameshift signals. BMC Genomics.

Boon, T. (1971a). Inactivation of Ribosomes In Vitro by Colicin E3 and Its Mechanism of Action. 4.

Boon, T. (1971b). Inactivation of Ribosomes In Vitro by Colicin E3. Proc. Natl. Acad. Sci. *68*, 2421–2425.

Bowman, C.M., Dahlberg, J.E., Ikemura, T., Konisky, J., and Nomura, M. (1971). Specific Inactivation of 16S Ribosomal RNA Induced by Colicin E3 In Vivo. Proc. Natl. Acad. Sci. *68*, 964–968.

Brown, R.F., Andrews, C.T., and Elcock, A.H. (2015). Stacking free energies of all DNA and RNA nucleoside pairs and dinucleoside-monophosphates computed using recently revised AMBER parameters and compared with experiment. J. Chem. Theory Comput. *11*, 2315–2328.

Buul, C.P.J.J. van, Visser, W., and Knippenberg, P.H. van (1984). Increased translational fidelity caused by the antibiotic kasugamycin and ribosomal ambiguity in mutants harbouring the ksgA gene. FEBS Lett. *177*, 119–124.

Chang, Y.-F., Imam, J.S., and Wilkinson, M.F. (2007). The Nonsense-Mediated Decay RNA Surveillance Pathway. Annu. Rev. Biochem. *76*, 51–74.

Chen, C., Stevens, B., Kaur, J., Smilansky, Z., Cooperman, B.S., and Goldman, Y.E. (2011). Allosteric vs. spontaneous exit-site (E-site) tRNA dissociation early in protein synthesis. Proc. Natl. Acad. Sci. *108*, 16980–16985.

Chen, G., Chang, K.-Y., Chou, M.-Y., Bustamante, C., and Tinoco, I. (2009). Triplex structures in an RNA pseudoknot enhance mechanical stability and increase efficiency of –1 ribosomal frameshifting. Proc. Natl. Acad. Sci. *106*, 12706–12711.

Chen, J., Petrov, A., Johansson, M., Tsai, A., O'Leary, S.E., and Puglisi, J.D. (2014). Dynamic pathways of −1 translational frameshifting. Nature *512*, 328–332.

Choi, J., and Puglisi, J.D. (2017). Three tRNAs on the ribosome slow translation elongation. Proc. Natl. Acad. Sci. *114*, 13691–13696.

Condon, D.E., Kennedy, S.D., Mort, B.C., Kierzek, R., Yildirim, I., and Turner, D.H. (2015). Stacking in RNA: NMR of Four Tetramers Benchmark Molecular Dynamics. J. Chem. Theory Comput. *11*, 2729–2742.

Connolly, K., Rife, J.P., and Culver, G. (2008). Mechanistic insight into the ribosome biogenesis functions of the ancient protein KsgA. Mol. Microbiol. *70*, 1062–1075.

Craigen, W.J., and Caskey, C.T. (1986). Expression of peptide chain release factor 2 requires high-efficiency frameshift. Nature *322*, 273–275.

Davis, R.C., and Tinoco, I. (1968). Temperature-dependent properties of dinucleoside phosphates. Biopolymers *6*, 223–242.

Demirci, H., Murphy, F., Belardinelli, R., Kelley, A.C., Ramakrishnan, V., Gregory, S.T., Dahlberg, A.E., and Jogl, G. (2010). Modification of 16S ribosomal RNA by the KsgA methyltransferase restructures the 30S subunit to optimize ribosome function. RNA *16*, 2319–2324.

Demo, G., Loveland, A.B., Svidritskiy, E., Gamper, H.B., Hou, Y.-M., and Korostelev, A.A. (2020). Structural basis for +1 ribosomal frameshifting during EF-G-catalyzed translocation. BioRxiv 2020.12.29.424751.

Douthwaite, S., Powers, T., Lee, J.Y., and Noller, H.F. (1989). Defining the structural requirements for a helix in 23 S ribosomal RNA that confers erythromycin resistance. J. Mol. Biol. *209*, 655–665.

Drummond, D.A., and Wilke, C.O. (2008). Mistranslation-Induced Protein Misfolding as a Dominant Constraint on Coding-Sequence Evolution. Cell *134*, 341–352.

Dunkle, J.A., Wang, L., Feldman, M.B., Pulk, A., Chen, V.B., Kapral, G.J., Noeske, J., Richardson, J.S., Blanchard, S.C., and Cate, J.H.D. (2011). Structures of the Bacterial Ribosome in Classical and Hybrid States of tRNA Binding. Science *332*, 981–984.

Fareed, G.C., Wilt, E.M., and Richardson, C.C. (1971). Enzymatic Breakage and Joining of Deoxyribonucleic Acid: VIII. HYBRIDS OF RIBO- AND DEOXYRIBONUCLEOTIDE HOMOPOLYMERS AS SUBSTRATES FOR POLYNUCLEOTIDE LIGASE OF BACTERIOPHAGE T4. J. Biol. Chem. *246*, 925–932.

Flower, A.M., and Mchenry, C.S. (1990). The γ subunit of DNA polymerase III holoenzyme of Escherichia coli is produced by ribosomal frameshifting. 5.

Frilander, M.J., and Steitz, J.A. (2001). Dynamic Exchanges of RNA Interactions Leading to Catalytic Core Formation in the U12-Dependent Spliceosome. Mol. Cell *7*, 217–226.

Golden, B.L., Gooding, A.R., Podell, E.R., and Cech, T.R. (1996). X-ray crystallography of large RNAs: heavy-atom derivatives by RNA engineering. RNA *2*, 1295–1305.

Helser, T.L., Davies, J.E., and Dahlberg, J.E. (1971). Change in Methylation of 16S Ribosomal RNA Associated with Mutation to Kasugamycin Resistance in Escherichia coli. Nature. New Biol. *233*, 12–14.

Helser, T.L., Davies, J.E., and Dahlberg, J.E. (1972). Mechanism of Kasugamycin Resistance in Escherichia coli. Nature. New Biol. *235*, 6–9.

Heus, H.A., and van Knippenberg, P.H. (1988). The 3' terminal colicin fragment of Escherichia coli 16S ribosomal RNA. Conformational details revealed by enzymic and chemical probing. J. Biomol. Struct. Dyn. *5*, 951–963.

Ho, C.K., and Shuman, S. (2002). Bacteriophage T4 RNA ligase 2 (gp24.1) exemplifies a family of RNA ligases found in all phylogenetic domains. Proc. Natl. Acad. Sci. *99*, 12709–12714.

Hong, S., Sunita, S., Maehigashi, T., Hoffer, E.D., Dunkle, J.A., and Dunham, C.M. (2018). Mechanism of tRNA-mediated +1 ribosomal frameshifting. Proc. Natl. Acad. Sci. *115*, 11226–11231.

Huang, C., and Yu, Y.-T. (2013). Synthesis and Labeling of RNA In Vitro. Curr. Protoc. Mol. Biol. Ed. Frederick M Ausubel Al *0 4*, Unit4.15.

Jafilan, S., Klein, L., Hyun, C., and Florián, J. (2012). Intramolecular Base Stacking of Dinucleoside Monophosphate Anions in Aqueous Solution. J. Phys. Chem. B *116*, 3613–3618.

Jenner, L.B., Demeshkina, N., Yusupova, G., and Yusupov, M. (2010). Structural aspects of messenger RNA reading frame maintenance by the ribosome. Nat. Struct. Mol. Biol. *17*, 555–560.

Kershaw, C.J., and O'Keefe, R.T. (2012). Splint ligation of RNA with T4 DNA ligase. Methods Mol. Biol. Clifton NJ *941*, 257–269.

Kibbe, W.A. (2007). OligoCalc: an online oligonucleotide properties calculator. Nucleic Acids Res. *35*, W43–W46.

Kim, H.-K., Liu, F., Fei, J., Bustamante, C., Gonzalez, R.L., and Tinoco, I. (2014). A frameshifting stimulatory stem loop destabilizes the hybrid state and impedes ribosomal translocation. Proc. Natl. Acad. Sci. U. S. A. *111*, 5538–5543.

Kleppe, K., Sande, J.H. van de, and Khorana, H.G. (1970). Polynucleotide Ligase-Catalyzed Joining of Deoxyribo-oligonucleotides on Ribopolynucleotide Templates and of Ribo-oligonucleotides on Deoxyribopolynucleotide Templates. Proc. Natl. Acad. Sci. *67*, 68–73.

Korostelev, A., Asahara, H., Lancaster, L., Laurberg, M., Hirschi, A., Zhu, J., Trakhanov, S., Scott, W.G., and Noller, H.F. (2008). Crystal structure of a translation termination complex formed with release factor RF2. Proc. Natl. Acad. Sci. *105*, 19684–19689.

Kunkel, T.A. (1985). Rapid and efficient site-specific mutagenesis without phenotypic selection. Proc. Natl. Acad. Sci. *82*, 488–492.

Kurland, C.G. (1992). Translational Accuracy and the Fitness of Bacteria. Annu. Rev. Genet. *26*, 29–50.

Labuda, D., Grosjean, H., Striker, G., and Pörschke, D. (1982). Codon:Anticodon and anticodon:Anticodon interaction. Evaluation of equilibrium and kinetic parameters of complexes involving a G:U wobble. Biochim. Biophys. Acta BBA - Gene Struct. Expr. *698*, 230–236.

Lancaster, L., and Noller, H.F. (2005). Involvement of 16S rRNA Nucleotides G1338 and A1339 in Discrimination of Initiator tRNA. Mol. Cell *20*, 623–632.

Larsen, B., Gesteland, R.F., and Atkins, J.F. (1997). Structural probing and mutagenic analysis of the stem-loop required for Escherichia coli dnaX ribosomal frameshifting: programmed efficiency of 50%11Edited By D. E. Draper. J. Mol. Biol. *271*, 47–60.

Li, Z., Stahl, G., and Farabaugh, P.J. (2001). Programmed +1 frameshifting stimulated by complementarity between a downstream mRNA sequence and an error-correcting region of rRNA. RNA *7*, 275–284.

Lingner, J., and Cech, T.R. (1996). Purification of telomerase from Euplotes aediculatus: requirement of a primer 3’ overhang. Proc. Natl. Acad. Sci. *93*, 10712–10717.

Matsufuji, S., Matsufuji, T., Wills, N.M., Gesteland, R.F., and Atkins, J.F. (1996). Reading two bases twice: mammalian antizyme frameshifting in yeast. EMBO J. *15*, 1360.

Moazed, D., and Noller, H. (1989a). Interaction of tRNA with 23S rRNA in the ribosomal A, P, and E sites. Cell.

Moazed, D., and Noller, H.F. (1989b). Intermediate states in the movement of transfer RNA in the ribosome. Nature *342*, 142–148.

Mohan, S., Donohue, J.P., and Noller, H.F. (2014). Molecular mechanics of 30S subunit head rotation. Proc. Natl. Acad. Sci. *111*, 13325–13330.

Moore, M.J., and Query, C.C. (2000). [7] Joining of RNAs by splinted ligation. In Methods in Enzymology, (Academic Press), pp. 109–123.

Moore, M.J., and Sharp, P.A. (1992). Site-specific modification of pre-mRNA: the 2’-hydroxyl groups at the splice sites. Science *256*, 992–997.

Namy, O., Rousset, J.-P., Napthine, S., and Brierley, I. (2004). Reprogrammed Genetic Decoding in Cellular Gene Expression. Mol. Cell *13*, 157–168.

Nandakumar, J., Ho, C.K., Lima, C.D., and Shuman, S. (2004). RNA Substrate Specificity and Structure-guided Mutational Analysis of Bacteriophage T4 RNA Ligase 2 *. J. Biol. Chem. *279*, 31337–31347.

Niblett, D., Nelson, C., Leung, C.S., Rexroad, G., Cozy, J., Zhou, J., Lancaster, L., and Noller, H.F. (2021). Mutations in domain IV of elongation factor EF-G confer −1 frameshifting. RNA *27*, 40–53.

Noller, H.F., Donohue, J.P., and Gutell, R.R. (2022). The universally conserved nucleotides of the small subunit ribosomal RNAs. RNA *28*, 623–644.

Norberg, J., and Nilsson, L. (1995). Stacking Free Energy Profiles for All 16 Natural Ribodinucleoside Monophosphates in Aqueous Solution. J. Am. Chem. Soc. *117*, 10832–10840.

O'Farrell, H.C., Pulicherla, N., Desai, P.M., and Rife, J.P. (2006). Recognition of a complex substrate by the KsgA/Dim1 family of enzymes has been conserved throughout evolution. RNA *12*, 725–733.

Peng, B.-Z., Bock, L.V., Belardinelli, R., Peske, F., Grubmüller, H., and Rodnina, M.V. (2019). Active role of elongation factor G in maintaining the mRNA reading frame during translation. Sci. Adv. *5*, eaax8030.

Poldermans, B., Bakker, H., and Van Knippenberg, P.H. (1980). Studies on the function of two adjacent N6,N6-dimethyladenosines near the 3' end of 16S ribosomal RNA of Escherichia coli. IV. The effect of the methylgroups on ribosomal subunit interaction. Nucleic Acids Res. *8*, 143–151.

Qin, P., Yu, D., Zuo, X., and Cornish, P.V. (2014). Structured mRNA induces the ribosome into a hyper-rotated state. EMBO Rep. *15*, 185–190.

Ritchie, D.B., Foster, D.A.N., and Woodside, M.T. (2012). Programmed −1 frameshifting efficiency correlates with RNA pseudoknot conformational plasticity, not resistance to mechanical unfolding. Proc. Natl. Acad. Sci. U. S. A. *109*, 16167–16172.

Sanders, C.L., and Curran, J.F. (2007). Genetic analysis of the E site during RF2 programmed frameshifting. RNA *13*, 1483–1491.

Sauert, M., Temmel, H., and Moll, I. (2015). Heterogeneity of the translational machinery: Variations on a common theme. Biochimie *114*, 39–47.

Savelsbergh, A., Katunin, V.I., Mohr, D., Peske, F., Rodnina, M.V., and Wintermeyer, W. (2003). An Elongation Factor G-Induced Ribosome Rearrangement Precedes tRNA-mRNA Translocation. Mol. Cell *11*, 1517–1523.

Schluenzen, F., Takemoto, C., Wilson, D.N., Kaminishi, T., Harms, J.M., Hanawa-Suetsugu, K., Szaflarski, W., Kawazoe, M., Shirouzu, M., Nierhaus, K.H., et al. (2006). The antibiotic kasugamycin mimics mRNA nucleotides to destabilize tRNA binding and inhibit canonical translation initiation. Nat. Struct. Mol. Biol. *13*, 871–878.

Schürer, H., Lang, K., Schuster, J., and Mörl, M. (2002). A universal method to produce in vitro transcripts with homogeneous 3' ends. Nucleic Acids Res. *30*, e56.

Schuwirth, B.S., Day, J.M., Hau, C.W., Janssen, G.R., Dahlberg, A.E., Cate, J.H.D., and Vila-Sanjurjo, A. (2006). Structural analysis of kasugamycin inhibition of translation. Nat. Struct. Mol. Biol. *13*, 879–886.

Senior, B.W., and Holland, I.B. (1971). Effect of Colicin E3 upon the 30S Ribosomal Subunit of Escherichia coli. Proc. Natl. Acad. Sci. U. S. A. *68*, 959–963.

Šponer, J., E. Riley, K., and Hobza, P. (2008). Nature and magnitude of aromatic stacking of nucleic acid bases. Phys. Chem. Chem. Phys. *10*, 2595–2610.

Stark, M.R., Pleiss, J.A., Deras, M., Scaringe, S.A., and Rader, S.D. (2006). An RNA ligase-mediated method for the efficient creation of large, synthetic RNAs. RNA *12*, 2014–2019.

Stephan, N.C., Ries, A.B., Boehringer, D., and Ban, N. (2021). Structural basis of successive adenosine modifications by the conserved ribosomal methyltransferase KsgA. Nucleic Acids Res. *49*, 6389–6398.

Stochmanski, S.J., Therrien, M., Laganière, J., Rochefort, D., Laurent, S., Karemera, L., Gaudet, R., Vyboh, K., Van Meyel, D.J., Di Cristo, G., et al. (2012). Expanded ATXN3 frameshifting events are toxic in Drosophila and mammalian neuron models. Hum. Mol. Genet. *21*, 2211–2218.

Thammana, P., and Held, W.A. (1974). Methylation of 16S RNA during ribosome assembly in vitro. Nature *251*, 682–686.

Tinoco Jr., I., Kim, H.-K., and Yan, S. (2013). Frameshifting dynamics. Biopolymers *99*, 1147–1166.

Traub, P., and Nomura, M. (1968). Structure and function of E. coli ribosomes. V. Reconstitution of functionally active 30S ribosomal particles from RNA and proteins. Proc. Natl. Acad. Sci. U. S. A. *59*, 777–784.

Traub, P., and Nomura, M. (1969). Structure and function of Escherichia coli ribosomes: VI. Mechanism of assembly of 30 s ribosomes studied in vitro. J. Mol. Biol. *40*, 391–413.

Traub, P., Mizushima, S., Lowry, C.V., and Nomura, M. (1971a). [41] Reconstitution of ribosomes from subribosomal components. In Methods in Enzymology, (Academic Press), pp. 391–407.

Traub, P., Mizushima, S., Lowry, C.V., and Nomura, M. (1971b). [41] Reconstitution of ribosomes from subribosomal components. In Methods in Enzymology, (Academic Press), pp. 391–407.

Turner, D.H. (1996). Thermodynamics of base pairing. Curr. Opin. Struct. Biol. *6*, 299–304.

Uemura, S., Aitken, C.E., Korlach, J., Flusberg, B.A., Turner, S.W., and Puglisi, J.D. (2010). Real-time tRNA transit on single translating ribosomes at codon resolution. Nature *464*, 1012–1017.

Van Charldorp, R., Heus, H.A., and Van Knippenberg, P.H. (1981). Adenosine dimethylation of 16S ribosomal RNA: effect of the methylgroups on local conformational stability as deduced from electrophoretic mobility of RNA fragments in denaturing polyacrylamide gels. Nucleic Acids Res. *9*, 267–275.

Varshney, U., Lee, C.P., and RajBhandary, U.L. (1991). Direct analysis of aminoacylation levels of tRNAs in vivo. Application to studying recognition of Escherichia coli initiator tRNA mutants by glutaminyl-tRNA synthetase. J. Biol. Chem. *266*, 24712–24718.

Walter, A.E., and Turner, D.H. (1994). Sequence dependence of stability for coaxial stacking of RNA helixes with Watson-Crick base paired interfaces. Biochemistry *33*, 12715–12719.

Watson, Z.L., Ward, F.R., Méheust, R., Ad, O., Schepartz, A., Banfield, J.F., and Cate, J.H. (2020). Structure of the bacterial ribosome at 2 Å resolution. ELife *9*.

Wills, N.M., and Atkins, J.F. (2006). The potential role of ribosomal frameshifting in generating aberrant proteins implicated in neurodegenerative diseases. RNA *12*, 1149–1153.

Zhou, J., Lancaster, L., Donohue, J.P., and Noller, H.F. (2013). Crystal Structures of EF-G-Ribosome Complexes Trapped in Intermediate States of Translocation. Science *340*, 1236086–1236086.

Zhou, J., Lancaster, L., Donohue, J.P., and Noller, H.F. (2019). Spontaneous ribosomal translocation of mRNA and tRNAs into a chimeric hybrid state. Proc. Natl. Acad. Sci. *116*, 7813–7818.

CHAPTER III

Role of universally conserved dimethyl adenosines near 3' end of 16S rRNA in translational fidelity

Abstract

Through *in vitro* translation with a slippery sequence mRNA, we have confirmed a role for the universally conserved dimethyl adenosines A1518 and A1519 of the 16S rRNA. This came as an extension to our abasic 1503 project due to an unexpected increase in frameshifting with our ligated synthetic wild-type control. Here, we express and purify ribosomes lacking dimethylation at A1518 and A1519 as well as the methyltransferase responsible for the modifications. We explore the effects of these methylations in ribosomal frameshifting to find that the 3' end of 16S rRNA contributes to reading frame maintenance of the P and E site mRNA.

Introduction

The universally conserved N6, N6-dimethyladenosines, A1518 and A1519, of the small subunit 16S ribosomal RNA (rRNA) have several known functions. These modifications serve as a marker in 16S rRNA regulation, maturation and biogenesis (Poldermans et al., 1980; Connolly et al., 2008). Dimethylation at these sites also assists in structural rearrangement of the

16S rRNA 3'-end stabilizing secondary and tertiary interactions of helices 44 and 45 (Van Charldorp et al., 1981; Demirci et al., 2010). It was established early on that methylation of both bases is catalyzed by a single methyltransferase, KsgA, at a late stage of 30S subunit assembly (Thammana and Held, 1974) and that bacteria resistant to the antibiotic kasugamycin lack dimethylation of the two conserved adenosines (KsgA mutants or knockouts) (Helser et al., 1971, 1972). However, there have been indications that dimethylation of A1518 and A1519 play a role in translational fidelity as well. Since *ksgA* mutants display an increased leakiness in nonsense and frameshift mutations *in vitro* it has been proposed that submethylation of A1518 and A1519 are likely factors in mistranslation (Buul et al., 1984) however these errors may be attributed to non-AUG initiation (O'Conner 1997).

We found that ribosomes lacking dimethylation at A1518 and A1519 of 16S rRNA showed slightly increased levels of frameshifting *in vitro*. First, we noticed this result in ribosomes containing 16S rRNA constructed by ligation with a synthetic RNA oligonucleotide bearing wild type sequence but missing these conserved modifications. We later confirmed that the lack of methylation was causing this slightly heightened frameshifting by comparing to ribosomes purified from a *ksgA* knockout strain. What potential role could these highly conserved modifications be playing with respect to reading frame maintenance?

Submethylation of A1518 and A1519 allows for resistance to kasugamycin (Ksg) (Helser et al., 1971, 1972) though binding of the antibiotic is not inhibited (Schuwirth et al., 2006). Instead, resistance to Ksg is linked to the structure of the mRNA at the junction P and E sites. Since Ksg binds to the mRNA tunnel mimicking nucleotides in the P and E sites (Schluenzen et al., 2006), we can tie the mechanism of binding to A1518 and A1519 modification. A1518 and A1519, or more specifically dimethylation at these sites, play a role in stabilizing Ksg binding and since Ksg mimics mRNA nucleotides between the P and E site there could be a role for stabilizing mRNA as well. To confirm that lack of methylation is responsible for the increased frameshifting seen in our synthetic wild-type control, we tested demethylated ribosomes from a *ksgA* knockout (ΔKsgA) strain *in vitro* and validated early accounts that these conserved modifications play a role in reading frame maintenance.

Results

Demethylated ribosomes confer weak increase in frameshifting

Ribosomes with demethylated 16S rRNA A1518 and A1519 were purified from a *ksgA* deletion strain (ΔKsgA) (Connolly et al., 2008) and confirmed by primer extension of the 16S rRNA 3'-end (see methods; Fig. 1, A). We also used 70S that was reconstituted with 16S rRNA constructed by ligation of a truncated natural 16S and a synthetic RNA which lacked

modification on the 3'-end. We then used *in vitro* translation of an mRNA bearing a slippery sequence (Niblett et al., 2021) to accurately measure the frequency of frameshifting. We found that ribosomes carrying 16S rRNA with demethylated A1518 and A1519, from ΔKsgA as well as the ligation reconstitution construct, showed a nearly 2-fold increase in frameshifting compared to tight coupled 70S (Fig. 1). Once methylated *in vitro* by purified KsgA methyltransferase, (see methods) the levels of frameshifting were rescued to levels that were indistinguishable from tight coupled (Fig. 2).

Discussion

Do universally conserved N6, N6-dimethyladenosines play a role in mRNA reading frame maintenance?

Using our synthetic ligation construct and KsgA knockout purified ribosomes, we saw that lack of methylation at A1518 and A1519 leads to slightly increased frameshifting *in vitro.* In order to build a model for A1518 and A1519 methylation in reading frame fidelity, we looked to previous work with kasugamycin binding. Structural studies have shown that the drug mimics mRNA nucleotides between the P and E sites (Schluenzen et al., 2006; Schuwirth et al., 2006). Since methylation of A1518 and A1519 play a role in the stability of Ksg binding in the mRNA tunnel, it's possible that a similar role is carried out for mRNA nucleotides—that is A1518 and A1519

stabilize mRNA near the P and E sites by controlling the width and rigidity of the mRNA tunnel.

There is a network of 16S rRNA interactions forming the mRNA tunnel between the P and E sites which control the width and rigidity of the tunnel for kasugamycin binding (Schuwirth et al., 2006). In this network, we propose the dimethylation of A1518 an A1519 contributes to proper stacking of 16S rRNA nucleotides surrounding the P and E site. The width and rigidity of the mRNA tunnel may help regulated mRNA processing near the P and E site, assisting in important interactions for reading frame maintenance.

Materials and methods

Purification of demethylated A1518 and A1519 ribosomes

Demethylated ribosomes were purified using established techniques (Moazed and Noller, 1989a) from ΔKsgA BW25113 cells originally constructed in the Keio Collection but acquired from the lab of Gloria Culver (Baba et al., 2006; Connolly et al., 2008). See chapter 4 for preparation of synthetic ligation construct methods.

Purification of KsgA methyltransferase

The histidine tagged KsgA methyltransferase was purified using methods based on previous work with some modification (O'Farrell et al., 2006; Stephan et al., 2021). E.coli BL21 cell cultures carrying pBAD-ksgA

plasmid were grown to an OD600 of 0.6 in the presence of ampicillin and induced with 2 mM Arabinose (Sigma-Aldrich). Cells were pelleted by centrifugation and lysed by french press at 18,000 psi, one pass in lysis buffer (50mM Tris-HCl pH 7.5, 300mM NaCl, 20mM imidazole pH 7.5, 10% glycerol and 6mM β-mercaptoethanol). Cleared lysate was bound to 2mL equilibrated Ni-NTA Agarose resin (Qiagen) by rotating at 4°C for one hour in lysis buffer. The bound resin was then washed 4 times with 10mLlysis buffer and histidine tagged KsgA was eluted by addition of 8mL elution buffer (50mM Tris-HCl pH 7.5, 50mM NaCl, 250mM imidazole pH 7.5, 10% glycerol and 6mM β-mercaptoethanol) collecting elution fractions in 2mL volumes. Fractions were combined and dialyzed in 10kDa molecular cutoff dialysis tubing overnight at 4°C in 1L buffer (50mM Tris-HCl pH 7.5, 400mM NaCl, 10% glycerol and 6mM β-mercaptoethanol) for storage.

Methylation of A1518 and A1519 *in vitro*

Demethylated 30S subunits were extracted from 70S particles purified previously from a KsgA deletion strain. Subunits were methylated *in vitro* using protocols established previously (O'Farrell et al., 2006) with minor changes. We used a final concentration of 20 μM KsgA methyltransferase to 2μM demethylated 30S (10-fold excess of enzyme) in a final buffer containing 40mM Tris-HCl pH 7.5, 40mM NH4Cl, 4mM MgCl2, 6mM β-mercaptoethanol and 0.2mM methyl-SAM (Sigma-Aldrich). We found that the reaction

completed after incubation at 37° for 2 hours. Methylated 30S subunits were then associated with natural 50S subunits and purified by ultracentrifugation through a 10%-35% sucrose gradient in buffer containing 25mM Tris-HCl pH 7.5, 100mM NH4Cl, 15mM MgCl2, 6mM β-mercaptoethanol.

Primer extension assay

Primer extension of the 16S 3' end was used to detect presence of methylation at A1518 and A1519. A DNA oligonucleotide was designed to anneal to the 3' end of 16S rRNA for extension: Primer DNA: 5'-TAAGGAGGTGATCCAACCGC -3'. The primer DNA was radiolabeled on the 5' end with [32]-P using polynucleotide kinase (NEB 10,000u/mL) and [g-32]-ATP for visualization on a gel. We annealed 0.3pmol of radioactively labeled DNA primer to 6pmol 16S rRNA extracted by phenol and chloroform in 10μL with a final buffer of 25mM Tris-HCl pH 7.5, 50mM KCl. We annealed in a 90°C water bath for 1 minute, followed by a slow cooling step to 47°C. Next, the primer was extended in a reaction mixture containing 0.4mM dNTPs (Thermo Scientific) and AMV reverse transcriptase (NEB) in buffer containing 25mM Tris-HCl pH 8.5, 10mM MgCL2, and 10mM DTT. We allowed the extension reaction to proceed at 42°C for 20 minutes. Samples were then precipitated with 84mM NaOAC pH 5.3 and 70% ethanol for resuspension in water. Primer extension gel consisted of 10% acrylamide and 7M Urea in 30cm plates and 1mm spacers, electrophoresis took place at 25watts for 30 minutes and the gel was dried at 80°C under vacuum for 30 minutes prior to

exposure to (screen) overnight. Gel was imaged using typhoon scanner and Image J processing.

In vitro translation assay

See material and methods section of chapter 2, assays in this section were completed with the same methods.

Tables and Figures

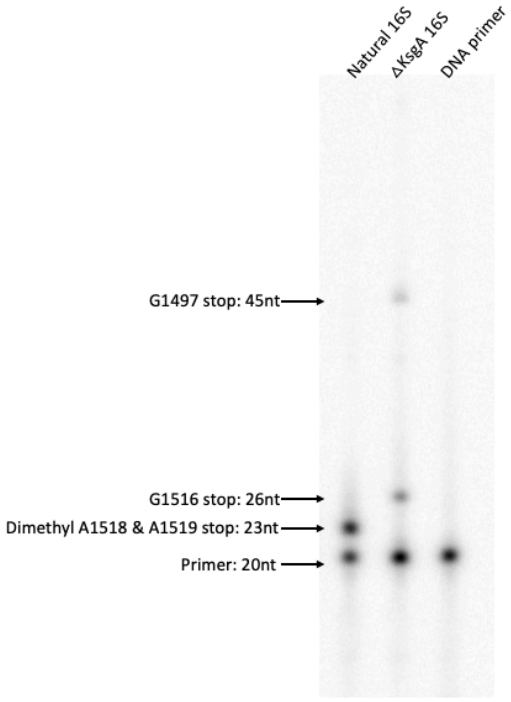

Figure 1. Primer extension of 16S 3' end confirms submethylation of A1518 and A1519. Since reverse transcriptase cannot process past dimethylation of a nucleotide, we see bands corresponding to extension products up until the reverse transcriptase encounters a modification creating a 'stop'. Natural 16S rRNA shows a hard stop with a 23-nucleotide extension

product indicating the presence of dimethylation at A1519 and A1518. In the ΔKsgA 16S rRNA lane, we see that this band is missing, indicating the lack of methylation at this site. Instead, we see extension of the primer until the reverse transcriptase encounters soft stops at known methylation sites, G1516 and G1497.

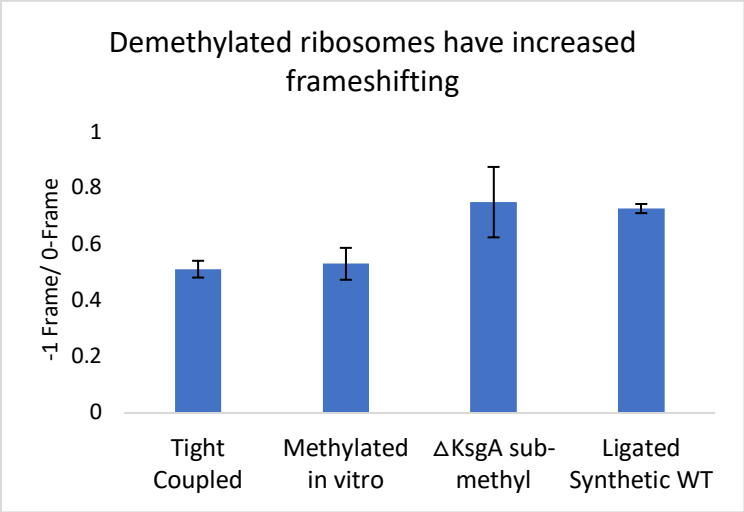

Figure 2. *In vitro* translation assay shows demethylated ribosomes have increased rates of frameshifting. *In vitro* translation activity was determined by ^{35}S-Met incorporation into either full length or truncated S2 protein product by -1 frameshift mRNA as in chapter 2 (n=5 for Methylated in vitro and ΔKsgA sub-methyl samples; n=8 for Tight Coupled and Ligated Synthetic WT samples)).

References

ABDI, N.M., and FREDRICK, K. (2005). Contribution of 16S rRNA nucleotides forming the 30S subunit A and P sites to translation in Escherichia coli. RNA *11*, 1624–1632.

Akiyama, B.M., and Stone, M.D. (2009). Chapter 2 - Assembly of Complex RNAs by Splinted Ligation. In Methods in Enzymology, (Academic Press), pp. 27–46.

Baan, R.A., Charldorp, R.V., Leerdam, E.V., Knippenberg, P.H.V., and Bosch, L. (1976). The 3'-terminus of 16 S ribosomal RNA of Escherichia coli. Isolation and purification of the terminal 49-nucleotide fragment at a milligram scale. FEBS Lett. *71*, 351–355.

Baba, T., Ara, T., Hasegawa, M., Takai, Y., Okumura, Y., Baba, M., Datsenko, K.A., Tomita, M., Wanner, B.L., and Mori, H. (2006). Construction of Escherichia coli K-12 in-frame, single-gene knockout mutants: the Keio collection. Mol. Syst. Biol. *2*, 2006.0008.

Baker, K.E., and Parker, R. (2004). Nonsense-mediated mRNA decay: terminating erroneous gene expression. Curr. Opin. Cell Biol. *16*, 293–299.

Bank, R.P.D. RCSB PDB: Policies.

Baranov, P.V., Gesteland, R.F., and Atkins, J.F. (2002). Recoding: translational bifurcations in gene expression. Gene *286*, 187–201.

Belew, A.T., Hepler, N.L., Jacobs, J., and Dinman, J. (2008). PRFdb: A database of computationally predicted eukaryotic programmed -1 ribosomal frameshift signals. BMC Genomics.

Boon, T. (1971a). Inactivation of Ribosomes In Vitro by Colicin E3 and Its Mechanism of Action. 4.

Boon, T. (1971b). Inactivation of Ribosomes In Vitro by Colicin E3. Proc. Natl. Acad. Sci. *68*, 2421–2425.

Bowman, C.M., Dahlberg, J.E., Ikemura, T., Konisky, J., and Nomura, M. (1971). Specific Inactivation of 16S Ribosomal RNA Induced by Colicin E3 In Vivo. Proc. Natl. Acad. Sci. *68*, 964–968.

Brown, R.F., Andrews, C.T., and Elcock, A.H. (2015). Stacking free energies of all DNA and RNA nucleoside pairs and dinucleoside-monophosphates computed using

recently revised AMBER parameters and compared with experiment. J. Chem. Theory Comput. *11*, 2315–2328.

Buul, C.P.J.J. van, Visser, W., and Knippenberg, P.H. van (1984). Increased translational fidelity caused by the antibiotic kasugamycin and ribosomal ambiguity in mutants harbouring the ksgA gene. FEBS Lett. *177*, 119–124.

Chang, Y.-F., Imam, J.S., and Wilkinson, M.F. (2007). The Nonsense-Mediated Decay RNA Surveillance Pathway. Annu. Rev. Biochem. *76*, 51–74.

Chen, C., Stevens, B., Kaur, J., Smilansky, Z., Cooperman, B.S., and Goldman, Y.E. (2011). Allosteric vs. spontaneous exit-site (E-site) tRNA dissociation early in protein synthesis. Proc. Natl. Acad. Sci. *108*, 16980–16985.

Chen, G., Chang, K.-Y., Chou, M.-Y., Bustamante, C., and Tinoco, I. (2009). Triplex structures in an RNA pseudoknot enhance mechanical stability and increase efficiency of –1 ribosomal frameshifting. Proc. Natl. Acad. Sci. *106*, 12706–12711.

Chen, J., Petrov, A., Johansson, M., Tsai, A., O'Leary, S.E., and Puglisi, J.D. (2014). Dynamic pathways of −1 translational frameshifting. Nature *512*, 328–332.

Choi, J., and Puglisi, J.D. (2017). Three tRNAs on the ribosome slow translation elongation. Proc. Natl. Acad. Sci. *114*, 13691–13696.

Condon, D.E., Kennedy, S.D., Mort, B.C., Kierzek, R., Yildirim, I., and Turner, D.H. (2015). Stacking in RNA: NMR of Four Tetramers Benchmark Molecular Dynamics. J. Chem. Theory Comput. *11*, 2729–2742.

Connolly, K., Rife, J.P., and Culver, G. (2008). Mechanistic insight into the ribosome biogenesis functions of the ancient protein KsgA. Mol. Microbiol. *70*, 1062–1075.

Craigen, W.J., and Caskey, C.T. (1986). Expression of peptide chain release factor 2 requires high-efficiency frameshift. Nature *322*, 273–275.

Davis, R.C., and Tinoco, I. (1968). Temperature-dependent properties of dinucleoside phosphates. Biopolymers *6*, 223–242.

Demirci, H., Murphy, F., Belardinelli, R., Kelley, A.C., Ramakrishnan, V., Gregory, S.T., Dahlberg, A.E., and Jogl, G. (2010). Modification of 16S ribosomal RNA by the KsgA methyltransferase restructures the 30S subunit to optimize ribosome function. RNA *16*, 2319–2324.

Demo, G., Loveland, A.B., Svidritskiy, E., Gamper, H.B., Hou, Y.-M., and Korostelev, A.A. (2020). Structural basis for +1 ribosomal frameshifting during EF-G-catalyzed translocation. BioRxiv 2020.12.29.424751.

Douthwaite, S., Powers, T., Lee, J.Y., and Noller, H.F. (1989). Defining the structural requirements for a helix in 23 S ribosomal RNA that confers erythromycin resistance. J. Mol. Biol. *209*, 655–665.

Drummond, D.A., and Wilke, C.O. (2008). Mistranslation-Induced Protein Misfolding as a Dominant Constraint on Coding-Sequence Evolution. Cell *134*, 341–352.

Dunkle, J.A., Wang, L., Feldman, M.B., Pulk, A., Chen, V.B., Kapral, G.J., Noeske, J., Richardson, J.S., Blanchard, S.C., and Cate, J.H.D. (2011). Structures of the Bacterial Ribosome in Classical and Hybrid States of tRNA Binding. Science *332*, 981–984.

Fareed, G.C., Wilt, E.M., and Richardson, C.C. (1971). Enzymatic Breakage and Joining of Deoxyribonucleic Acid: VIII. HYBRIDS OF RIBO- AND DEOXYRIBONUCLEOTIDE HOMOPOLYMERS AS SUBSTRATES FOR POLYNUCLEOTIDE LIGASE OF BACTERIOPHAGE T4. J. Biol. Chem. *246*, 925–932.

Flower, A.M., and Mchenry, C.S. (1990). The γ subunit of DNA polymerase III holoenzyme of Escherichia coli is produced by ribosomal frameshifting. 5.

Frilander, M.J., and Steitz, J.A. (2001). Dynamic Exchanges of RNA Interactions Leading to Catalytic Core Formation in the U12-Dependent Spliceosome. Mol. Cell *7*, 217–226.

Golden, B.L., Gooding, A.R., Podell, E.R., and Cech, T.R. (1996). X-ray crystallography of large RNAs: heavy-atom derivatives by RNA engineering. RNA *2*, 1295–1305.

Helser, T.L., Davies, J.E., and Dahlberg, J.E. (1971). Change in Methylation of 16S Ribosomal RNA Associated with Mutation to Kasugamycin Resistance in Escherichia coli. Nature. New Biol. *233*, 12–14.

Helser, T.L., Davies, J.E., and Dahlberg, J.E. (1972). Mechanism of Kasugamycin Resistance in Escherichia coli. Nature. New Biol. *235*, 6–9.

Heus, H.A., and van Knippenberg, P.H. (1988). The 3’ terminal colicin fragment of Escherichia coli 16S ribosomal RNA. Conformational details revealed by enzymic and chemical probing. J. Biomol. Struct. Dyn. *5*, 951–963.

Ho, C.K., and Shuman, S. (2002). Bacteriophage T4 RNA ligase 2 (gp24.1) exemplifies a family of RNA ligases found in all phylogenetic domains. Proc. Natl. Acad. Sci. *99*, 12709–12714.

Hong, S., Sunita, S., Maehigashi, T., Hoffer, E.D., Dunkle, J.A., and Dunham, C.M. (2018). Mechanism of tRNA-mediated +1 ribosomal frameshifting. Proc. Natl. Acad. Sci. *115*, 11226–11231.

Huang, C., and Yu, Y.-T. (2013). Synthesis and Labeling of RNA In Vitro. Curr. Protoc. Mol. Biol. Ed. Frederick M Ausubel Al *0 4*, Unit4.15.

Jafilan, S., Klein, L., Hyun, C., and Florián, J. (2012). Intramolecular Base Stacking of Dinucleoside Monophosphate Anions in Aqueous Solution. J. Phys. Chem. B *116*, 3613–3618.

Jenner, L.B., Demeshkina, N., Yusupova, G., and Yusupov, M. (2010). Structural aspects of messenger RNA reading frame maintenance by the ribosome. Nat. Struct. Mol. Biol. *17*, 555–560.

Kershaw, C.J., and O'Keefe, R.T. (2012). Splint ligation of RNA with T4 DNA ligase. Methods Mol. Biol. Clifton NJ *941*, 257–269.

Kibbe, W.A. (2007). OligoCalc: an online oligonucleotide properties calculator. Nucleic Acids Res. *35*, W43–W46.

Kim, H.-K., Liu, F., Fei, J., Bustamante, C., Gonzalez, R.L., and Tinoco, I. (2014). A frameshifting stimulatory stem loop destabilizes the hybrid state and impedes ribosomal translocation. Proc. Natl. Acad. Sci. U. S. A. *111*, 5538–5543.

Kleppe, K., Sande, J.H. van de, and Khorana, H.G. (1970). Polynucleotide Ligase-Catalyzed Joining of Deoxyribo-oligonucleotides on Ribopolynucleotide Templates and of Ribo-oligonucleotides on Deoxyribopolynucleotide Templates. Proc. Natl. Acad. Sci. *67*, 68–73.

Korostelev, A., Asahara, H., Lancaster, L., Laurberg, M., Hirschi, A., Zhu, J., Trakhanov, S., Scott, W.G., and Noller, H.F. (2008). Crystal structure of a translation termination complex formed with release factor RF2. Proc. Natl. Acad. Sci. *105*, 19684–19689.

Kunkel, T.A. (1985). Rapid and efficient site-specific mutagenesis without phenotypic selection. Proc. Natl. Acad. Sci. *82*, 488–492.

Kurland, C.G. (1992). Translational Accuracy and the Fitness of Bacteria. Annu. Rev. Genet. *26*, 29–50.

Labuda, D., Grosjean, H., Striker, G., and Pörschke, D. (1982). Codon:Anticodon and anticodon:Anticodon interaction. Evaluation of equilibrium and kinetic parameters of complexes involving a G:U wobble. Biochim. Biophys. Acta BBA - Gene Struct. Expr. *698*, 230–236.

Lancaster, L., and Noller, H.F. (2005). Involvement of 16S rRNA Nucleotides G1338 and A1339 in Discrimination of Initiator tRNA. Mol. Cell *20*, 623–632.

Larsen, B., Gesteland, R.F., and Atkins, J.F. (1997). Structural probing and mutagenic analysis of the stem-loop required for Escherichia coli dnaX ribosomal frameshifting: programmed efficiency of 50%11Edited By D. E. Draper. J. Mol. Biol. *271*, 47–60.

Li, Z., Stahl, G., and Farabaugh, P.J. (2001). Programmed +1 frameshifting stimulated by complementarity between a downstream mRNA sequence and an error-correcting region of rRNA. RNA *7*, 275–284.

Lingner, J., and Cech, T.R. (1996). Purification of telomerase from Euplotes aediculatus: requirement of a primer 3’ overhang. Proc. Natl. Acad. Sci. *93*, 10712–10717.

Matsufuji, S., Matsufuji, T., Wills, N.M., Gesteland, R.F., and Atkins, J.F. (1996). Reading two bases twice: mammalian antizyme frameshifting in yeast. EMBO J. *15*, 1360.

Moazed, D., and Noller, H. (1989a). Interaction of tRNA with 23S rRNA in the ribosomal A, P, and E sites. Cell.

Moazed, D., and Noller, H.F. (1989b). Intermediate states in the movement of transfer RNA in the ribosome. Nature *342*, 142–148.

Mohan, S., Donohue, J.P., and Noller, H.F. (2014). Molecular mechanics of 30S subunit head rotation. Proc. Natl. Acad. Sci. *111*, 13325–13330.

Moore, M.J., and Query, C.C. (2000). [7] Joining of RNAs by splinted ligation. In Methods in Enzymology, (Academic Press), pp. 109–123.

Moore, M.J., and Sharp, P.A. (1992). Site-specific modification of pre-mRNA: the 2’-hydroxyl groups at the splice sites. Science *256*, 992–997.

Namy, O., Rousset, J.-P., Napthine, S., and Brierley, I. (2004). Reprogrammed Genetic Decoding in Cellular Gene Expression. Mol. Cell *13*, 157–168.

Nandakumar, J., Ho, C.K., Lima, C.D., and Shuman, S. (2004). RNA Substrate Specificity and Structure-guided Mutational Analysis of Bacteriophage T4 RNA Ligase 2 *. J. Biol. Chem. *279*, 31337–31347.

Niblett, D., Nelson, C., Leung, C.S., Rexroad, G., Cozy, J., Zhou, J., Lancaster, L., and Noller, H.F. (2021). Mutations in domain IV of elongation factor EF-G confer −1 frameshifting. RNA *27*, 40–53.

Noller, H.F., Donohue, J.P., and Gutell, R.R. (2022). The universally conserved nucleotides of the small subunit ribosomal RNAs. RNA *28*, 623–644.

Norberg, J., and Nilsson, L. (1995). Stacking Free Energy Profiles for All 16 Natural Ribodinucleoside Monophosphates in Aqueous Solution. J. Am. Chem. Soc. *117*, 10832–10840.

O'Farrell, H.C., Pulicherla, N., Desai, P.M., and Rife, J.P. (2006). Recognition of a complex substrate by the KsgA/Dim1 family of enzymes has been conserved throughout evolution. RNA *12*, 725–733.

Peng, B.-Z., Bock, L.V., Belardinelli, R., Peske, F., Grubmüller, H., and Rodnina, M.V. (2019). Active role of elongation factor G in maintaining the mRNA reading frame during translation. Sci. Adv. *5*, eaax8030.

Poldermans, B., Bakker, H., and Van Knippenberg, P.H. (1980). Studies on the function of two adjacent N6,N6-dimethyladenosines near the 3' end of 16S ribosomal RNA of Escherichia coli. IV. The effect of the methylgroups on ribosomal subunit interaction. Nucleic Acids Res. *8*, 143–151.

Qin, P., Yu, D., Zuo, X., and Cornish, P.V. (2014). Structured mRNA induces the ribosome into a hyper-rotated state. EMBO Rep. *15*, 185–190.

Ritchie, D.B., Foster, D.A.N., and Woodside, M.T. (2012). Programmed −1 frameshifting efficiency correlates with RNA pseudoknot conformational plasticity, not resistance to mechanical unfolding. Proc. Natl. Acad. Sci. U. S. A. *109*, 16167–16172.

Sanders, C.L., and Curran, J.F. (2007). Genetic analysis of the E site during RF2 programmed frameshifting. RNA *13*, 1483–1491.

Sauert, M., Temmel, H., and Moll, I. (2015). Heterogeneity of the translational machinery: Variations on a common theme. Biochimie *114*, 39–47.

Savelsbergh, A., Katunin, V.I., Mohr, D., Peske, F., Rodnina, M.V., and Wintermeyer, W. (2003). An Elongation Factor G-Induced Ribosome Rearrangement Precedes tRNA-mRNA Translocation. Mol. Cell *11*, 1517–1523.

Schluenzen, F., Takemoto, C., Wilson, D.N., Kaminishi, T., Harms, J.M., Hanawa-Suetsugu, K., Szaflarski, W., Kawazoe, M., Shirouzu, M., Nierhaus, K.H., et al. (2006). The antibiotic kasugamycin mimics mRNA nucleotides to destabilize tRNA binding and inhibit canonical translation initiation. Nat. Struct. Mol. Biol. *13*, 871–878.

Schürer, H., Lang, K., Schuster, J., and Mörl, M. (2002). A universal method to produce in vitro transcripts with homogeneous 3′ ends. Nucleic Acids Res. *30*, e56.

Schuwirth, B.S., Day, J.M., Hau, C.W., Janssen, G.R., Dahlberg, A.E., Cate, J.H.D., and Vila-Sanjurjo, A. (2006). Structural analysis of kasugamycin inhibition of translation. Nat. Struct. Mol. Biol. *13*, 879–886.

Senior, B.W., and Holland, I.B. (1971). Effect of Colicin E3 upon the 30S Ribosomal Subunit of Escherichia coli. Proc. Natl. Acad. Sci. U. S. A. *68*, 959–963.

Šponer, J., E. Riley, K., and Hobza, P. (2008). Nature and magnitude of aromatic stacking of nucleic acid bases. Phys. Chem. Chem. Phys. *10*, 2595–2610.

Stark, M.R., Pleiss, J.A., Deras, M., Scaringe, S.A., and Rader, S.D. (2006). An RNA ligase-mediated method for the efficient creation of large, synthetic RNAs. RNA *12*, 2014–2019.

Stephan, N.C., Ries, A.B., Boehringer, D., and Ban, N. (2021). Structural basis of successive adenosine modifications by the conserved ribosomal methyltransferase KsgA. Nucleic Acids Res. *49*, 6389–6398.

Stochmanski, S.J., Therrien, M., Laganière, J., Rochefort, D., Laurent, S., Karemera, L., Gaudet, R., Vyboh, K., Van Meyel, D.J., Di Cristo, G., et al. (2012). Expanded ATXN3 frameshifting events are toxic in Drosophila and mammalian neuron models. Hum. Mol. Genet. *21*, 2211–2218.

Thammana, P., and Held, W.A. (1974). Methylation of 16S RNA during ribosome assembly in vitro. Nature *251*, 682–686.

Tinoco Jr., I., Kim, H.-K., and Yan, S. (2013). Frameshifting dynamics. Biopolymers *99*, 1147–1166.

Traub, P., and Nomura, M. (1968). Structure and function of E. coli ribosomes. V. Reconstitution of functionally active 30S ribosomal particles from RNA and proteins. Proc. Natl. Acad. Sci. U. S. A. *59*, 777–784.

Traub, P., and Nomura, M. (1969). Structure and function of Escherichia coli ribosomes: VI. Mechanism of assembly of 30 s ribosomes studied in vitro. J. Mol. Biol. *40*, 391–413.

Traub, P., Mizushima, S., Lowry, C.V., and Nomura, M. (1971a). [41] Reconstitution of ribosomes from subribosomal components. In Methods in Enzymology, (Academic Press), pp. 391–407.

Traub, P., Mizushima, S., Lowry, C.V., and Nomura, M. (1971b). [41] Reconstitution of ribosomes from subribosomal components. In Methods in Enzymology, (Academic Press), pp. 391–407.

Turner, D.H. (1996). Thermodynamics of base pairing. Curr. Opin. Struct. Biol. *6*, 299–304.

Uemura, S., Aitken, C.E., Korlach, J., Flusberg, B.A., Turner, S.W., and Puglisi, J.D. (2010). Real-time tRNA transit on single translating ribosomes at codon resolution. Nature *464*, 1012–1017.

Van Charldorp, R., Heus, H.A., and Van Knippenberg, P.H. (1981). Adenosine dimethylation of 16S ribosomal RNA: effect of the methylgroups on local conformational stability as deduced from electrophoretic mobility of RNA fragments in denaturing polyacrylamide gels. Nucleic Acids Res. *9*, 267–275.

Varshney, U., Lee, C.P., and RajBhandary, U.L. (1991). Direct analysis of aminoacylation levels of tRNAs in vivo. Application to studying recognition of Escherichia coli initiator tRNA mutants by glutaminyl-tRNA synthetase. J. Biol. Chem. *266*, 24712–24718.

Walter, A.E., and Turner, D.H. (1994). Sequence dependence of stability for coaxial stacking of RNA helixes with Watson-Crick base paired interfaces. Biochemistry *33*, 12715–12719.

Watson, Z.L., Ward, F.R., Méheust, R., Ad, O., Schepartz, A., Banfield, J.F., and Cate, J.H. (2020). Structure of the bacterial ribosome at 2 Å resolution. ELife *9*.

Wills, N.M., and Atkins, J.F. (2006). The potential role of ribosomal frameshifting in generating aberrant proteins implicated in neurodegenerative diseases. RNA *12*, 1149–1153.

Zhou, J., Lancaster, L., Donohue, J.P., and Noller, H.F. (2013). Crystal Structures of EF-G-Ribosome Complexes Trapped in Intermediate States of Translocation. Science *340*, 1236086–1236086.

Zhou, J., Lancaster, L., Donohue, J.P., and Noller, H.F. (2019). Spontaneous ribosomal translocation of mRNA and tRNAs into a chimeric hybrid state. Proc. Natl. Acad. Sci. *116*, 7813–7818.

CHAPTER IV

A Non-Denaturing Method for Splinted Ligation of Large Functional RNAs

Abstract

The ability to introduce modified nucleotides into a large RNA, while preserving its native functional activity, has the potential to greatly expand the range of RNA biochemistry and biophysics. The most widely used method for constructing such modified RNAs is by DNA splint-directed RNA ligation using RNA ligases. However, following completion of ligation, removal of a bound DNA splint without disruption of the higher-order structure of the RNA presents a challenge to construction of large functional RNAs containing introduced modifications. Here, we present a method for efficient removal of DNA splints under mild conditions using a partially non-complementary tailed DNA splint. We ligate a 1493-nucleotide 16S rRNA fragment to a synthetic 49-mer to create a 1542-nucleotide semi-synthetic 16S ribosomal RNA. After our improved splint ligation protocol, the resulting ligated 16S rRNA retains its ability to undergo *in vitro* reconstitution to yield active 70S ribosomes. This approach should be generally applicable to ligation of any large functional RNA.

Introduction

RNA researchers have long used introduction of site-specific nucleotide modifications to probe the structure and function of these important biological molecules. Improvements in RNA ligation techniques have allowed for synthesis of novel constructs containing site-specific internal modifications such as nucleotides with 2'-deoxy or 2'-O-methyl (Moore and Sharp, 1992), photo-cross-linkable groups (Golden et al., 1996), fluorescent dyes (Akiyama and Stone, 2009) or radioactive phosphates (Huang and Yu, 2013). Bridging two RNAs with a DNA splint and then sealing the nicked RNA with T4 DNA Ligase (Kleppe et al., 1970; Fareed et al., 1971; Moore and Sharp, 1992; Kershaw and O'Keefe, 2012) or T4 RNA Ligase 2 (Ho and Shuman, 2002; Nandakumar et al., 2004) has become the most efficient way to build modified RNAs with minimal off-target side products (Moore and Query, 2000; Stark et al., 2006).

An important remaining hurdle to this powerful approach lies in purification of the desired RNA products from their hybridized DNA splint oligonucleotides while preserving the structure of the RNA. This purification has primarily been achieved using polyacrylamide gel electrophoresis under denaturing conditions. However, this method typically results in low yields, especially with larger RNAs, contamination with fragments of polyacrylamide and disruption of the higher-order structure of the RNA. While it is possible to use non-denaturing methods such as sucrose gradient centrifugation or size-

exclusion chromatography to separate large ligation products from small un-ligated fragments, there have not been successful methods for removal of the annealed DNA splint oligonucleotide while avoiding denaturation of the ligated RNA product. Removal of the DNA splint using DNase digestion is often inefficient, and typically requires denaturing gel purification to remove any remaining DNA fragments that may be able to re-hybridize to the RNA ligation product. For these reasons, we sought to develop a method by which DNA splints can be quantitatively removed from RNA ligation products on a preparative scale under non-denaturing conditions.

In our approach, we designed DNA splints complementary to the junction of the RNA ligation targets but flanked by non-complementary 5' and 3' tails (Fig. 1). The non-complementary tails then allow removal of the DNA splint by annealing to an antisplint DNA with complete complementarity to the tailed splint DNA (Figs 1; 2). The antisplint DNA efficiently outcompetes the RNA ligation product for hybridization with the tailed splint and remains stably annealed to the antisplint while the RNA product is purified under non-denaturing conditions.

Results

The following example uses ligation of the 1493-nucleotide 16S rRNA colicin E3 cleavage product (Boon, 1971b; Bowman et al., 1971; Senior and Holland, 1971) to a synthetic 49-mer RNA containing the remaining 3'-

terminal sequence of 16S rRNA resulting in a semi-synthetic 16S rRNA capable of reconstitution into active 30S ribosomal subunits.

Optimization of Splinted Ligation

For efficient splinted ligation, the DNA oligonucleotide splint must be optimized to anneal stably and with high sequence specificity to the target RNAs at the ligation site. A series of splints of varying lengths were designed to anneal to the junction between the 3' end of the 1493-nucleotide 16S rRNA colicin E3 cleavage product and the 5' end of a synthetic 49-nucleotide RNA oligonucleotide (Table 1; Fig. 2). The extent of complementarity of the DNA splint to each target RNA was varied from 15 to 20 base pairs to determine the minimal length that conferred stable annealing to the ends of both RNAs. Since the 16S rRNA is itself highly structured near the ligation site, we found it necessary to create lengthy complementary regions. The complementary region of the DNA splint was then extended on its 5' and 3' ends by 10-15 additional nucleotides to create non-complementary tails (Figs. 1,2). When designing the tailed splints, it was important to avoid potential secondary structure and self-annealing within the splint sequence itself, by adjusting the sequences of the non-complementary tails accordingly (Fig. 2, A).

Since the two RNA sequences have different base pairing stabilities, we tested ligation efficiency using 4 different tailed splint designs (TS1, TS2, TS3 and TS4; Table 1) containing complementary sequences with lengths

varying from 13-18 nt and non-complementary tails varying from 6-15 nt. The initial ligation efficiency of 5'-[^{32}P]-labeled synthetic 49mer RNA to 1493mer 16S colicin E3 fragment (cut 16S) (Fig. 3). Though ligation efficiency was low overall, less than 10%, tailed splint 3 (TS3) resulted in the highest amount of ligation product as monitored by [^{32}P]-49mer migration on denaturing gel following ligation. A main factor in ligation efficiency is optimal annealing of ligation precursors to the DNA splint. To increase ligation efficiency, the tailed DNA splint could be pre-incubated with the two RNA targets prior to addition of ligase. This annealing step allows for the tailed DNA splint to compete with the secondary structure of the RNAs, more efficiently directing ligation.

Prior to optimizing annealing conditions, we tested the ability of 16S rRNA to be reconstituted into functional ribosomes as a function of increasing temperatures. Though it is common practice to heat the 16S rRNA to 40^{o}C during *in vitro* reconstitution (Traub and Nomura, 1968) we asked whether its functionality survives higher incubation temperatures, to favor annealing of the DNA splint. We tested the efficiency of *in vitro* reconstitution of 16S rRNA following 30-minute incubations at 46^{o}, 52^{o}, and 58^{o}C (Fig. 4). We found that 16S rRNA heated to 46^{o} in buffer containing 20mM Tris-HCL pH 7.5, 50mM KCL, 5mM $MgCl_2$, 0.5mM Spermine was reconstituted into 70S ribosomes at an efficiency identical to that of untreated 16S rRNA. However, reconstitution was slightly inhibited after incubation at 52^{o}C and reduced by half at 58^{o}C.

Accordingly, we chose to focus on an annealing temperature of 46^{o} for further optimization.

Next, annealing conditions were monitored by hybridization of 5'-[^{32}P]-labeled TS3 DNA to the colicin E3 16S rRNA fragment and synthetic 49mer RNA (Fig. 5). Efficiency of annealing TS3 to the colicin E3-digested 16S rRNA was followed by co-migration of the labeled DNA splint with the large 16S rRNA fragment in a non-denaturing gel (Fig. 5A), using a 3-fold molar excess of [^{32}P]-splint TS3 and 49mer RNA. We first extended the time of annealing at 46^{o} from 5 min to 5 h and found the efficiency of annealing to increase from 20% to a final plateau at 52% after 2 h of incubation (Fig, 5B). We next tested the effects of different stoichiometries of splint, 49mer and 1493mer on annealing efficiency, following the co-migration of [^{32}P]-labeled 49mer with the large rRNA fragment (Fig. 5C). As expected, increasing the amount of DNA splint and synthetic 49mer RNA relative to 1493mer fragment resulted in increased annealing efficiency. An optimal efficiency of 65% was achieved with a 3-fold molar excess of DNA splint and 2-fold molar excess of synthetic 49mer RNA over the 1493mer rRNA fragment (Fig. 5D). Our final annealing conditions were thus 2μM synthetic 49mer, 1μM 1493mer 16S rRNA fragment and 3μM TS3 DNA, incubated at 46^{o}C for 2 hours followed by slow cooling to 30^{o}C. With an annealing efficiency of around 65%, ligation efficiency reached 61% on a preparative scale (Fig. 6)

Optimization of Splint Displacement from Ligation Product by Antisplint Hybridization

Following ligation, we tested removal of the DNA splint from the ligation product using a [^{32}P]-labeled tailed splint and an antisplint DNA with full complementarity to the tailed splint (Fig. 7). Hybridization of anti-TS3 to TS3 was initially tested at 37^{o} for 10 minutes with increasing amount of antisplint DNA (Fig. 7A). The displacement of TS3 from full length 16S rRNA was linear until reaching a plateau between 1.3 and 2-molar excess of antisplint to TS3 (Fig. 7B). To minimize the possibility of binding the antisplint DNA to off-target sites, we limited the concentration of antisplint DNA to a 1.3-fold molar excess. Next, we tested splint removal at temperatures between 4^{o} and 75^{o}, incubating for 10 min at temperatures of 37^{o}C and higher, and for 30 min at the lower temperatures, followed by quenching on ice (Fig. 7C). The tailed splint DNA partially dissociated at 4^{o} (41%), increasing to 82% at 37^{o}C, and over 90% at 46^{o} (Fig. 7D). Although removal was nearly quantitative (98%) at 75^{o}, we limited the temperature to 46^{o} to minimize disruption of the higher-order structure of the rRNA. Our final procedure for removal of the tailed splint from the RNA ligation product uses a 1.3-fold molar excess of antisplint DNA to the amount of tailed splint used in the ligation reaction at 46^{o}C for 10 minutes, followed by slow cooling to 30^{o}C and quenching on ice for further purification.

Purification of Ligation Product

Removal of the splint-antisplint DNA duplex and free synthetic 49mer RNA from the RNA ligation product was carried out by sucrose gradient ultracentrifugation, which efficiently separates the 1542-nucleotide 16S rRNA ligation product from the much smaller DNAs and un-ligated 49mer RNA. The 1542-nucleotide 16S rRNA ligation product was separated from the 60 bp splint-antisplint DNA duplex and the 49-nucleotide synthetic RNA using a 10-30% sucrose gradient and centrifugation at 35,000 RPM at 4^{o} for 18 hours (Fig. 8).

The 16S rRNA ligation product was collected, exchanged into sucrose-free buffer, and tested for functionality by *in vitro* reconstitution into 70S ribosomes with total 30S proteins (TP30) and excess 50S subunits as described (Traub et al., 1971). The efficiency of reconstitution of the 16S rRNA ligation product into 70S was about 70% of that of natural 16S rRNA (Fig. 9A). The activity of the reconstituted, semi-synthetic 70S ribosomes in *in vitro* synthesis of a full-length protein was 77% of that of natural tight-couple 70S ribosomes, and 95% of the activity of ribosomes reconstituted *in vitro* with natural 16S rRNA (Fig. 9B; C).

Discussion

The RNA ligation method described here uses a DNA splint specifically complementary to the RNA sequences flanking the ligation junction site, but also contains non-complementary tails at its 5' and 3' ends to allow quantitative removal of the DNA splint using a fully complementary antisplint DNA under mild conditions. This approach is so simple yet so powerful since the fully complementary splint-antisplint DNA duplex has a much lower free energy of base-pairing than that of the duplex formed between the tailed DNA splint and the RNA ligation product. At equilibrium, the splinting DNA is displaced from the ligated RNA product. This allows for removal of the DNA splint under conditions that preserve the higher-order structure and thus the functional properties of the RNA. The ligation example described here has been used to introduce an abasic nucleotide into a specific position in the 1542-nucleotide 16S ribosomal RNA (Smart et al. REF?) but should be generally applicable to the study of any large RNA, especially when preservation of the higher-order structure of the RNA is an important consideration.

Use of tailed oligonucleotides has successfully been applied to the study of functional RNAs in other experimental contexts. Affinity purification of telomerase RNA was accomplished by annealing a tailed, avidin-labeled DNA oligonucleotide to the telomerase RNA template, which was eluted by adding a complementary DNA to outcompete the bound RNA (Lingner and Cech, 1996). Similarly, a tailed 2'-O-methyl RNA oligonucleotide that blocks a

critical step in assembly of the U12-dependent spliceosome was efficiently released by binding a second, fully complementary 2-O-methyl RNA oligonucleotide (Frilander and Steitz, 2001).

Design of tailed DNA splints must strike a balance between the lengths of complementary and non-complementary segments that will create stable annealing to the RNAs at the ligation junction while remaining easy to remove with an antisplint DNA. For the highly structured 16S rRNA, we observed both efficient annealing and removal with 15-20 nucleotides of complementary sequence to each RNA, for a total of 30-40 nucleotides of complementarity across the ligation junction, and a total of 15-20-nucleotides of non-complementary tails (Fig. 2). A typical starting point would be to create a long sequence of complementarity to the RNA targets across the ligation junction, followed by addition of 5' and 3' tails that total about half that length. This would likely be followed by further optimization. For example, splints TS1 and TS4 have similar lengths of complementary and non-complementary sequences yet show different ligation efficiencies (Fig. 3) This is likely attributable to the lengths and sequences of the complements to each target RNA. Another important step is to perform a search (for example, using 'OligoCalc' (Kibbe, 2007)) for any potential self-annealing into hairpin or other secondary structure that might compete with annealing to the target RNAs, and adjust the splint sequence accordingly.

Experimental Procedures

End-Labeling Tailed DNA Splints and Synthetic 49-mer RNA

Tailed splint DNA (IDT) or synthetic RNA (Dharmacon) oligonucleotides were incubated at a final concentration of 1.25μM in an 80μL reaction volume with 2μL of γ-[^{32}P]-ATP (PerkinElmer), 8μL 10X PNK buffer (700mM Tris-HCL pH 7.5, 500mM $MgCl_2$, 500mM DTT), and 1μL of polynucleotide kinase (10,000U/mL, NEB) at 37°C for 5 minutes, then immediately heat-inactivated at 68°C for 15 minutes. Unincorporated γ-[^{32}P]-ATP was removed with a Sephadex G25 spin-column. Working solutions were made by addition of non-radioactive oligonucleotide to a final concentration of 5μM with specific activity of 20,000 cpm/μL.

Optimization of DNA Splint Annealing to Target RNAs

Initial ligation efficiency with TS1, TS2, TS3, and TS4 was monitored by tracking [^{32}P]-labeled synthetic 49mer RNA migration on a denaturing 7M urea 4% polyacrylamide gel (Fig. 3). The ligation test was carried out at 37° for 1h with 8 units of T4RNA ligase (10,000U/mL, NEB), 1μM 1493bp colicin E3 digestion product, 3μM 49bp synthetic RNA, and 3μM each tailed DNA splint (TS1, TS2, TS3, and TS4) as well as controlled by a reaction lacking

splint DNA in 50mM Tris-HCl pH 7.5, 5mM MgCl2, 1mM DTT, and 0.5mM ATP buffer (NEB) (Fig. 3).

Once TS3 was determined to lead to highest amount of ligation product, splint annealing conditions were optimized, monitored by tracking mobility of [^{32}P]-labeled TS3 in non-denaturing 4% (29:1 acrylamide;bis-acrylamide) polyacrylamide gels following annealing to colicin E3 cut 16S rRNA (Fig. 5). Optimization of incubation time for annealing (Fig. 5A) was carried out in a 10μL volume with 1μM 1493mer Colicin E3 product, and 3μM labeled splint TS3 at 46°C in annealing buffer (20mM Tris-HCL pH 7.5, 50mM KCL, 5mM $MgCl_2$, 0.5mM Spermine). We found that 16S rRNA was able to reconstitute at higher temperatures with the addition of $MgCL_2$ and Spermidine in the buffers so our annealing buffer included these. We next tested the effects of different stoichiometries of splint, 49mer and 1493mer on annealing efficiency, following the co-migration of [^{32}P]-labeled 49mer with the large rRNA fragment (Fig. 5C). While keeping the amount of 1493mer constant, we tested using equimolar amounts of 49mer RNA and TS3 as well as 2-fold and 3-fold molar excess of each at 46° for 2 hours in annealing buffer. Concentrations of each nucleic acid component was determined by A260 reading prior to mixing in annealing reactions. The final concentrations in 10μL for different stoichiometric annealing reaction are as follows:

Stoichiometry	0.0.1	0.1.1	1.1.1	1.2.2	1.2.3	1.3.2

1493mer RNA (μM)	0	0	1	1	1	1
TS3 DNA (μM)	0	1	1	2	2	3
49mer RNA (μM)	1	1	1	2	3	2

Following annealing, the reactions were moved directly from the 46°C water bath into a small dish of water from the bath and allowed to sit at room temperature until the system reached a temperature of 30° over about 20 minutes (slow cooling step). The annealing reactions were then placed on ice and mixed with an equal volume of 2X native loading buffer (40% sucrose, 0.2% TBE buffer) and loaded directly onto a 4% non-denaturing polyacrylamide gel in TBE buffer (1% Tris base, 0.6% boric acid, 0.1% EDTA). All 4% polyacrylamide gels were poured using 25cm plates and 1mm spacers then ran at 30 watts for 1 h at 4° for native gels and room temperature for denaturing gels. The gels were then directly blotted onto Whatman 3MM CHR paper and dried for 30 minutes at 80°C under vacuum. Dried gels were exposed overnight, scanned with a Typhoon Phosphorimager and quantified with image J (Schneider, Rasband, and Eliceiri 2012). For optimal annealing of tailed DNA splint TS3 to target RNAs, the final concentrations were 1μM 1493mer Colicin E3 16S rRNA fragment, 2μM 49mer synthetic RNA, and 2μM TS3 splint DNA, in annealing buffer (20mM Tris-HCL pH 7.5, 50mM KCL, 5mM $MgCl_2$, 0.5mM Spermine). All reagents

were combined on ice, followed by a 2-hour incubation at 46°, slow cooling to 30°C and placed on ice prior to ligation.

Ligation Procedure

Following annealing of the two RNAs to TS3, we increased the volume by 10-fold on ice to give a final concentration of 0.1μM 16S rRNA 1493mer in buffer containing 50mM Tris-HCl pH 7.5, 5mM MgCl2, 1mM DTT, and 0.5mM ATP. At this step, the final buffering conditions for ligation following annealing was 52mM Tris-HCL pH 7.5, 5mM KCL, 5.5mM $MgCl_2$, 0.05mM Spermidine, 1mM DTT, and 0.5mM ATP. Finally, T4 RNA ligase 2 (homemade following Ho and Shuman 2002) to a final concentration of 0.005mg/mL. The ligation reaction was incubated at 37° for 1 hour. Next, the ligase was denatured by addition of SDS to a final concentration of 0.25% and the RNA precipitated in 0.3M NaOAc pH 5.3 and 2.5 volumes of ethanol placed at -20°C overnight or in a dry-ice bath for 15 min, followed by centrifugation at 10,000 RPM for 30 minutes at 4°C to recover the nucleic acids, which were resuspended in annealing buffer. Ligation products were analyzed by electrophoresis on a 7M urea denaturing 4% polyacrylamide gel using 25cm plates and 1mm spacers at 10 W for 19h at room temperature then stained with 0.2% methylene blue in 0.4M sodium acetate (Fig. 6).

Removal of Splints from 16S rRNA with Anti-splint DNA

Annealing of TS3 DNA to full-length 16S rRNA ligation product was done in a large-scale master mix with 3μM final TS3 and 1μM 16S rRNA then aliquoted on ice for testing different antisplint hybridization optimization conditions. Removal of splint with antisplint DNA was first optimized by ratio of antisplint to splint of 0- to 2-fold (0μM-6μM) at 37° for 10 minutes in annealing buffer (20mM Tris-HCL pH 7.5, 50mM KCL, 5mM $MgCl_2$, 0.5mM Spermine) (Fig. 7A). Following antisplint titration, we tested hybridization of antisplint at different temperatures from 4° to 75° (Fig. 7C). Optimal conditions for splint removal were 1.2-fold molar excess of antisplint to tailed splint DNA, at a temperature of 46° for 10 minutes followed by slow cooling to 30°C, then placement on ice. Labeled products were analyzed by 4% polyacrylamide native gel using methods established earlier.

Sucrose Gradient Purification of Ligated 16S rRNA Product

Following removal of DNA splint from the ligated 16S rRNA product, the rRNA was purified by sucrose gradient ultracentrifugation. The reaction was loaded onto a 10%-30% w/v sucrose gradient in 25mM Tris-HCl pH 7.5, 60mM NH4Cl, 5mM MgCl2, 5mM β-mercaptoethanol, and centrifuged in an SW-41 rotor at 35,000 RPM for 18h at 4°. The 16S rRNA was collected using a density gradient fractionator following UV absorbance at 260 nm, and exchanged into buffer containing 25 mM Tris-HCl (pH 7.5), 60 mM NH_4Cl and

10 mM $MgCl_2$ and concentrated to 10-20uM using an Amicon spin concentrator with a 100 kDa MW cutoff.

Reconstitution of Ligated 16S rRNA into 70S ribosomes

Purified semi-synthetic 16S rRNA ligation product was mixed with total 30S ribosomal proteins (TP30) and reconstituted into 30S subunits using previously established protocols (Traub et al., 1971). The reconstituted 30S were associated with natural 50S subunits and loaded onto a 10-35% w/v sucrose gradient in 25 mM Tris-HCl (pH 7.5), 100 mM NH_4Cl, 15 mM $MgCl_2$, 5 mM β-mercaptoethanol and centrifuged in an SW-41 rotor at 22,000 RPM for 18 h at 4°. The 70S ribosomes were collected as described above and exchanged into buffer containing 25mM Tris-HCl (pH 7.5), 100mM NH_4Cl and 10mM $MgCl_2$ and concentrated to 1-10 μM as described above.

Testing Functionality by *In Vitro* Translation

The activity of reconstituted ribosomes was tested by *in vitro* translation of a full-length protein as previously described (Niblett et al., 2021). Results were analyzed by electrophoresis on a SDS polyacrylamide gel (15%), dried under vacuum for 30 minutes at 80°C, then visualized and quantified as described above.

Acknowledgements

We thank Laura Lancaster for her advice in designing and troubleshooting these methods. We thank Stewart Schuman (Cornell Medical School) for advice on RNA ligation and a generous gift of plasmid DNA for expression and purification of T4 RNA ligase 2.

Tables and Figures

Table 1. Tailed Splint Constructs[a]

	Splint Sequences	Lengths (nt)
	TS1	
5' tail	CCAATTGGAT	10
splint	CGGTTACCTTGTTACGAC|TTCACCCCAGTCATGAATCAC	18 I 21
3' tail	TTTCACCATT	10
	TS2	
5' tail	CGTCCAAGATGATGC	15
splint	GTTACCTTGTTACGAC|TTCACCCCAGTCA	16 I 13

3' tail	ACTTAGTGTTTCACC	15
	TS3	
5' tail	GAGTAT	6
splint	CGGTTACCTTGTTACGAC|TTCACCCCAGTCATGAATCAC AAAG	18 I 25
3' tail	ACCATTCGCGG	11
	TS4	
5' tail	GGGATGCCAA	10
splint	ACCTTGTTACGAC|TTCACCCCAGTCATGAATCACAAAG	13 I 25
3' tail	ACCATTCGCGGG	12

[a]Regions complementary to the rRNA sequences flanking the ligation junction (|) are underlined. The 5' and 3' tails are non-complementary to the rRNA.

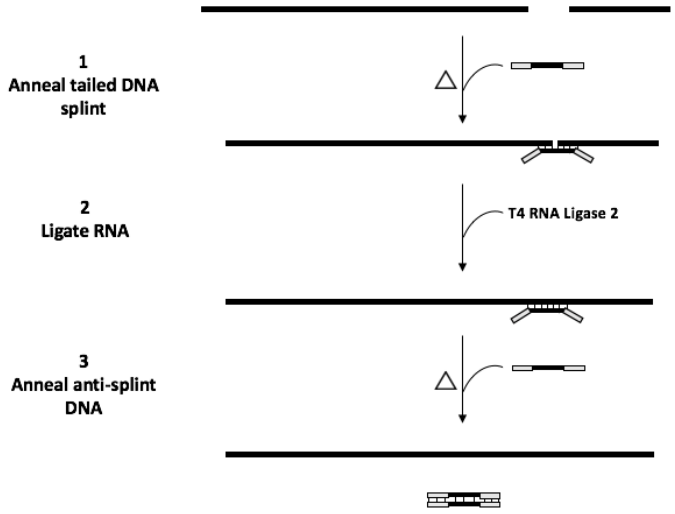

Figure 1. Scheme for tailed DNA splint displacement by annealing to a tailed anti-splint DNA.

A DNA splint contains an internal section (black) that is complementary to the ends of the RNA substrates flanking the site of ligation, and two non-complementary tails (white). Following ligation, the tailed splint is removed by annealing with a tailed anti-splint DNA that is fully complementary to the tailed splint.

A.

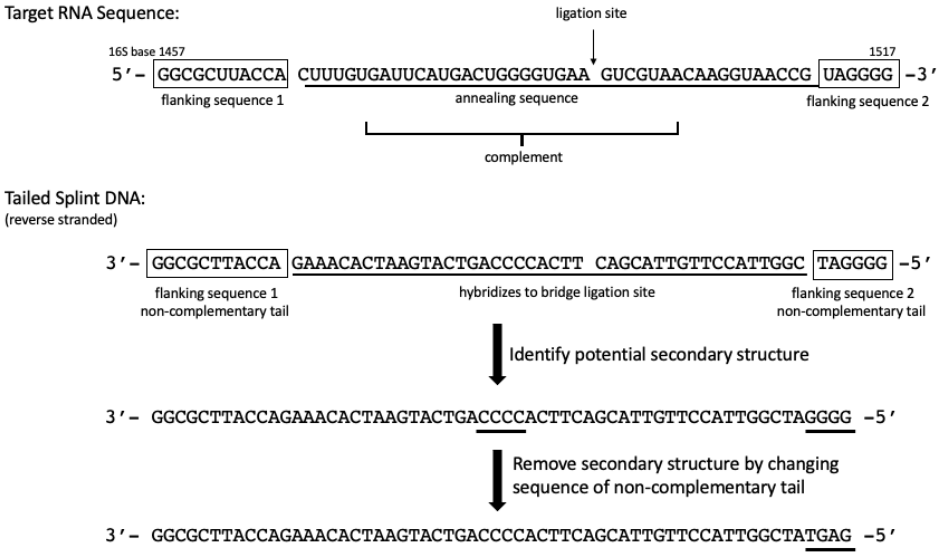

B.

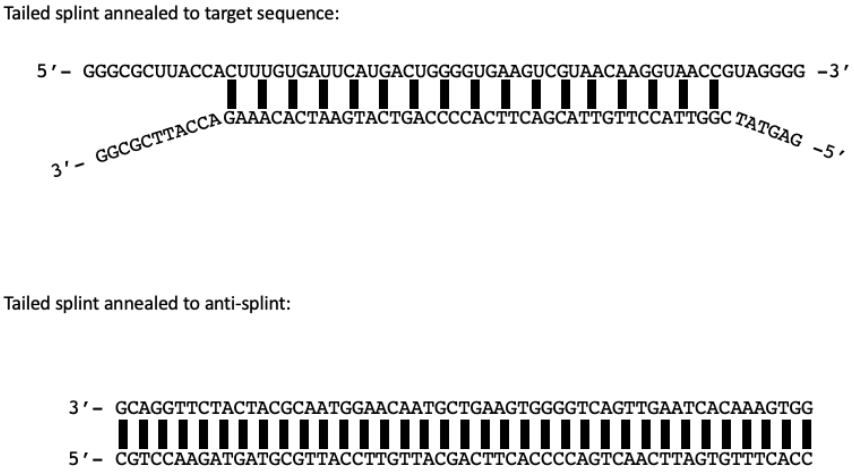

Figure 2. Tailed Splint DNA Design Methods

A tailed DNA splint is designed to complementarily bridge the RNA ligation site and have two flanking non-complement tails (A). An antisplint DNA

oligonucleotide is designed to have full complementarity to the tailed splint, allowing recovery of RNA ligation product from tailed DNA splint (B).

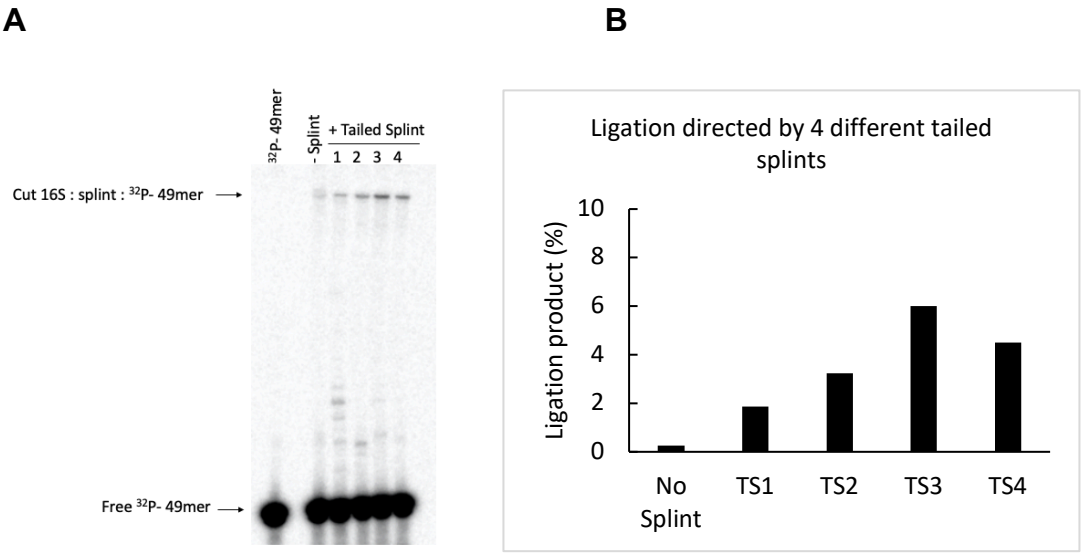

Figure 4. Initial ligation comparison with 4 different tailed splints

Tailed DNA splints, TS1-4, compared in ligation efficiency using a 3-molar excess of labeled 49mer RNA over 1493mer 16S fragment at 37°C for one hour. (A) Denaturing 7M urea, 4% polyacrylamide gel showing ligation of synthetic [^{32}P]-49mer RNA to 1493mer (Cut) 16S rRNA fragment as directed by tailed DNA splints 1-4 or without addition of a DNA splint. (B) Ligation efficiency (%) without addition of DNA splint and with addition of 4 different tailed DNA splints TS1-4 (sequences found in Table 1; n=1).

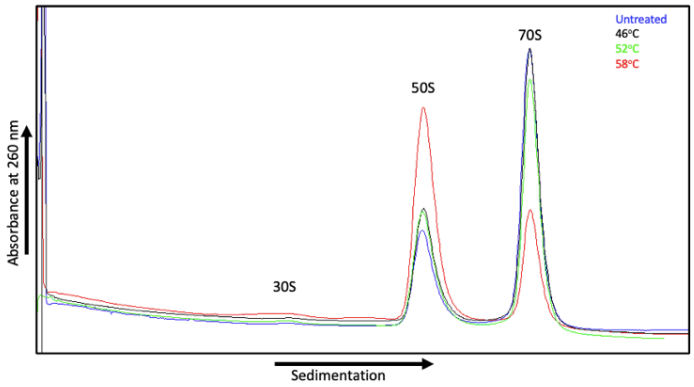

Figure 4. Ribosome reconstitutions with heated 16S rRNA

Analytical 10%-35% w/v sucrose gradients of 70S ribosome reconstitutions scanned with BioComp to get absorbance peaks at 260nm. The 70S ribosomes contain 16S rRNA that has been either left untreated (blue) or heated to 46^{o}C (black), 52^{o}C (green), or 58^{o}C (red) in annealing buffer (20mM Tris-HCL pH 7.5, 50mM KCL, 5mM $MgCl_2$, 0.5mM Spermine) for 30 minutes.

A **B**

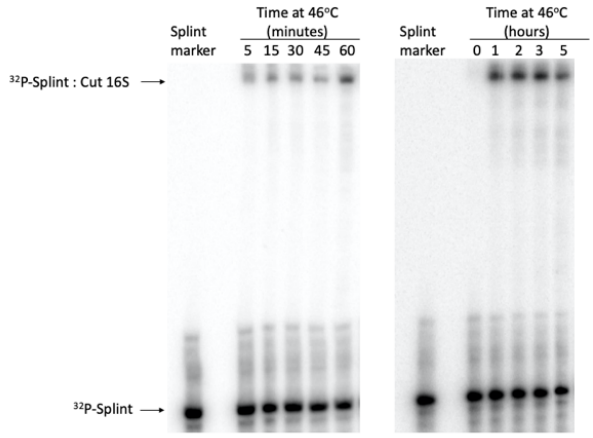
Splint marker
Time at 46°C (minutes)
5 15 30 45 60
Splint marker
Time at 46°C (hours)
0 1 2 3 5
32P-Splint : Cut 16S
32P-Splint

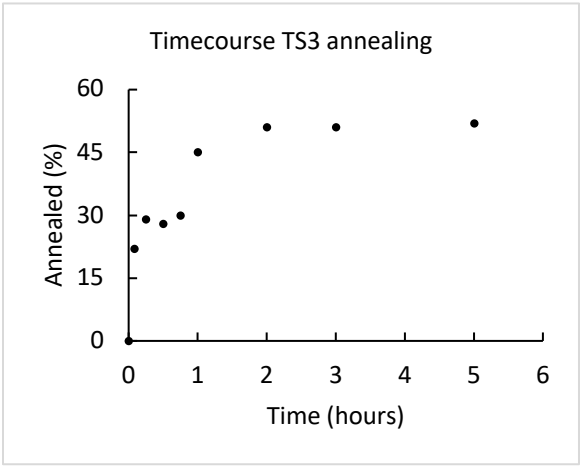
Timecourse TS3 annealing
Annealed (%)
60
45
30
15
0
0 1 2 3 4 5 6
Time (hours)

C

D

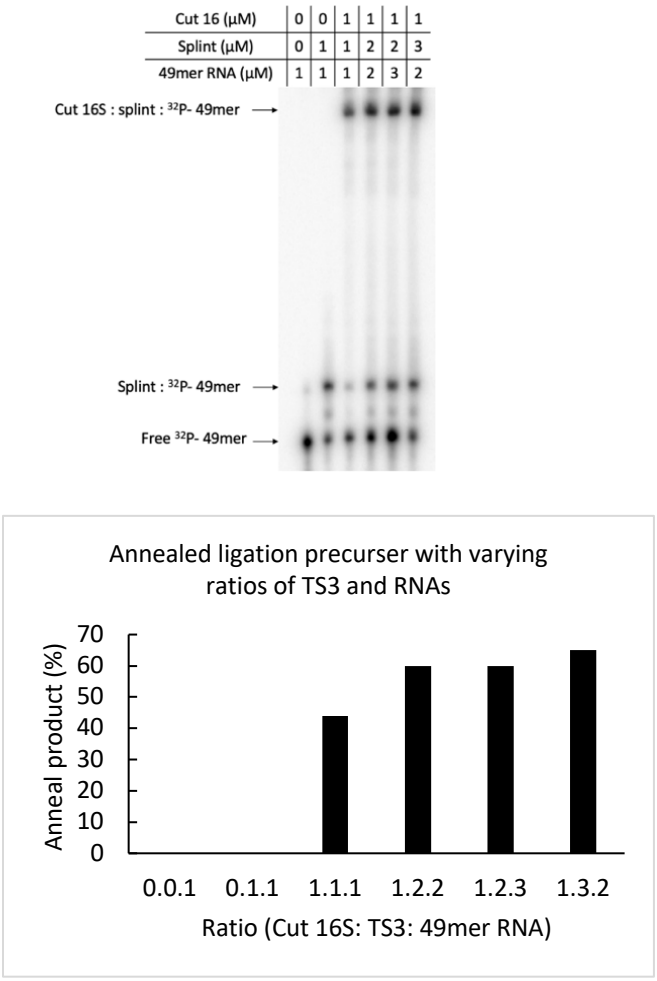

Figure 5. Tailed DNA splint annealing to RNA targets

Annealing of TS3 DNA to *E. coli* 16S rRNA 1493bp fragment from colicin E3 digestion and 49bp synthetic RNA oligo under optimization conditions. (A) Native 4% polyacrylamide gel showing time course of [^{32}P]-tailed DNA splint annealing to 1493mer (colicin E3 cut) 16S rRNA fragment. (B) Time course data averaged from 3 experiments and plotted as a function of annealed [^{32}P]-tailed DNA splint percent over time. (C) Determining optimal stoichiometric

ratio of TS3 and synthetic [^{32}P]-49mer RNA to 1493mer (cut) 16S rRNA fragment monitored by native 4% polyacrylamide gel. (D) Histogram analysis of stoichiometric annealing results. The ratio corresponds to concentration (μM) of each component in panel (C) for example 0.0.1 corresponds to 0μM Cut 16S 1493mer, 0μM TS3, and 1μM [^{32}P]-49mer RNA (n=1).

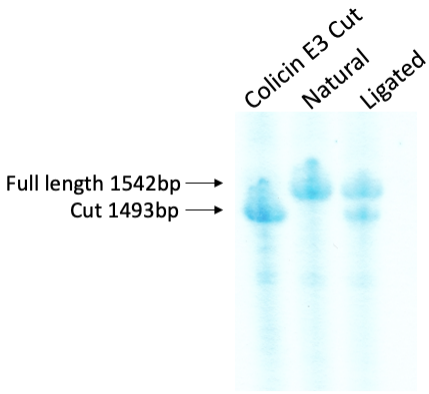

Figure 6. Ligation Efficiency

Denaturing 4% polyacrylamide and 7M urea RNA-stained gel showing ligation of the semi-synthtic16S rRNA on the preparative scale. Final ligation product is compared to natural 16S rRNA and the colicin E3 cut 1493mer 16S rRNA fragment.

A **B**

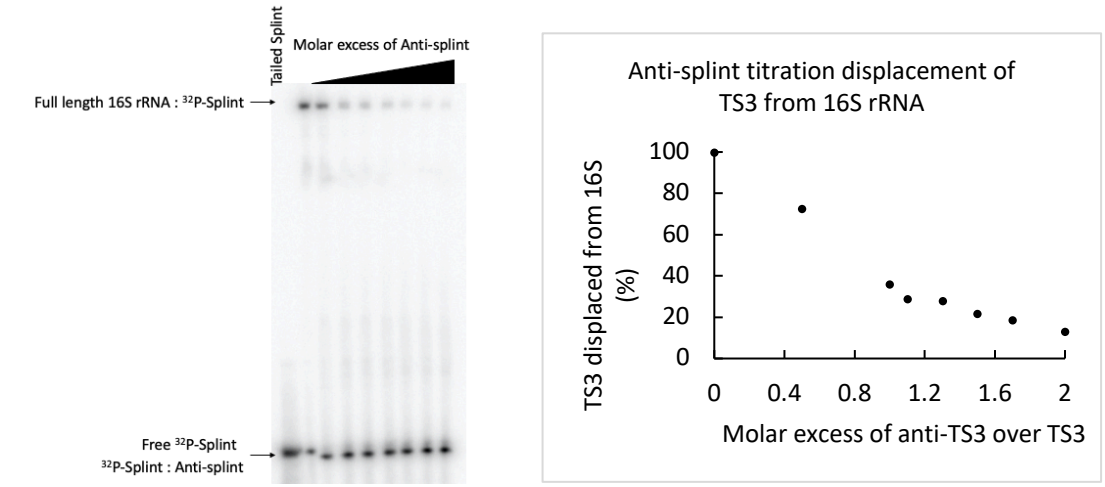

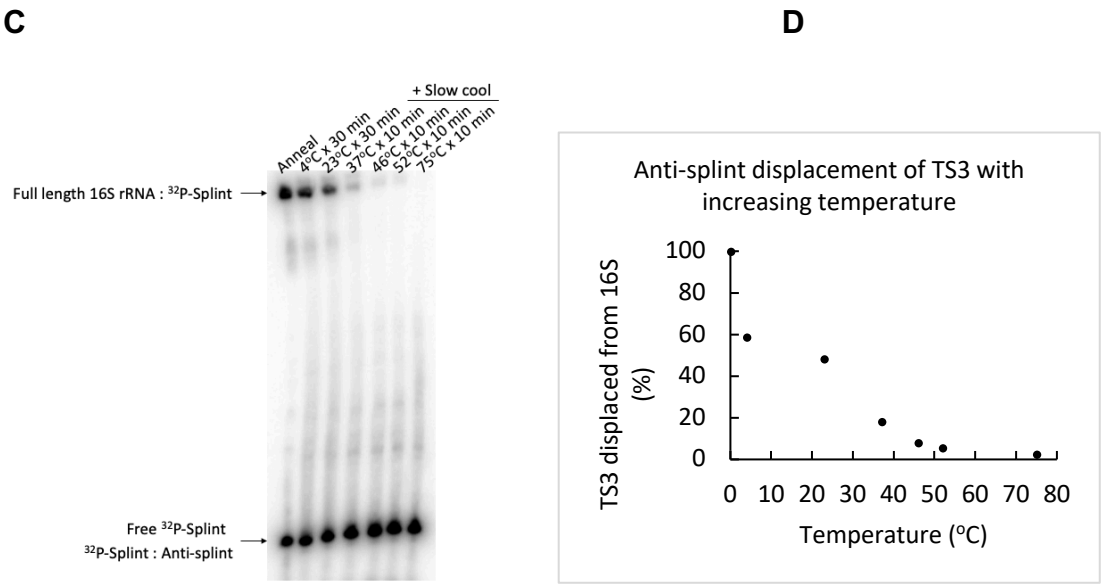

Figure 7. Displacement of tailed splint DNA from RNA product by hybridization with antisplint DNA

Displacement of TS3 from ligation product under optimization conditions. (A) Native 4% polyacrylamide gel showing displacement of [^{32}P]-labeled TS3 DNA from full-length *E. coli* 16S rRNA with increasing concentrations of anti-splint DNA carried out for 10 minutes at 37° in annealing buffer, data analysis

is shown in (B). Temperature optimization with 1.3-molar excess anti-splint DNA carried out for indicated times at indicated temperatures followed by a brief incubation on ice prior to loading gel (C and D) (n=2).

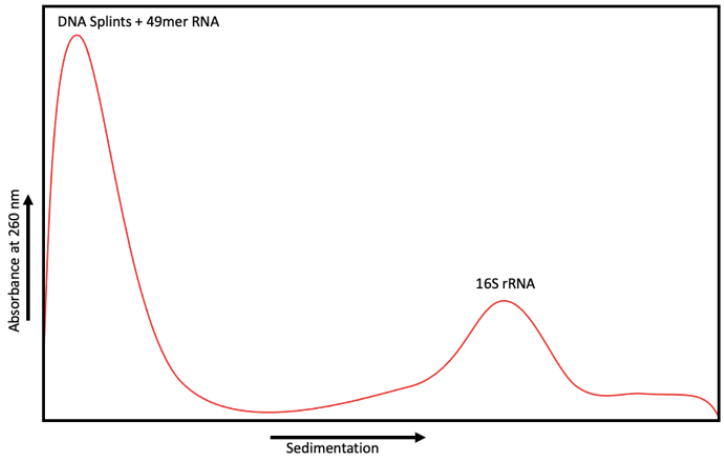

Figure 8. Purification of ligation product from DNA contaminants

Preparative 10%-30% w/v sucrose density gradient data from fractionator as indicated by peak absorbance at 260nm. The peak on the far left is attributed to DNA splint and antisplint hybrids as well as excess synthetic 49mer RNA while the peak on the right corresponds to the full-length 16S rRNA product. The ligation product peak is collected from the gradient and used for functional studies.

A

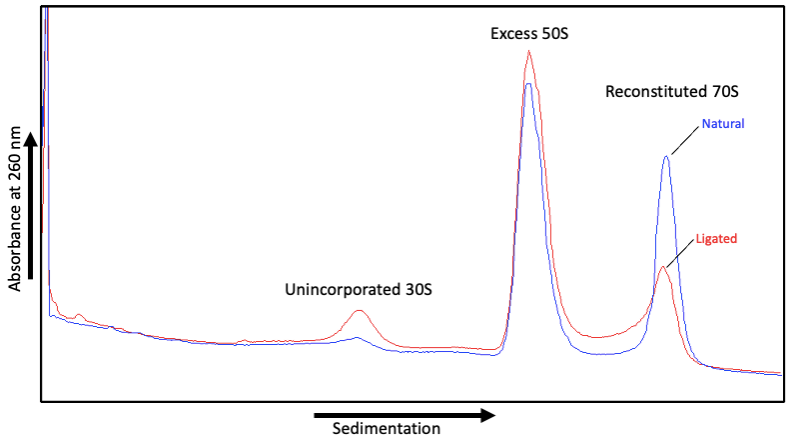

B

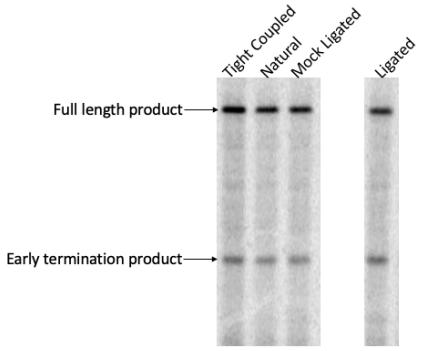

C

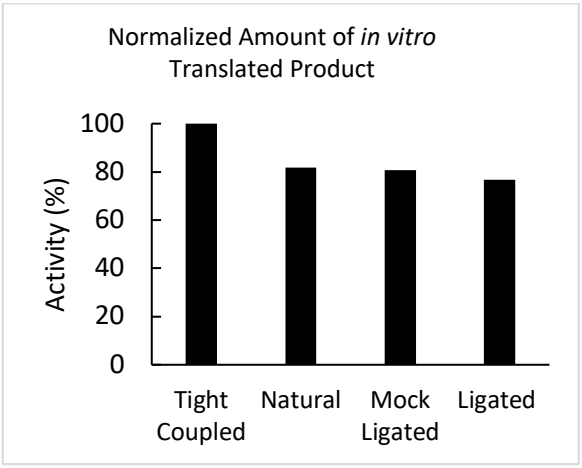

Figure 9. Functional ligation product

Functionality of our 16S rRNA ligation product was determined by ability to form functional 70S particles (A) Schematic of 10% - 35% w/v sucrose gradient scanned at 260nm absorbance to indicate reconstitution of ribosomes with natural 16S rRNA (blue) and ligated 16S product (red). After purification, the ligated and reconstituted 70S was used in an *in vitro*

translation assay visualized by ^{35}S-Met incorporation into protein product (B). Controls in this assay were tight coupled 70S from MRE600, natural 16S reconstituted, and a mock ligation performed on natural 16S followed by reconstitution. The total amount of *in vitro* synthesized product intensity was measure in ImageJ for direct comparison, normalized to the tight coupled 70S control (C) (n=2).

References

ABDI, N.M., and FREDRICK, K. (2005). Contribution of 16S rRNA nucleotides forming the 30S subunit A and P sites to translation in Escherichia coli. RNA *11*, 1624–1632.

Akiyama, B.M., and Stone, M.D. (2009). Chapter 2 - Assembly of Complex RNAs by Splinted Ligation. In Methods in Enzymology, (Academic Press), pp. 27–46.

Baan, R.A., Charldorp, R.V., Leerdam, E.V., Knippenberg, P.H.V., and Bosch, L. (1976). The 3'-terminus of 16 S ribosomal RNA of Escherichia coli. Isolation and purification of the terminal 49-nucleotide fragment at a milligram scale. FEBS Lett. *71*, 351–355.

Baba, T., Ara, T., Hasegawa, M., Takai, Y., Okumura, Y., Baba, M., Datsenko, K.A., Tomita, M., Wanner, B.L., and Mori, H. (2006). Construction of Escherichia coli K-12 in-frame, single-gene knockout mutants: the Keio collection. Mol. Syst. Biol. *2*, 2006.0008.

Baker, K.E., and Parker, R. (2004). Nonsense-mediated mRNA decay: terminating erroneous gene expression. Curr. Opin. Cell Biol. *16*, 293–299.

Bank, R.P.D. RCSB PDB: Policies.

Baranov, P.V., Gesteland, R.F., and Atkins, J.F. (2002). Recoding: translational bifurcations in gene expression. Gene *286*, 187–201.

Belew, A.T., Hepler, N.L., Jacobs, J., and Dinman, J. (2008). PRFdb: A database of computationally predicted eukaryotic programmed -1 ribosomal frameshift signals. BMC Genomics.

Boon, T. (1971a). Inactivation of Ribosomes In Vitro by Colicin E3 and Its Mechanism of Action. 4.

Boon, T. (1971b). Inactivation of Ribosomes In Vitro by Colicin E3. Proc. Natl. Acad. Sci. *68*, 2421–2425.

Bowman, C.M., Dahlberg, J.E., Ikemura, T., Konisky, J., and Nomura, M. (1971). Specific Inactivation of 16S Ribosomal RNA Induced by Colicin E3 In Vivo. Proc. Natl. Acad. Sci. *68*, 964–968.

Brown, R.F., Andrews, C.T., and Elcock, A.H. (2015). Stacking free energies of all DNA and RNA nucleoside pairs and dinucleoside-monophosphates computed using recently revised AMBER parameters and compared with experiment. J. Chem. Theory Comput. *11*, 2315–2328.

Buul, C.P.J.J. van, Visser, W., and Knippenberg, P.H. van (1984). Increased translational fidelity caused by the antibiotic kasugamycin and ribosomal ambiguity in mutants harbouring the ksgA gene. FEBS Lett. *177*, 119–124.

Chang, Y.-F., Imam, J.S., and Wilkinson, M.F. (2007). The Nonsense-Mediated Decay RNA Surveillance Pathway. Annu. Rev. Biochem. *76*, 51–74.

Chen, C., Stevens, B., Kaur, J., Smilansky, Z., Cooperman, B.S., and Goldman, Y.E. (2011). Allosteric vs. spontaneous exit-site (E-site) tRNA dissociation early in protein synthesis. Proc. Natl. Acad. Sci. *108*, 16980–16985.

Chen, G., Chang, K.-Y., Chou, M.-Y., Bustamante, C., and Tinoco, I. (2009). Triplex structures in an RNA pseudoknot enhance mechanical stability and increase efficiency of –1 ribosomal frameshifting. Proc. Natl. Acad. Sci. *106*, 12706–12711.

Chen, J., Petrov, A., Johansson, M., Tsai, A., O'Leary, S.E., and Puglisi, J.D. (2014). Dynamic pathways of −1 translational frameshifting. Nature *512*, 328–332.

Choi, J., and Puglisi, J.D. (2017). Three tRNAs on the ribosome slow translation elongation. Proc. Natl. Acad. Sci. *114*, 13691–13696.

Condon, D.E., Kennedy, S.D., Mort, B.C., Kierzek, R., Yildirim, I., and Turner, D.H. (2015). Stacking in RNA: NMR of Four Tetramers Benchmark Molecular Dynamics. J. Chem. Theory Comput. *11*, 2729–2742.

Connolly, K., Rife, J.P., and Culver, G. (2008). Mechanistic insight into the ribosome biogenesis functions of the ancient protein KsgA. Mol. Microbiol. *70*, 1062–1075.

Craigen, W.J., and Caskey, C.T. (1986). Expression of peptide chain release factor 2 requires high-efficiency frameshift. Nature *322*, 273–275.

Davis, R.C., and Tinoco, I. (1968). Temperature-dependent properties of dinucleoside phosphates. Biopolymers *6*, 223–242.

Demirci, H., Murphy, F., Belardinelli, R., Kelley, A.C., Ramakrishnan, V., Gregory, S.T., Dahlberg, A.E., and Jogl, G. (2010). Modification of 16S ribosomal RNA by the KsgA methyltransferase restructures the 30S subunit to optimize ribosome function. RNA *16*, 2319–2324.

Demo, G., Loveland, A.B., Svidritskiy, E., Gamper, H.B., Hou, Y.-M., and Korostelev, A.A. (2020). Structural basis for +1 ribosomal frameshifting during EF-G-catalyzed translocation. BioRxiv 2020.12.29.424751.

Douthwaite, S., Powers, T., Lee, J.Y., and Noller, H.F. (1989). Defining the structural requirements for a helix in 23 S ribosomal RNA that confers erythromycin resistance. J. Mol. Biol. *209*, 655–665.

Drummond, D.A., and Wilke, C.O. (2008). Mistranslation-Induced Protein Misfolding as a Dominant Constraint on Coding-Sequence Evolution. Cell *134*, 341–352.

Dunkle, J.A., Wang, L., Feldman, M.B., Pulk, A., Chen, V.B., Kapral, G.J., Noeske, J., Richardson, J.S., Blanchard, S.C., and Cate, J.H.D. (2011). Structures of the Bacterial Ribosome in Classical and Hybrid States of tRNA Binding. Science *332*, 981–984.

Fareed, G.C., Wilt, E.M., and Richardson, C.C. (1971). Enzymatic Breakage and Joining of Deoxyribonucleic Acid: VIII. HYBRIDS OF RIBO- AND DEOXYRIBONUCLEOTIDE HOMOPOLYMERS AS SUBSTRATES FOR POLYNUCLEOTIDE LIGASE OF BACTERIOPHAGE T4. J. Biol. Chem. *246*, 925–932.

Flower, A.M., and Mchenry, C.S. (1990). The γ subunit of DNA polymerase III holoenzyme of Escherichia coli is produced by ribosomal frameshifting. 5.

Frilander, M.J., and Steitz, J.A. (2001). Dynamic Exchanges of RNA Interactions Leading to Catalytic Core Formation in the U12-Dependent Spliceosome. Mol. Cell *7*, 217–226.

Golden, B.L., Gooding, A.R., Podell, E.R., and Cech, T.R. (1996). X-ray crystallography of large RNAs: heavy-atom derivatives by RNA engineering. RNA *2*, 1295–1305.

Helser, T.L., Davies, J.E., and Dahlberg, J.E. (1971). Change in Methylation of 16S Ribosomal RNA Associated with Mutation to Kasugamycin Resistance in Escherichia coli. Nature. New Biol. *233*, 12–14.

Helser, T.L., Davies, J.E., and Dahlberg, J.E. (1972). Mechanism of Kasugamycin Resistance in Escherichia coli. Nature. New Biol. *235*, 6–9.

Heus, H.A., and van Knippenberg, P.H. (1988). The 3' terminal colicin fragment of Escherichia coli 16S ribosomal RNA. Conformational details revealed by enzymic and chemical probing. J. Biomol. Struct. Dyn. *5*, 951–963.

Ho, C.K., and Shuman, S. (2002). Bacteriophage T4 RNA ligase 2 (gp24.1) exemplifies a family of RNA ligases found in all phylogenetic domains. Proc. Natl. Acad. Sci. *99*, 12709–12714.

Hong, S., Sunita, S., Maehigashi, T., Hoffer, E.D., Dunkle, J.A., and Dunham, C.M. (2018). Mechanism of tRNA-mediated +1 ribosomal frameshifting. Proc. Natl. Acad. Sci. *115*, 11226–11231.

Huang, C., and Yu, Y.-T. (2013). Synthesis and Labeling of RNA In Vitro. Curr. Protoc. Mol. Biol. Ed. Frederick M Ausubel Al *0 4*, Unit4.15.

Jafilan, S., Klein, L., Hyun, C., and Florián, J. (2012). Intramolecular Base Stacking of Dinucleoside Monophosphate Anions in Aqueous Solution. J. Phys. Chem. B *116*, 3613–3618.

Jenner, L.B., Demeshkina, N., Yusupova, G., and Yusupov, M. (2010). Structural aspects of messenger RNA reading frame maintenance by the ribosome. Nat. Struct. Mol. Biol. *17*, 555–560.

Kershaw, C.J., and O'Keefe, R.T. (2012). Splint ligation of RNA with T4 DNA ligase. Methods Mol. Biol. Clifton NJ *941*, 257–269.

Kibbe, W.A. (2007). OligoCalc: an online oligonucleotide properties calculator. Nucleic Acids Res. *35*, W43–W46.

Kim, H.-K., Liu, F., Fei, J., Bustamante, C., Gonzalez, R.L., and Tinoco, I. (2014). A frameshifting stimulatory stem loop destabilizes the hybrid state and impedes ribosomal translocation. Proc. Natl. Acad. Sci. U. S. A. *111*, 5538–5543.

Kleppe, K., Sande, J.H. van de, and Khorana, H.G. (1970). Polynucleotide Ligase-Catalyzed Joining of Deoxyribo-oligonucleotides on Ribopolynucleotide Templates

and of Ribo-oligonucleotides on Deoxyribopolynucleotide Templates. Proc. Natl. Acad. Sci. *67*, 68–73.

Korostelev, A., Asahara, H., Lancaster, L., Laurberg, M., Hirschi, A., Zhu, J., Trakhanov, S., Scott, W.G., and Noller, H.F. (2008). Crystal structure of a translation termination complex formed with release factor RF2. Proc. Natl. Acad. Sci. *105*, 19684–19689.

Kunkel, T.A. (1985). Rapid and efficient site-specific mutagenesis without phenotypic selection. Proc. Natl. Acad. Sci. *82*, 488–492.

Kurland, C.G. (1992). Translational Accuracy and the Fitness of Bacteria. Annu. Rev. Genet. *26*, 29–50.

Labuda, D., Grosjean, H., Striker, G., and Pörschke, D. (1982). Codon:Anticodon and anticodon:Anticodon interaction. Evaluation of equilibrium and kinetic parameters of complexes involving a G:U wobble. Biochim. Biophys. Acta BBA - Gene Struct. Expr. *698*, 230–236.

Lancaster, L., and Noller, H.F. (2005). Involvement of 16S rRNA Nucleotides G1338 and A1339 in Discrimination of Initiator tRNA. Mol. Cell *20*, 623–632.

Larsen, B., Gesteland, R.F., and Atkins, J.F. (1997). Structural probing and mutagenic analysis of the stem-loop required for Escherichia coli dnaX ribosomal frameshifting: programmed efficiency of 50%11Edited By D. E. Draper. J. Mol. Biol. *271*, 47–60.

Li, Z., Stahl, G., and Farabaugh, P.J. (2001). Programmed +1 frameshifting stimulated by complementarity between a downstream mRNA sequence and an error-correcting region of rRNA. RNA *7*, 275–284.

Lingner, J., and Cech, T.R. (1996). Purification of telomerase from Euplotes aediculatus: requirement of a primer 3’ overhang. Proc. Natl. Acad. Sci. *93*, 10712–10717.

Matsufuji, S., Matsufuji, T., Wills, N.M., Gesteland, R.F., and Atkins, J.F. (1996). Reading two bases twice: mammalian antizyme frameshifting in yeast. EMBO J. *15*, 1360.

Moazed, D., and Noller, H. (1989a). Interaction of tRNA with 23S rRNA in the ribosomal A, P, and E sites. Cell.

Moazed, D., and Noller, H.F. (1989b). Intermediate states in the movement of transfer RNA in the ribosome. Nature *342*, 142–148.

Mohan, S., Donohue, J.P., and Noller, H.F. (2014). Molecular mechanics of 30S subunit head rotation. Proc. Natl. Acad. Sci. *111*, 13325–13330.

Moore, M.J., and Query, C.C. (2000). [7] Joining of RNAs by splinted ligation. In Methods in Enzymology, (Academic Press), pp. 109–123.

Moore, M.J., and Sharp, P.A. (1992). Site-specific modification of pre-mRNA: the 2'-hydroxyl groups at the splice sites. Science *256*, 992–997.

Namy, O., Rousset, J.-P., Napthine, S., and Brierley, I. (2004). Reprogrammed Genetic Decoding in Cellular Gene Expression. Mol. Cell *13*, 157–168.

Nandakumar, J., Ho, C.K., Lima, C.D., and Shuman, S. (2004). RNA Substrate Specificity and Structure-guided Mutational Analysis of Bacteriophage T4 RNA Ligase 2 *. J. Biol. Chem. *279*, 31337–31347.

Niblett, D., Nelson, C., Leung, C.S., Rexroad, G., Cozy, J., Zhou, J., Lancaster, L., and Noller, H.F. (2021). Mutations in domain IV of elongation factor EF-G confer −1 frameshifting. RNA *27*, 40–53.

Noller, H.F., Donohue, J.P., and Gutell, R.R. (2022). The universally conserved nucleotides of the small subunit ribosomal RNAs. RNA *28*, 623–644.

Norberg, J., and Nilsson, L. (1995). Stacking Free Energy Profiles for All 16 Natural Ribodinucleoside Monophosphates in Aqueous Solution. J. Am. Chem. Soc. *117*, 10832–10840.

O'Farrell, H.C., Pulicherla, N., Desai, P.M., and Rife, J.P. (2006). Recognition of a complex substrate by the KsgA/Dim1 family of enzymes has been conserved throughout evolution. RNA *12*, 725–733.

Peng, B.-Z., Bock, L.V., Belardinelli, R., Peske, F., Grubmüller, H., and Rodnina, M.V. (2019). Active role of elongation factor G in maintaining the mRNA reading frame during translation. Sci. Adv. *5*, eaax8030.

Poldermans, B., Bakker, H., and Van Knippenberg, P.H. (1980). Studies on the function of two adjacent N6,N6-dimethyladenosines near the 3' end of 16S ribosomal RNA of Escherichia coli. IV. The effect of the methylgroups on ribosomal subunit interaction. Nucleic Acids Res. *8*, 143–151.

Qin, P., Yu, D., Zuo, X., and Cornish, P.V. (2014). Structured mRNA induces the ribosome into a hyper-rotated state. EMBO Rep. *15*, 185–190.

Ritchie, D.B., Foster, D.A.N., and Woodside, M.T. (2012). Programmed −1 frameshifting efficiency correlates with RNA pseudoknot conformational plasticity, not resistance to mechanical unfolding. Proc. Natl. Acad. Sci. U. S. A. *109*, 16167–16172.

Sanders, C.L., and Curran, J.F. (2007). Genetic analysis of the E site during RF2 programmed frameshifting. RNA *13*, 1483–1491.

Sauert, M., Temmel, H., and Moll, I. (2015). Heterogeneity of the translational machinery: Variations on a common theme. Biochimie *114*, 39–47.

Savelsbergh, A., Katunin, V.I., Mohr, D., Peske, F., Rodnina, M.V., and Wintermeyer, W. (2003). An Elongation Factor G-Induced Ribosome Rearrangement Precedes tRNA-mRNA Translocation. Mol. Cell *11*, 1517–1523.

Schluenzen, F., Takemoto, C., Wilson, D.N., Kaminishi, T., Harms, J.M., Hanawa-Suetsugu, K., Szaflarski, W., Kawazoe, M., Shirouzu, M., Nierhaus, K.H., et al. (2006). The antibiotic kasugamycin mimics mRNA nucleotides to destabilize tRNA binding and inhibit canonical translation initiation. Nat. Struct. Mol. Biol. *13*, 871–878.

Schürer, H., Lang, K., Schuster, J., and Mörl, M. (2002). A universal method to produce in vitro transcripts with homogeneous 3′ ends. Nucleic Acids Res. *30*, e56.

Schuwirth, B.S., Day, J.M., Hau, C.W., Janssen, G.R., Dahlberg, A.E., Cate, J.H.D., and Vila-Sanjurjo, A. (2006). Structural analysis of kasugamycin inhibition of translation. Nat. Struct. Mol. Biol. *13*, 879–886.

Senior, B.W., and Holland, I.B. (1971). Effect of Colicin E3 upon the 30S Ribosomal Subunit of Escherichia coli. Proc. Natl. Acad. Sci. U. S. A. *68*, 959–963.

Šponer, J., E. Riley, K., and Hobza, P. (2008). Nature and magnitude of aromatic stacking of nucleic acid bases. Phys. Chem. Chem. Phys. *10*, 2595–2610.

Stark, M.R., Pleiss, J.A., Deras, M., Scaringe, S.A., and Rader, S.D. (2006). An RNA ligase-mediated method for the efficient creation of large, synthetic RNAs. RNA *12*, 2014–2019.

Stephan, N.C., Ries, A.B., Boehringer, D., and Ban, N. (2021). Structural basis of successive adenosine modifications by the conserved ribosomal methyltransferase KsgA. Nucleic Acids Res. *49*, 6389–6398.

Stochmanski, S.J., Therrien, M., Laganière, J., Rochefort, D., Laurent, S., Karemera, L., Gaudet, R., Vyboh, K., Van Meyel, D.J., Di Cristo, G., et al. (2012). Expanded ATXN3

frameshifting events are toxic in Drosophila and mammalian neuron models. Hum. Mol. Genet. *21*, 2211–2218.

Thammana, P., and Held, W.A. (1974). Methylation of 16S RNA during ribosome assembly in vitro. Nature *251*, 682–686.

Tinoco Jr., I., Kim, H.-K., and Yan, S. (2013). Frameshifting dynamics. Biopolymers *99*, 1147–1166.

Traub, P., and Nomura, M. (1968). Structure and function of E. coli ribosomes. V. Reconstitution of functionally active 30S ribosomal particles from RNA and proteins. Proc. Natl. Acad. Sci. U. S. A. *59*, 777–784.

Traub, P., and Nomura, M. (1969). Structure and function of Escherichia coli ribosomes: VI. Mechanism of assembly of 30 s ribosomes studied in vitro. J. Mol. Biol. *40*, 391–413.

Traub, P., Mizushima, S., Lowry, C.V., and Nomura, M. (1971a). [41] Reconstitution of ribosomes from subribosomal components. In Methods in Enzymology, (Academic Press), pp. 391–407.

Traub, P., Mizushima, S., Lowry, C.V., and Nomura, M. (1971b). [41] Reconstitution of ribosomes from subribosomal components. In Methods in Enzymology, (Academic Press), pp. 391–407.

Turner, D.H. (1996). Thermodynamics of base pairing. Curr. Opin. Struct. Biol. *6*, 299–304.

Uemura, S., Aitken, C.E., Korlach, J., Flusberg, B.A., Turner, S.W., and Puglisi, J.D. (2010). Real-time tRNA transit on single translating ribosomes at codon resolution. Nature *464*, 1012–1017.

Van Charldorp, R., Heus, H.A., and Van Knippenberg, P.H. (1981). Adenosine dimethylation of 16S ribosomal RNA: effect of the methylgroups on local conformational stability as deduced from electrophoretic mobility of RNA fragments in denaturing polyacrylamide gels. Nucleic Acids Res. *9*, 267–275.

Varshney, U., Lee, C.P., and RajBhandary, U.L. (1991). Direct analysis of aminoacylation levels of tRNAs in vivo. Application to studying recognition of Escherichia coli initiator tRNA mutants by glutaminyl-tRNA synthetase. J. Biol. Chem. *266*, 24712–24718.

Walter, A.E., and Turner, D.H. (1994). Sequence dependence of stability for coaxial stacking of RNA helixes with Watson-Crick base paired interfaces. Biochemistry *33*, 12715–12719.

Watson, Z.L., Ward, F.R., Méheust, R., Ad, O., Schepartz, A., Banfield, J.F., and Cate, J.H. (2020). Structure of the bacterial ribosome at 2 Å resolution. ELife *9*.

Wills, N.M., and Atkins, J.F. (2006). The potential role of ribosomal frameshifting in generating aberrant proteins implicated in neurodegenerative diseases. RNA *12*, 1149–1153.

Zhou, J., Lancaster, L., Donohue, J.P., and Noller, H.F. (2013). Crystal Structures of EF-G-Ribosome Complexes Trapped in Intermediate States of Translocation. Science *340*, 1236086–1236086.

Zhou, J., Lancaster, L., Donohue, J.P., and Noller, H.F. (2019). Spontaneous ribosomal translocation of mRNA and tRNAs into a chimeric hybrid state. Proc. Natl. Acad. Sci. *116*, 7813–7818.